

# Recent Developments in Machine Learning Methods for Stochastic Control and Games

Ruimeng Hu <sup>\*</sup>      Mathieu Laurière <sup>†</sup>

## Abstract

In this paper, we give an overview of recently developed machine learning methods for stochastic control problems and games. The main focus is on deep learning methods that have unlocked the possibility to solve such problems even when the structure is complex or the dimension is high, which is not feasible with traditional numerical methods. The new approaches build on recent breakthrough machine learning methods for high-dimensional partial differential equations or backward stochastic differential equations, or on model-free reinforcement learning for Markov decision processes. This review summarizes state-of-the-art works at the crossroad of machine learning and stochastic control and games. It also discusses connections with real applications and identifies unsolved challenges.

## Contents

<b>1</b>	<b>Introduction</b>	<b>2</b>
1.1	Some high-dimensional examples in applications	3
1.2	An illustrative linear quadratic model	4
1.3	Organization of the survey	6
<b>2</b>	<b>Stochastic Control Problems</b>	<b>7</b>
2.1	Formulation of stochastic control	7
2.2	Direct parameterization	9
2.2.1	Global and local in time approaches	9
2.2.2	Stochastic control with delay	11
2.2.3	Mean-field type control	13
2.3	BSDE-based deep learning algorithms	17
2.3.1	Deep backward stochastic differential equation (Deep BSDE) method	17
2.3.2	Deep backward dynamic programming (DBDP)	18
2.4	Primal-Dual approaches	19
2.5	PDE-based algorithms	20
<b>3</b>	<b>Stochastic Differential Games</b>	<b>21</b>
3.1	$N$ -player stochastic games	22
3.1.1	Open-loop Nash equilibrium	23
3.1.2	Markovian Nash equilibrium	24
3.2	Mean-field games	29
3.2.1	Theoretical background	31
3.2.2	The Sig-DFP algorithm for mean-field games with common noise	35
3.2.3	Deep learning for mean-field PDE systems	38
3.2.4	Deep learning for McKean-Vlasov FBSDE systems	41

<sup>\*</sup>Department of Mathematics, and Department of Statistics and Applied Probability, University of California, Santa Barbara, CA 93106-3080, USA, *rhu@ucsb.edu*.

<sup>†</sup>NYU-ECNU Institute of Mathematical Sciences, and Center for Data Science and Artificial Intelligence, New York University Shanghai, 200122, China, *mathieu.lauriere@nyu.edu*.

3.2.5	Deep learning for mean-field master equation	43
<b>4</b>	<b>Reinforcement Learning</b>	<b>46</b>
4.1	Reinforcement learning for stochastic control problems	47
4.1.1	Markov decision processes	47
4.1.2	Mean-field MDP and reinforcement learning for mean-field control problems	51
4.2	Reinforcement learning for stochastic differential games	53
4.2.1	Multi-agent reinforcement learning (MARL)	53
4.2.2	Reinforcement learning for mean-field games	54
<b>5</b>	<b>Conclusion and Perspectives</b>	<b>55</b>
<b>A</b>	<b>Deep Learning Tools</b>	<b>70</b>
A.1	Neural network architectures	70
A.1.1	Feedforward fully connected neural networks	70
A.1.2	Recurrent neural networks	70
A.1.3	Long short-term memory	71
A.1.4	Expressive power of neural networks	71
A.2	Stochastic gradient descent and its variants	72
<b>B</b>	<b>Preliminaries on SDDE</b>	<b>72</b>
<b>C</b>	<b>Pseudo-codes of Algorithms</b>	<b>73</b>
<b>D</b>	<b>List of Acronyms</b>	<b>75</b>
<b>E</b>	<b>List of Frequently Used Notations</b>	<b>76</b>

## 1 Introduction

Stochastic optimal control and games have been extensively studied throughout the twentieth century and have found a wide range of applications in many areas such as finance, social sciences, operations research, and epidemic management problems, to cite just a few. In recent years, computational methods for stochastic control and games have seen great progress with the help of machine learning tools. A striking example of recent breakthrough in applied mathematics using such tools is the numerical resolution of general nonlinear parabolic partial differential equations and backward stochastic differential equations in high dimensions [83, 82, 124, 227]. In short, stochastic control problems study how an agent optimally controls a stochastic *dynamical system*. The agent perceives some observations of the system's state and, based on these observations, can decide to influence the evolution of the state. The goal is to optimize an objective function that typically incorporates the cost of controlling the system and the reward for reaching some state. One of the most popular methods to solve such problems is dynamic programming, developed by Richard Bellman in the 1950s [25]. However, this method suffers from what Bellman called the *curse of dimensionality*, meaning that its complexity increases drastically with the number of possible states. This is a major issue for systems evolving in continuous and high dimensional spaces since they can not be approximated by a small number of states. In such cases, using exact dynamic programming becomes infeasible from the computational viewpoint. The complexity may also come from the structure of the system's evolution. For example, in some cases, the system's evolution or its observation is subject to delay, which appears in many real-world applications, *e.g.*, in economics, mechanics, or biology. To model the delay feature, the dynamics of the controlled system will depend not only on the current state but also on the history prior to the current time, which makes the problem path-dependent and thus infinite-dimensional.

On the other hand, stochastic differential game theory, initiated by [147], combines theory and optimal control, and provides a framework for modeling and analyzing behavior of strategic agents in the context of a dynamical system. The theory has been extensively employed across many disciplines, including

management science, economics, social science, and biology. One of the core objectives in differential games is to compute Nash equilibria, *i.e.*, strategy profiles according to which no player has an incentive to deviate unilaterally [201]. However, computing Nash equilibria in  $N$ -agent games is a notoriously hard problem, and the direct computation of Nash equilibria is extremely demanding in terms of time and memory [75] even for moderately large  $N$ . The mean-field game paradigm has been introduced independently by Lasry and Lions in [174] and by Huang, Malhamé and Caines in [142] to provide a tractable approximation of games with very large populations. A mean-field game is a game with a continuum of infinitesimal agents, where any single agent does not influence the rest of the population, which forms the mean field with which each agent interacts. This framework provides an efficient way to compute approximate Nash equilibria for symmetric  $N$ -agent games when  $N$  is large. However, challenges remain in terms of computational complexity for games with high dimensional or complex environments, or when common noise affects the population dynamics. Furthermore, in the intermediate regime when  $N$  is moderately large, the mean-field theory does not provide a good approximation of the  $N$ -player game. In such cases, one may still face a high-dimensional problem. To make these challenges more concrete, we discuss some illustrative examples.

## 1.1 Some high-dimensional examples in applications

We first discuss an example to financial markets. Many problems in economics or finance involve multiple interacting agents. For instance, we may consider a group of traders who buy and sell stocks in a financial market such as the S&P 500, a free-float weighted measurement stock market index of 500 of the largest companies listed on stock exchanges in the United States. Each trader's portfolio describes the investment in stocks available on the market. To describe the investments of the whole group of traders, we need to incorporate all the trader's portfolios, and hence this description can be very high dimensional. However, if the traders have similar risk preferences, it is sufficient to study how one representative trader optimizes their payoff to understand the whole group's behavior. Any single agent has only a negligible impact on the stocks' prices. However, the impact of the group might be significant because if everyone wants to buy or sell the same stock, then the price will probably be shifted up or down. The portfolio optimization problem then becomes to find a Nash equilibrium. Each agent can anticipate that every other agent will behave like themselves and can thus predict the impact of the group on the stocks' prices. The mean-field game paradigm provides a rigorous framework in which each agent, taken individually, has no impact at all on the group's dynamics, and the problem is to find a fixed point at the population level. This simplifies the analysis. A first approach to describe the solution is through a forward-backward system of partial differential equations (PDEs) composed of a Fokker-Plank (FP) equation for the population distribution and a Hamilton-Jacobi-Bellman (HJB) equation for the value function of an infinitesimal player. However, several difficulties arise. Firstly, even solving the optimal control problem for the representative agent can be challenging: Given the number of stocks, the problem is in high dimension, and using an exact dynamic programming algorithm can be computationally too expensive. Secondly, even if the agent's portfolio state is in a low dimension, the optimal strategy may depend on the average state or control of the group. If the agents are trading the same stocks, then their trading strategies are all subject to the same source of randomness, which implies that the group's average strategy itself is stochastic. In the context of mean-field games, this is formalized through the notion of common noise. In such cases, the PDEs of the forward-backward system characterizing the solutions are no longer deterministic but stochastic, making the system considerably harder to solve. Another approach characterizes the solution by a forward-backward system of stochastic differential equations (FBSDEs) which involves the conditional distribution of the forward and the backward processes, given the common noise. A third approach consists in describing the solution by a PDE on the space of probability distributions, but here again, this PDE is difficult to solve since it is posed on a high or infinite-dimensional space. In any case, in this application to optimal trading and as in many others, realistic models lead to the need to approximate functions of high or infinite-dimensional inputs. All together, it makes crucial to develop efficient and accurate deep learning algorithms and theories for computing optimal controls and Nash equilibria in high dimensions.

Our second example arises in infectious disease control of multiple regions. In a classic compartmental epidemiological model, each individual in a geographical region is assigned a label, for instance, **S**usceptible, **E**xposed, **I**nfectious, **R**emoved, **V**accinated. The transmission of a virus, being infected or recovered, moves individuals from one compartment to another, and this transition is usually described by stochastic

dynamical equations. When a disease outbreak is reported, the region planner needs to take measurements to control its spread. The ongoing COVID-19 includes issuing lockdown or work from home policies, developing vaccines and later expanding equitable vaccine distribution, providing telehealth programs, distributing free testing kits, educating the public on how the virus transits, and focusing on surface disinfection. As a region planner, the decisions are usually made by weighting different costs, including the economic loss due to less productivity during lockdown policy or work from home policy, the economic value of life due to death of infected individuals, and various social-welfare costs due to measurements mentioned above, and many more. Moreover, as the world is more interconnected than ever before, one region's decision will inevitably influence its neighboring regions. For instance, in the US, the decision made by the New York governor will affect the situation in New Jersey as so many people travel daily between the two states. Imagining that both state governors make decisions representing their own benefits but also take into account others' rational decisions, and they may even compete for the scarce resource (frontline workers, personal protective equipment, *etc.*), these are precisely the features of a non-cooperative game. A Nash equilibrium computed from such a game will definitely provide some qualitative guidance and insights for policymakers on the impact of certain policies. However, even with only three states (New York, New Jersey, and Pennsylvania) and a simple stochastic SEIR model as in [239, 240], this problem's state space is already twelve dimensions. Figure 1 below showcases the equilibrium lockdown policy corresponding to the multi-region SEIR model solved by a deep learning algorithm proposed in [122] (see Section 3.1.2) between the three states. The model parameters are estimated from real data posted by the Centers for Disease Control and Prevention (CDC). In general, the problem dimension is proportional to the number of compartments in the epidemiological model multiplied by the number of regions considered. For the most basic SIR model, the dimension of the problem for US governors will be  $3 \times 50 = 150$ .

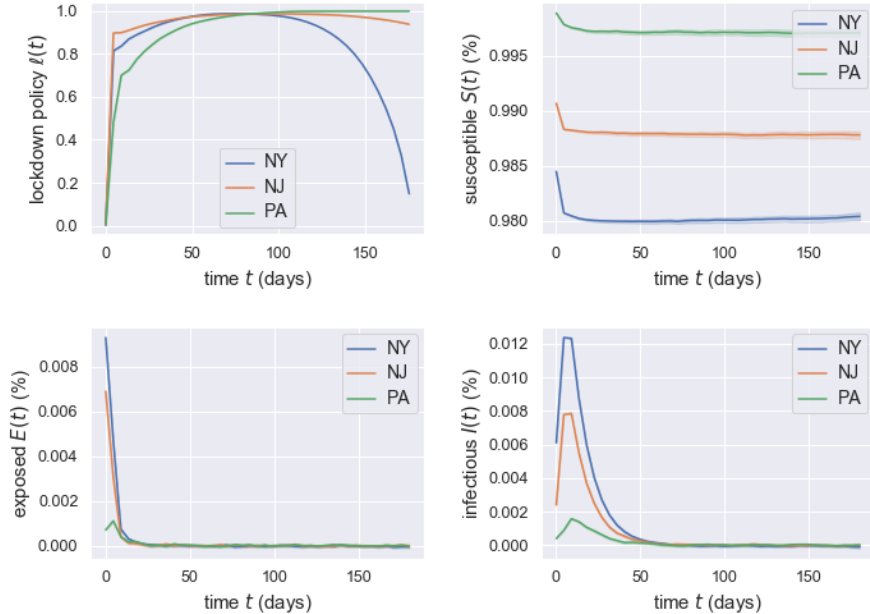


Figure 1: A case study of the COVID-19 pandemic in three states: New York (NY), New Jersey (NJ), and Pennsylvania (PA) in [239]. Plots of optimal policies (top-left), Susceptibles (top-right), Exposed (bottom-left), and Infectious (bottom-right) for three states: New York (blue), New Jersey (orange), and Pennsylvania (green). Large  $\ell$  indicates high intensity of lockdown policy. Choices of parameters are referred to [239, Section 4.2].

## 1.2 An illustrative linear quadratic model

To illustrate numerical methods and show that they can correctly compute the problem's solution, it is convenient to have examples with analytical or semi-explicit solutions. We present here an example

introduced in [49] to model the interactions in a system of banks. This model and other similar models with linear-quadratic structures admit a closed-form solution and have found applications in various fields.

We consider a stochastic differential game with  $N$  players, and we denote by  $\mathcal{I} = \{1, 2, \dots, N\}$  the set of players. Each player is interpreted as a bank and the state is its log-reserve. Let  $T$  be a finite time horizon. At each time  $t \in [0, T]$ , player  $i \in \mathcal{I}$  has a state  $X_t^i \in \mathbb{R}$  and takes an action  $\alpha_t^i \in \mathbb{R}$ . The information structure will be discussed later and for now we proceed informally but we can think of  $\alpha_t^i$  as a stochastic process adapted to a filtration that represents the information available to player  $i$ . The dynamics of the controlled state process on  $[0, T]$  are given by

$$dX_t^i = [a(\bar{X}_t - X_t^i) + \alpha_t^i] dt + \sigma \left( \rho dW_t^0 + \sqrt{1 - \rho^2} dW_t^i \right), \quad X_0^i \sim \mu_0, \quad i \in \mathcal{I}, \quad \bar{X}_t = \frac{1}{N} \sum_{i=1}^N X_t^i,$$

where  $\mu_0$  is a given initial distribution and  $\mathbf{W} = [W^0, W^1, \dots, W^N]$  are  $(N+1)$   $m$ -dimensional independent Brownian motions. We shall call  $W^i$  the idiosyncratic (i.e., individual) noises and  $W^0$  the common noise. The parameter  $\rho \in [0, 1]$  characterizes the noise correlation between agents. Here  $a(\bar{X}_t - X_t^i)$  represents the rate at which bank  $i$  borrows from or lends to other banks in the lending market, while  $\alpha_t^i$  denotes its control rate of cash flows to a central bank. Furthermore,  $\bar{X}_t = \frac{1}{N} \sum_{i=1}^N X_t^i$  denotes the average state. The  $N$  dynamics are thus coupled since all the states  $\mathbf{X}_t = [X_t^1, \dots, X_t^N]$  affect the drift of every agent. Given a set of strategies  $(\boldsymbol{\alpha}_t)_{t \in [0, T]} = ([\alpha_t^1, \dots, \alpha_t^N])_{t \in [0, T]}$ , the cost incurred to player  $i$  is

$$J^i(\boldsymbol{\alpha}) = \mathbb{E} \left[ \int_0^T f^i(t, \mathbf{X}_t, \boldsymbol{\alpha}_t) dt + g^i(\mathbf{X}_T) \right],$$

where the running cost  $f^i : [0, T] \times \mathbb{R}^N \times \mathbb{R}^N \rightarrow \mathbb{R}$  and the terminal cost  $g^i : \mathbb{R}^N \rightarrow \mathbb{R}$  are given by

$$f^i(t, \mathbf{x}, \boldsymbol{\alpha}) = \frac{1}{2}(\alpha^i)^2 - q\alpha^i(\bar{x} - x^i) + \frac{\epsilon}{2}(\bar{x} - x^i)^2, \quad g^i(\mathbf{x}) = \frac{c}{2}(\bar{x} - x^i)^2, \quad \bar{x} = \frac{1}{N} \sum_{i=1}^N x^i.$$

where  $\mathbf{x} = [x^1, \dots, x^N]$  and  $\boldsymbol{\alpha} = [\alpha^1, \dots, \alpha^N]$ . All the parameters are non-negative. Here  $\frac{1}{2}(\alpha^i)^2$  denotes the quadratic cost of the control, and  $-q\alpha^i(\bar{x} - x^i)$  models the incentive to borrowing or lending: bank  $i$  will want to borrow if  $X_t^i$  is smaller than  $\bar{X}_t$  and lend if  $X_t^i$  is larger than  $\bar{X}_t$ . The quadratic term  $(\bar{x} - x^i)^2$  in  $f^i$  and  $g^i$  penalizes the deviation from the average, given the other players' states. Player  $i$  chooses  $(\alpha_t^i)_{t \in [0, T]}$  to minimize her cost  $J^i(\boldsymbol{\alpha})$  within some set of admissible strategies. We assume  $q \leq \epsilon^2$  so that the Hamiltonian is jointly convex in state and control variables, ensuring that there is at most one best response and then at most one Nash equilibrium. In the original work [49, Section 3.1], open-loop and closed-loop equilibria are characterized using semi-explicit formulas through ordinary differential equations (ODEs).

As the number of agents  $N$  grows to infinity, the idiosyncratic noises have a smaller and smaller influence on  $\bar{X}$ , which, in the limit, depends only on the common noise  $W^0$ . This is formalized in the following mean field game (MFG). Let  $(W_t)_{0 \leq t \leq T}$  and  $(W_t^0)_{0 \leq t \leq T}$  be independent  $m$ -dimensional Brownian motions. We shall refer to  $W$  as the idiosyncratic noise of the representative player and to  $W^0$  as the common noise of the system. We consider the stochastic control problem

$$\inf_{\alpha} \mathbb{E} \left\{ \int_0^T \left[ \frac{\alpha_t^2}{2} - q\alpha_t(m_t - X_t) + \frac{\epsilon}{2}(m_t - X_t)^2 \right] dt + \frac{c}{2}(m_T - X_T)^2 \right\},$$

where  $dX_t = [a(m_t - X_t) + \alpha_t] dt + \sigma(\rho dW_t^0 + \sqrt{1 - \rho^2} dW_t)$ ,  $X_0 \sim \mu_0$  (1.1)

where the representative agent controls her state  $X$  through a control process  $\alpha$ . Here  $m_t = \mathbb{E}[X_t | \mathcal{F}_t^{W^0}]$  is the conditional population mean given the common noise. As in the  $N$ -player case, one advantage of LQ models lies in the existence of an analytical solution for the mean-field equilibrium, which can provide a benchmark to test numerical algorithms. In this model, at equilibrium, we have

$$m_t = \mathbb{E}[X_0] + \rho\sigma W_t^0, \quad t \in [0, T], \quad (1.2)$$

$$\alpha_t = (q + \eta_t)(m_t - X_t), \quad t \in [0, T], \quad (1.3)$$

where  $\eta$  is a deterministic function of time solving the Riccati equation,

$$\dot{\eta}_t = 2(a + q)\eta_t + \eta_t^2 - (\epsilon - q^2), \quad \eta_T = c.$$

The solution is given by

$$\eta_t = \frac{-(\epsilon - q^2)(e^{(\delta^+ - \delta^-)(T-t)} - 1) - c(\delta^+ e^{(\delta^+ - \delta^-)(T-t)} - \delta^-)}{(\delta^- e^{(\delta^+ - \delta^-)(T-t)} - \delta^+) - c(e^{(\delta^+ - \delta^-)(T-t)} - 1)}.$$

where  $\delta^\pm = -(a + q) \pm \sqrt{R}$ ,  $R = (a + q)^2 + (\epsilon - q^2) > 0$ . At equilibrium, i.e., when all the payers use the equilibrium control, and the minimal expected cost for a representative player is

$$u(0, x_0 - \mathbb{E}[x_0]), \quad \text{with } u(t, x) = \frac{\eta_t}{2} x^2 + \frac{1}{2} \sigma^2 (1 - \rho^2) \int_t^T \eta_s \, ds.$$

Even though the state is in dimension one only, the presence of the common noise means that the optimal control is a function of the common noise. In this example, the equilibrium control actually depends on the common noise only through the first conditional moment of the distribution. In this case, the equilibrium can be found using neural networks which take as inputs not only the individual player's state but also an estimate of this first conditional moment. This idea can be extended to scenarios where the dependence on the common noise occurs only through a finite dimensional vector of information; see [56, Test cases 5 and 6] for more details. However, this approach requires estimating aggregate quantities, for example by simulating a finite but large population of particles for many realizations of the common noise. When the interactions are through moments, another approach is to use only one realization of the idiosyncratic noise for each realization of the common noise: In [193], based on the rough path theory, a single-loop algorithm called signatured deep fictitious play has been proposed. The proposed algorithm can accurately capture the effect of common uncertainty changes on mean-field equilibria without further training of neural networks, as previously needed in the existing machine learning algorithms. We will provide more details on this method in Section 3.2.2 below. Figure 2 showcases the performance for this LQ MFG with common noise, where the benchmark trajectories are simulated according to (1.1) with  $m_t$  and  $\alpha_t$  in (1.2) and (1.3).

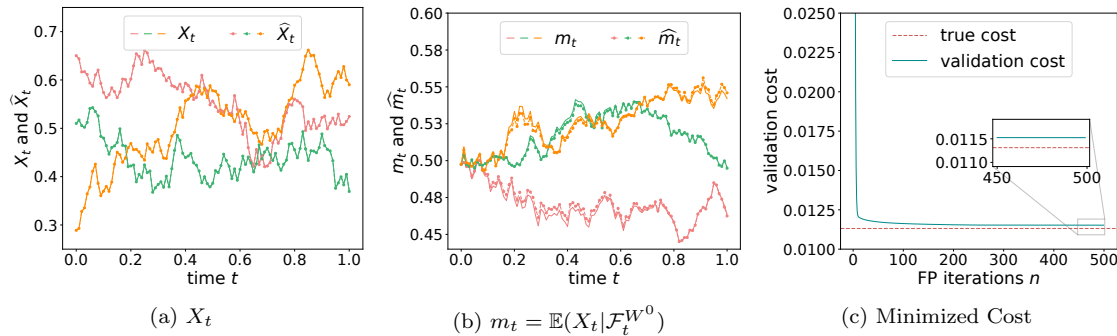


Figure 2: The illustrative linear quadratic model in Section 1.2. Panels (a) and (b) give three trajectories of  $X_t$ ,  $m_t = \mathbb{E}[X_t | \mathcal{F}_t^{W^0}]$  (solid lines) and their approximations  $\hat{X}_t$  (dashed lines) using different realizations of  $(X_0, W, W^0)$  from validation data. Panel (c) shows the minimized cost computed using validation data over fictitious play iterations. Parameter choices are given in [193, Section 5].

### 1.3 Organization of the survey

In the rest of this survey, we review recent developments in machine learning methods and theory for stochastic control and differential games. We shall also identify unsolved challenges, and make connections to real applications. We first review deep learning algorithms for stochastic control problems in Section 2.

In Section 3, we focus on deep learning for stochastic differential games, including (moderately large)  $N$ -player games and mean-field games. In Section 4, we review the basic principles underpinning model-free reinforcement learning methods for stochastic control and games. We make conclusive remarks and discuss unsolved challenges in Section 5. In the appendix, we provide more background on two main tools of modern machine learning, namely, neural networks architectures and stochastic gradient descent. We also summarize all the acronyms and the notations frequently used in this paper.

**The scope of the survey.** This paper focuses on the recent developed neural network-based algorithms aiming at high-dimensional problems. The main reason why we focus on the stochastic setting is that in the deterministic setting, the problems can usually be tackled using open loop controls by reducing the problem to two point boundary value problem [156, 242], which can be solved in high dimension without machine learning.

Besides the methods reviewed in this paper, there is a rich literature on methods, some of them related to machine learning but without neural networks. For example, to cite just a few examples, Markov chain based methods [38], regression based methods [18, 34], and approaches based on PDEs and BSDEs [68, 89]; see, *e.g.*, the survey papers [165, 153] and the references therein. Furthermore, we focus mostly on standard classes of stochastic control problems and games but many other problems are considered in the literature. For instance, we do not discuss in this paper optimal switching and optimal stopping problems, for which numerical algorithms have been extensively developed, *e.g.*, in [161, 137, 23, 24, 138, 145, 171, 218, 219, 91, 21].

## 2 Stochastic Control Problems

We start by reviewing the development of machine learning methods for stochastic optimal control problems, also called simply stochastic control (SC) problems. SC is a long-standing topic that studies stochastic dynamic systems that are controlled so as to achieve optimal performance. It has applications in many areas, including but not limited to engineering, economics, and mathematical finance. Some existing methods have been reviewed in, *e.g.*, works by Pham and co-authors [210, 95]. In this section, we shall focus on reviewing methods based on deep learning for solving standard SC problems, or problems with delay and mean-field type SC problems, BSDE-based deep learning algorithms, primal-dual approaches, and PDE-based algorithms. We focus here on the algorithms and we refer to Appendix A for more some basic introduction to neural networks and deep learning.

### 2.1 Formulation of stochastic control

Let  $T < \infty$  be a time horizon. Let  $(\Omega, \mathcal{F}, \mathbb{P})$  be a probability space supporting an  $m$ -dimensional Brownian motion  $W = (W_t)_{t \in [0, T]}$ , and  $\mathbb{F} = (\mathcal{F}_t)_{t \in [0, T]}$  be the natural filtration generated by  $W$ . In the most common case, a stochastic control problem is formulated as follows. Let  $d$  and  $k$  be integers for the dimensions of the state and the action. Let  $\mathcal{A} \subset \mathbb{R}^k$  denote the set of admissible actions. Let  $b, \sigma, f, g$  be Borel-measurable functions,

$$(b, \sigma, f) : [0, T] \times \mathbb{R}^d \times \mathcal{A} \rightarrow (\mathbb{R}^d, \mathbb{R}^{d \times m}, \mathbb{R}), \quad g : \mathbb{R}^d \rightarrow \mathbb{R}. \quad (2.1)$$

We denote by  $\mathbb{A}$  the set of so-called admissible controls. This set describes the integrability and measurability conditions required on  $\alpha$ . We usually require that  $\alpha$  is square-integrable. For measurability, two popular choices are that either  $\alpha$  should be a  $\mathcal{F}_t$ -progressively measurable process, or  $\alpha$  should be expressed as a measurable function of  $(t, X_t)$ . The former case is called *adaptive controls* (also called *open-loop*) while the latter one is referred to as *Markovian controls* or *closed-loop controls in feedback form* (we use the two terms interchangeably in the sequel). We will sometimes consider *closed-loop controls*, which means controls that are adapted to the filtration generated by  $X$ . We shall see that different choices of  $\mathbb{A}$  might lead to different algorithm designs in Section 2.2.

**Definition 2.1** (Stochastic control problem). *An agent controls her state process  $X$  through an action process  $\alpha$  taking values respectively in  $\mathbb{R}^d$  and  $\mathcal{A}$ , where the dynamics of  $X$  are given by the stochastic differential equation (SDE),*

$$dX_t = b(t, X_t, \alpha_t) dt + \sigma(t, X_t, \alpha_t) dW_t, \quad X_0 = x_0. \quad (2.2)$$

The agent aims to minimize the expected cost

$$J(\alpha) : \alpha \mapsto \mathbb{E} \left[ \int_0^T f(t, X_t, \alpha_t) dt + g(X_T) \right], \quad (2.3)$$

over the set of admissible action processes, denoted by  $\mathbb{A}$  and to be discussed below.

We briefly describe how the above problem can be tackled by PDEs, or (F)BSDEs.

**PDE approach.** When considering Markovian controls, one can define the value function  $u : [0, T] \times \mathbb{R}^d \rightarrow \mathbb{R}$ ,

$$u(t, x) = \inf_{\alpha} \mathbb{E} \left[ \int_t^T f(s, X_s, \alpha_s) ds + g(X_T) | X_t = x \right],$$

and employ the dynamic programming principle (DPP) [209, Section 3]:  $u(T, x) = g(x)$  and for any stopping time  $\tau \in [t, T]$

$$u(t, x) = \inf_{\alpha} \mathbb{E} \left[ \int_t^{\tau} f(s, X_s, \alpha_s) ds + u(\tau, X_{\tau}) | X_t = x \right].$$

Then one can derive the Hamilton-Jacobi-Bellman (HJB) equation, which describes the evolution of the value function. Under suitable conditions,  $u$  solves

$$\begin{cases} \partial_t u(t, x) + \min_{\alpha \in \mathcal{A}} H(t, x, \nabla_x u(t, x), \text{Hess}_x u(t, x), \alpha) = 0, & (t, x) \in [0, T) \times \mathbb{R}^d \\ u(T, x) = g(x), & x \in \mathbb{R}^d \end{cases} \quad (2.4)$$

where the Hamiltonian  $H$  is defined as

$$H(t, x, p, q, \alpha) = b(t, x, \alpha) \cdot p + \frac{1}{2} \text{Tr}(\sigma(t, x, \alpha) \sigma(t, x, \alpha)^T q) + f(t, x, \alpha), \quad (2.5)$$

and  $\text{Hess}_x u(t, x)$  as the Hessian matrix of  $u$  with respect to  $x$ . If (2.4) has a classical solution, then the optimal control is given by

$$\hat{\alpha}(t, x) = \hat{\alpha}(t, x, \nabla_x u(t, x), \text{Hess}_x u(t, x)) = \arg \min_{\alpha \in \mathcal{A}} H(t, x, \nabla_x u(t, x), \text{Hess}_x u(t, x), \alpha).$$

**BSDE approach.** The connection between SC and BSDEs can be established in two different ways: by representing the value function or its derivative as the solution of a BSDE. When the volatility is uncontrolled, that is,  $\sigma(t, x, \alpha)$  is free of  $\alpha$ , then  $\hat{\alpha}$  does not depend on  $\text{Hess}_x u(t, x)$  and the PDE (2.4) becomes semi-linear

$$\begin{aligned} \partial_t u(t, x) + \frac{1}{2} \text{Tr}(\sigma(t, x) \sigma(t, x)^T \text{Hess}_x u(t, x)) + b(t, x, \hat{\alpha}(t, x, \nabla_x u(t, x))) \cdot \nabla_x u(t, x) \\ + f(t, x, \hat{\alpha}(t, x, \nabla_x u(t, x))) = 0. \end{aligned}$$

In this case, suppose that there exist functions  $\tilde{b}(t, x)$  and  $h(t, x, z)$  such that

$$\tilde{b}(t, x) \cdot \nabla_x u(t, x) + h(t, x, \sigma(t, x)^T \nabla_x u(t, x)) = b(t, x, \hat{\alpha}(t, x, \nabla_x u(t, x))) \cdot \nabla_x u(t, x) + f(t, x, \hat{\alpha}(t, x, \nabla_x u(t, x))).$$

Then the nonlinear Feynman-Kac formula [204] gives the following BSDE interpretation of  $u$ ,

$$\begin{cases} d\mathcal{X}_t = \tilde{b}(t, \mathcal{X}_t) dt + \sigma(t, \mathcal{X}_t) dW_t, & \mathcal{X}_0 \sim \mu_0, \\ d\mathcal{Y}_t = -h(t, \mathcal{X}_t, \mathcal{Z}_t) dt + \mathcal{Z}_t dW_t, & \mathcal{Y}_T = g(\mathcal{X}_T), \end{cases} \quad (2.6)$$

through the relations

$$\mathcal{Y}_t = u(t, \mathcal{X}_t), \quad \mathcal{Z}_t = \sigma(t, \mathcal{X}_t)^T \nabla_x u(t, \mathcal{X}_t).$$

If  $\mu_0 = \delta_{x_0}$  is concentrated on a single initial state  $x_0$ , then the optimal value is given by the value of the BSDE solution at time 0, *i.e.*,  $\inf_\alpha J(\alpha) = \mathcal{Y}_0$ . If  $\tilde{b}(t, x)$  is chosen to be identically zero, this equality can also be obtained by the comparison principle of BSDEs [47, Proposition 4.1].

In the controlled volatility case, the PDE (2.4) is fully nonlinear, and its solution is connected to a solution of the second order BSDE (2BSDE) [69]. If one chooses  $\tilde{b}(t, x)$  and  $\Sigma(t, x)$  such that  $h$  is determined by

$$H(t, x, p, q, \hat{\alpha}(t, x, p, q)) = \tilde{b}(t, x) \cdot p + h(t, x, p, q) + \frac{1}{2} \text{Tr}(\Sigma(t, x) \Sigma(t, x)^T q),$$

then the solution to the 2BSDE

$$\begin{cases} d\mathcal{X}_t = \tilde{b}(t, \mathcal{X}_t) dt + \Sigma(t, \mathcal{X}_t) dW_t, & \mathcal{X}_0 = x_0, \\ d\mathcal{Y}_t = -h(t, \mathcal{X}_t, \mathcal{Y}_t, \mathcal{Z}_t) dt + \mathcal{Z}_t^T \Sigma(t, \mathcal{X}_t) dW_t, & \mathcal{Y}_T = g(\mathcal{X}_T), \\ d\mathcal{Z}_t = \mathcal{A}_t dt + \Gamma_t \Sigma(t, \mathcal{X}_t) dW_t, & \mathcal{Z}_T = \nabla_x g(\mathcal{X}_T), \end{cases} \quad (2.7)$$

gives an interpretation of the solution to the PDE (2.4) through the relations

$$\mathcal{Y}_t = u(t, \mathcal{X}_t), \quad \mathcal{Z}_t = \nabla_x u(t, \mathcal{X}_t), \quad \Gamma_t = \text{Hess}_x u(t, \mathcal{X}_t), \quad \mathcal{A}_t = \mathfrak{L} \nabla_x u(t, \mathcal{X}_t),$$

where  $\mathfrak{L}$  denotes the infinitesimal generator of  $\mathcal{X}$ .

**FBSDE approach.** The Pontryagin stochastic maximum principle provides the connection to the FBSDE, where the forward equation is coupled with the backward equation. Define the generalized Hamiltonian  $\mathcal{H}$  by

$$\mathcal{H}(t, x, y, z, \alpha) = b(t, x, \alpha)y + \text{Tr}(\sigma^T(t, x, \alpha)z) + f(t, x, \alpha).$$

If the Hamiltonian  $\mathcal{H}$  is convex in  $(x, \alpha)$ , and  $(X_t, Y_t, Z_t)$  solves

$$\begin{cases} dX_t = b(t, X_t, \hat{\alpha}_t) dt + \sigma(t, X_t, \hat{\alpha}_t) dW_t, & X_0 = x_0, \\ dY_t = -\nabla_x \mathcal{H}(t, X_t, Y_t, Z_t, \hat{\alpha}_t) dt + Z_t dW_t, & Y_T = \partial_x g(X_T), \\ \hat{\alpha}_t = \inf_\alpha \mathcal{H}(t, X_t, Y_t, Z_t, \alpha), \end{cases}$$

then  $\hat{\alpha}$  is the optimal control. If the value function is smooth enough, then

$$Y_t = \nabla_x u(t, X_t), \quad Z_t = \sigma(t, X_t, \hat{\alpha}_t)^T \text{Hess}_x u(t, X_t).$$

For machine learning algorithms introduced in the following sections, if a temporal discretization is needed, we shall consider, for simplicity, a uniform grid  $\pi$  on the interval  $[0, T]$ , *i.e.*, a partition  $0 = t_0 < t_1 \dots < t_{N_T} = T$ , with  $t_n - t_{n-1} = \Delta t = T/N_T$ .

## 2.2 Direct parameterization

We refer to the first class of algorithms as direct parameterization methods, which directly replace the control function by a neural network with appropriate inputs. Such ideas can be traced back to earlier works such as *e.g.* [214, 143, 182, 97], in which neural networks are used for control and optimal control problems in relatively low dimension and with shallow networks.

### 2.2.1 Global and local in time approaches

There are two types of direct parameterization methods, depending on how the neural networks get trained.

**Global in time approach.** We start with the method which trains the neural networks used for the control using the whole time horizon at once. More recently, Han and E [121] were the first to generalize this type of methods to solve problems in high dimensions by using recent modern machine learning techniques such as deep neural networks and efficient built-in stochastic gradient descent solvers. This has motivated fruitful studies on high-dimensional control problems. In particular, the algorithms reviewed below in

Sections 2.2.2 and 2.2.3 for SC problems with delay and mean field control are both in the spirit of [121]. More precisely, [121] solved the following discrete time version of (2.2)–(2.3),

$$\begin{aligned}\check{X}_{t_{n+1}} &= \check{X}_{t_n} + b(t_n, \check{X}_{t_n}, \alpha_{t_n})\Delta t + \sigma(t_n, \check{X}_{t_n}, \alpha_{t_n})\Delta \check{W}_{t_n}, \\ &\min_{(\alpha_{t_n})_n} \mathbb{E} \left[ \sum_{n=0}^{N_T-1} f(t_n, \check{X}_{t_n}, \alpha_{t_n})\Delta t + g(\check{X}_T) \right],\end{aligned}\quad (2.8)$$

where  $\Delta \check{W}_{t_n} = \check{W}_{t_{n+1}} - \check{W}_{t_n}$  are i.i.d random variables with distribution  $\mathcal{N}(0, \Delta t)$ . Focusing on Markovian controls, they approximate at each time step the control  $\alpha_{t_n}$  in (2.8) by a feedforward neural network  $\alpha_{t_n}(\cdot; \theta_n)$  taking inputs  $\check{X}_{t_n}$ , where  $\theta_n$  denotes all NN's parameters at time  $t_n$ . We thus obtain the following cost, which is interpreted as a loss that can be minimized by SGD:

$$\check{J}(\theta) = \mathbb{E} \left[ \sum_{n=0}^{N_T-1} f(t_n, \check{X}_{t_n}^\theta, \alpha_{t_n}(\check{X}_{t_n}^\theta; \theta_n))\Delta t + g(\check{X}_T^\theta) \right], \quad \theta = (\theta_n)_{n=0}^{N_T}, \quad (2.9)$$

where  $(\check{X}_{t_n}^\theta)_{n=1}^{N_T}$  follows

$$\check{X}_{t_{n+1}}^\theta = \check{X}_{t_n}^\theta + b(t_n, \check{X}_{t_n}^\theta, \alpha_{t_n}(\check{X}_{t_n}^\theta; \theta_n))\Delta t + \sigma(t_n, \check{X}_{t_n}^\theta, \alpha_{t_n}(\check{X}_{t_n}^\theta; \theta_n))\Delta \check{W}_{t_n}. \quad (2.10)$$

In practice, the expected value in (2.9) is approximated by the following quantity based on Monte Carlo simulations:

$$L(\theta, S) = \frac{1}{N} \sum_{j=1}^N \left[ \sum_{n=0}^{N_T-1} f(t_n, \check{X}_{t_n}^{j,\theta}, \alpha_{t_n}(\check{X}_{t_n}^{j,\theta}; \theta_n))\Delta t + g(\check{X}_T^{j,\theta}) \right],$$

where  $\{(\check{X}_{t_n}^{j,\theta})_{n=1}^{N_T}\}_{j=1,\dots,N}$  are sample paths of  $(\check{X}_{t_n}^\theta)_{n=1}^{N_T}$  in (2.10) using i.i.d. samples of  $(\Delta \check{W}_{t_n})_{n=1}^{N_T}$ .

Constraints on the states and the controls can be taken into account by adding penalty terms in the loss function as in *e.g.* [121].

**Remark 2.2.** *Alternatively, one can use a single neural network  $(t, x) \mapsto \alpha(t, x; \theta)$  and evaluate it at  $(t, x) = (t_n, \check{X}_{t_n})$ ,  $n = 0, \dots, N_T - 1$ . In this case, the network can directly capture the time continuity in the control process (if it is continuous). Furthermore, it can be trained for various grids of points in time, and after training it can be used for arbitrary time points.*

**Local in time approach.** The second approach has been proposed by Bachouch, Huré, Langrené and Pham in [17]. It combines classical dynamic programming (DP) and deep neural networks for approximating the control and possibly the value function. There are two main versions. The first version, called NNContPI, is designed as follows. Assuming that the optimal controls at time steps  $t_{n+1}, \dots, t_{N_T-1}$  are already learnt with neural network parameters  $\hat{\theta}_{n+1}, \dots, \hat{\theta}_{N_T-1}$ , the optimal control at time  $t_n$  is approximated by a neural network  $\alpha_{t_n}(\cdot; \hat{\theta}_n)$  where the optimized parameters are determined by

$$\hat{\theta}_n \in \arg \min_{\theta} \mathbb{E} \left[ f(t_n, \check{X}_{t_n}^\theta, \alpha_{t_n}(\check{X}_{t_n}^\theta; \theta))\Delta t + \sum_{n'=n+1}^{N_T-1} f(t_{n'}, \check{X}_{t_{n'}}^\theta, \alpha_{t_{n'}}(\check{X}_{t_{n'}}^\theta; \hat{\theta}_{n'}))\Delta t + g(\check{X}_T^\theta) \right], \quad (2.11)$$

where  $(\check{X}_{t_n}^\theta)_{n'=n+1}^{N_T}$  follows (2.10) with  $\alpha_{t_n}(\cdot; \theta), \alpha_{t_{n+1}}(\cdot; \hat{\theta}_{n+1}), \dots, \alpha_{t_{N_T-1}}(\cdot; \hat{\theta}_{N_T-1})$  being used. Then, as always, the expected value is approximated by sample paths of  $\check{X}^{j,\theta}$ , and the optimal  $\hat{\theta}_n$  is obtained by SGD as described in Appendix A. The second version, termed as Hybrid-now, further approximates the value function (*i.e.*, the cost-to-go) at time  $t_{n+1}$  using a deep neural network to avoid repeated computation of the last two terms in (2.11). More precisely, given the learnt approximated value function  $V_{t_{n+1}}(\cdot; \hat{\theta}_{n+1})$  at time  $t_{n+1}$ , the optimal policy at time  $t_n$  is determined in a manner that is similar to the NNContPI algorithm

$$\hat{\theta}_n \in \arg \min_{\theta} \mathbb{E} [f(t_n, \check{X}_{t_n}^\theta, \alpha_{t_n}(\check{X}_{t_n}^\theta; \theta))\Delta t + V_{t_{n+1}}(\check{X}_{t_{n+1}}^\theta; \hat{\theta}_{n+1})],$$

and the value function  $V_{t_n}$  at time  $t_n$  is then approximated by another neural network  $V_{t_n}(\cdot; \tilde{\theta}_n)$  whose parameters are determined by

$$\tilde{\theta}_n \in \arg \min_{\theta} \mathbb{E} \left[ |f(t_n, \check{X}_{t_n}^\theta, \alpha_{t_n}(\check{X}_{t_n}^\theta; \hat{\theta}_n))\Delta t + V_{t_{n+1}}(\check{X}_{t_{n+1}}^\theta; \tilde{\theta}_{n+1}) - V_{t_n}(\check{X}_{t_n}^\theta; \theta)|^2 \right].$$

**Remark 2.3.** The first approach discussed above (global in time, developed by [121]) learns all the optimal controls  $\alpha_{t_n}(\cdot; \hat{\theta}_n)$ ,  $n = 0, \dots, N_T - 1$  at once, by performing a unique SGD with a loss function that involves the whole time horizon, while the second approach [17] learns  $\alpha_{t_n}$  sequentially and backwardly, for  $n = N_T - 1, N_T - 2, \dots, 0$ . Though the first work may be efficient since NNs for optimal controls at each time are designed in practice to share parameters and they are getting trained at the same time, it may encounter vanishing or exploding gradient problem for large  $N_T$  as remarked in [17].

**Remark 2.4.** It is common to use the same architecture for the neural networks  $\alpha_{t_n}$  of all the time steps. Even with the same architecture, the parameters can be different, which yields different functions for different time steps.

**Remark 2.5** (Theoretical analysis). In [144], the authors provided the consistency and rates of convergence for the control and the value function subject to universal approximation error of the neural networks.

### 2.2.2 Stochastic control with delay

In direct parameterization approaches as discussed above, the neural network is used to approximate the optimal control or the value function. The type of inputs depends on the class of controls considered in the optimal control problem. For Markovian controls, which are used in [121] and [17], the input shall be  $\check{X}_{t_n}$  for  $\alpha_{t_n}(\cdot; \theta_n)$ . For open-loop controls, one can naturally consider  $(\check{W}_{t_0}, \dots, \check{W}_{t_n})$ , while for closed-loop controls, one can use  $(\check{X}_{t_0}, \dots, \check{X}_{t_n})$  as inputs of the neural network. However the sequence length increases with the number of time steps, which leads to a high computational cost. Furthermore, passing the whole sequence as a single input does not make use of the time structure. For these reasons, other architectures have been considered.

We now illustrate the direct parameterization methods by studying SC problems with delay. Such problems have found many applications, *e.g.*, modeling systems with the aftereffect in mechanics and engineering, biology, and medicine [163, Chapter 1], time-to-build problems in economics [166, 14], modeling the ‘‘carryover’’ or ‘‘distributed lag’’ advertising effect in marketing [102, 103], and portfolio selection under the market with memory and delayed responses in finance [203, 87, 85, 184].

Note that feedforward neural network (FNN) architecture is the most common architecture in deep learning and performs well as function approximators of Markovian controls. Another popular type of neural networks is recurrent neural networks (RNNs). In a study by Han and Hu [123], it is shown that RNNs have better performance in control problems with a delay effect.

To distinguish between the value of a process at a given time and the portion of trajectory ending at time  $t$  with  $\delta$  history, for any process  $P$ , we denote by  $\underline{P}_t = (\underline{P}_t(s))_{s \in [-\delta, 0]}$  the trajectory of  $P$  from time  $t - \delta$  to  $t$ , *i.e.*,  $\underline{P}_t(s) = P_{t+s}$ , for  $-\delta \leq s \leq 0$ . Specifically, we consider a SC problem in which the state process  $X$  is characterized by a stochastic delay differential equation (SDDE),

$$\begin{cases} dX_t = b(t, \underline{X}_t, \alpha_t) dt + \sigma(t, \underline{X}_t, \alpha_t) dW_t, & t \in [0, T], \\ X_t = \varphi_t, & t \in [-\delta, 0], \end{cases} \quad (2.12)$$

and the objective function is given by

$$J(\alpha) = \mathbb{E} \left[ \int_0^T f(t, \underline{X}_t, \alpha_t) dt + g(\underline{X}_T) \right]. \quad (2.13)$$

Here  $\delta \geq 0$  is the fixed delay, and  $(\varphi_t)_{t \in [-\delta, 0]}$  is a given process on  $[-\delta, 0]$  for the initial condition of  $X$ , and  $X_t$  denotes the value of the state process at time  $t$  as usual. The SDDE (2.12) has been well studied in the literature [197, 198] (see also Appendix B some preliminaries on SDDEs).

The key difficulty is that, when optimizing over closed-loop controls, one should in principle take into account the whole trajectory of the state, which is computationally costly. The authors in [123] analyzed this problem with a focus on the deep neural networks’ (DNNs) architecture design in order to handle the high-dimensionality arising from the delay. Without loss of generality, let us consider that the fixed delay  $\delta < \infty$  covers  $N_\delta$  subintervals, *i.e.*,  $\delta = N_\delta \Delta t$ , the partition on  $[0, T]$  is extended to  $[-\delta, 0]$ ,

$$-\delta = t_{-N_\delta} \leq t_{-N_\delta+1} \leq \dots \leq t_0 = 0, \text{ with } t_{n+1} - t_n \equiv \Delta t, \forall n = -N_\delta, \dots, -1.$$

and the discretized version of (2.12)–(2.13) becomes

$$\begin{aligned}\check{X}_{t_{n+1}} &= \check{X}_{t_n} + b(t_n, \underline{\check{X}}_{t_n}, \alpha_{t_n})\Delta t + \sigma(t_n, \underline{\check{X}}_{t_n}, \alpha_{t_n})\Delta \check{W}_{t_n}, \\ &\quad \inf_{\{\alpha_{t_n}\}_{n=0}^{N_T-1}} \mathbb{E} \left[ \sum_{n=0}^{N_T-1} f(t_n, \underline{\check{X}}_{t_n}, \alpha_{t_n})\Delta t + g(\underline{\check{X}}_T) \right],\end{aligned}\tag{2.14}$$

where for each  $n$ ,  $\underline{\check{X}}_{t_n}$  represents the discrete path with  $N_\delta$  lags and  $\Delta \check{W}_{t_n}$  is the increment in Brownian motions,

$$\underline{\check{X}}_{t_n} = (\check{X}_{t_{n-N_\delta}}, \dots, \check{X}_{t_n}), \quad \Delta \check{W}_{t_n} = \check{W}_{t_{n+1}} - \check{W}_{t_n}.$$

Here  $\alpha_{t_n}$  is a function of time and the past state trajectory  $\underline{\check{X}}_{t_n}$  taking values in  $\mathbb{R}^k$ . The next two architectures are proposed for approximating  $\alpha_{t_n}$ .

**Feedforward architecture.** Motivated by the path-dependent structure of the considered problems (the change of current state only depends on the history up to lag  $\delta$ ), a natural idea is to approximate  $\alpha_{t_n}$  by a feedforward neural network taking the state history up to lag  $\bar{\delta}$  as the input. Note here it could be  $\bar{\delta} \neq \delta$  since one may not know the underlying true  $\delta$  a priori. Without loss of generality, one can assume  $\bar{\delta} = N_\delta h$  ( $N_\delta \in \mathbb{N}^+$ ) and define  $\bar{X}_{t_n} \equiv (\check{X}_{t_{n-N_\delta}}, \dots, \check{X}_{t_n}) \in \mathbb{R}^{d \times (N_\delta+1)}$ . Then the control at time  $t_n$  can be approximated by a feedforward fully connected network taking  $\bar{X}_{t_n}$  as input.

**Recurrent architecture.** Alternatively, the sequence  $\bar{X}_{t_n}$  can be processed by a recurrent neural network (RNN), such as a long-short term memory (LSTM) neural network. The basic principle of an RNN is that the elements of the sequence are processed one by one by applying the same neural network in a recurrent manner, and some information is saved between two applications until the output is calculated. Here, we can use a single RNN for all time steps. At time  $t_n$ , to produce the value of the control, it uses  $\bar{X}_{t_n}$  as an input, along with the information saved from the previous time step. We refer to Appendix A.1.2 and Appendix A.1.3 for more details.

**Remark 2.6.** *Although for both feedforward neural networks and RNN, the input dimensions remains constant as  $k$  changes, using the former requires prior knowledge of  $\delta$ . For the feedforward fully connected neural network, one feeds the discretized state values (2.14) of length  $N_\delta + 1$ , so to obtain the best performance, one needs to get a good estimate  $\bar{\delta}$  of  $\delta$  first. On the other hand, for the RNN, one only needs to provide the current state value  $X_{t_n}$ . Notice that in an LSTM all input information up to time  $t_n$  is summarized by the  $n^{\text{th}}$  cell, but if the optimal control depends only on the past up to  $\delta$ , the forget gates allows to drop out the unneeded information. The exact way information should be dropped is determined by the neural network parameters training. Though the authors in [123] only experimented LSTM, other variations of RNNs such as gated recurrent units (GRUs) [70] or peephole LSTM [96] can be considered.*

Before illustrating the above method, we stress that other methods also exist. For example, [181] uses a deep learning technique inspired by the physics-informed neural networks (PINNs) and applies it to solve a mean-variance portfolio selection with execution delay.

#### Numerical illustration: a linear-quadratic regulator problem with delay.

LQ problems with delay was first investigated by Kolmanovskii and Shaikhet [163]. In the version presented here, the aim is to minimize

$$\begin{aligned}\mathbb{E}_\varphi \left[ \int_0^T (X_t + e^{\lambda\delta} A_3 Y_t)^T Q(t) (X_t + e^{\lambda\delta} A_3 Y_t) + \alpha_t^T R(t) \alpha_t dt + (X_T + e^{\lambda\delta} A_3 Y_T)^T G (X_T + e^{\lambda\delta} A_3 Y_T) \right], \\ \text{subject to } dX_t = (A_1(t)X_t + A_2(t)Y_t + A_3Z_t + B(t)\alpha_t) dt + \sigma(t) dW_t, \quad t \in [0, T],\end{aligned}\tag{2.15}$$

where  $X_0 = \varphi \in L^2(\Omega, C([- \delta, 0], \mathbb{R}^d))$  is a given initial segment,  $Y_t = \int_{-\delta}^0 e^{\lambda s} X_{t+s} ds$  is the distributed delay and  $Z_t = X_{t-\delta}$  is the discrete delay,  $A_1, A_2, Q \in L^\infty([0, T]; \mathbb{R}^{d \times d})$ ,  $B \in L^\infty([0, T]; \mathbb{R}^{d \times k})$ ,  $R \in$

$L^\infty([0, T]; \mathbb{R}^{k \times k})$  are deterministic matrix-valued functions,  $\sigma \in L^2([0, T]; \mathbb{R}^{d \times m})$  is a deterministic matrix-valued function,  $A_3, G \in \mathbb{R}^{d \times d}$  are deterministic matrices. It is assumed that  $Q(t), G$  are positive semi-definite and  $R(t)$  is positive definite for all  $t \in [0, T]$  and continuous on  $[0, T]$ . To have a tractable solution, a further relation is prescribed,

$$A_2(t) = e^{\lambda\delta}(\lambda I_d + A_1(t) + e^{\lambda\delta}A_3)A_3, \quad (2.16)$$

where  $I_d$  is the identity matrix with rank  $d$ . This example was studied in [19, Section 4], and the main results are also summarized in [123].

We present below results for a ten-dimensional example. The model parameters are chosen as follows. The dimensions are  $d = k = m = 10$ , and  $\lambda = 0.1$ . In (2.15),  $A_1, A_3, B, \sigma$  are constant coefficient matrices (generated randomly),  $Q, R, G$  are constant matrices proportional to identity matrices, and  $A_2$  is determined by (2.16). For implementation details, we refer to [123]. The left panel of Figure 3 displays the total cost on the validation data against training time. The values are averaged every 200 steps. The feedforward model takes the state history as inputs up to lag  $\bar{\delta} = \delta$  with  $N_{\bar{\delta}} = 40$ . The right panel of Figure 3 displays the optimized cost as a function of the processed lag time  $\bar{\delta}$  from 0.2 to 1 with step size 0.1, while the actual lag  $\delta = 1$ . If the chosen lag time  $\bar{\delta}$  is smaller than the actual lag  $\delta$  time, there is a loss of information when the feedforward network processes the data. As expected, we observe that the cost increases as the lag time processed by the feedforward model decreases. A higher optimized cost indicates that the model can only find a strictly sub-optimal strategy due to the lack of information. Figure 4 displays one sample path (first five dimensions only) of the optimal state  $X$  and control  $\alpha$  provided by two neural networks in comparison with the analytical solution, in which the LSTM architecture presents a better agreement. The lag time  $\bar{\delta}$  processed by the feedforward model is chosen to be the same as  $\delta$ . One main drawback of the feedforward model is that it requires to know the true lag time  $\delta$  a priori to determine the network's size.

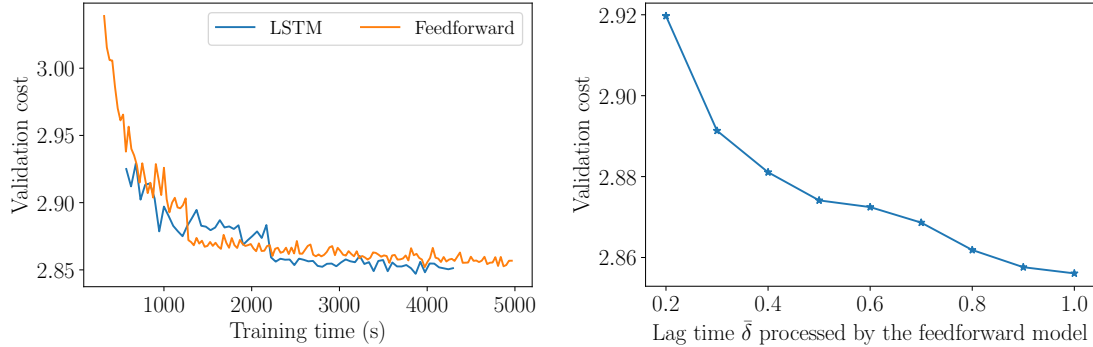


Figure 3: The linear-quadratic regulator problem with delay in Section 2.2.2. Left: Training curve of two models in the example of linear-quadratic problem. Right: The effect of lag time  $\bar{\delta}$  processed by the feedforward model in the example of linear-quadratic problem. The lag time  $\delta$  in the actual system is 1.

### 2.2.3 Mean-field type control

We now discuss how direct parameterization methods can be adapted for mean field control (MFC) problems, which are an extension of standard optimal control in which there are mean field interactions. MFC can be interpreted as a social optimum but also has applications in risk, *e.g.*, heating or electric loads management [158, 192], risk management in finance [11] or optimal control with a cost involving a conditional expectation [6, 202], to cite just a few examples. We refer to [28] for more background on MFC.

As before, let  $\mathcal{A} \subset \mathbb{R}^k$  denote the set of admissible actions and let  $\mathbb{A}$  be the set of so-called admissible controls. We denote by  $\mathcal{P}_2(\mathbb{R}^d)$  the set of probability measures on  $\mathbb{R}^d$  which admit a second moment. Let  $b, \sigma, f, g$  be Borel-measurable functions,

$$(b, \sigma, f) : [0, T] \times \mathbb{R}^d \times \mathcal{P}_2(\mathbb{R}^d) \times \mathcal{A} \rightarrow (\mathbb{R}^d, \mathbb{R}^{d \times m}, \mathbb{R}), \quad g : \mathcal{P}_2(\mathbb{R}^d) \times \mathbb{R}^d \rightarrow \mathbb{R}.$$

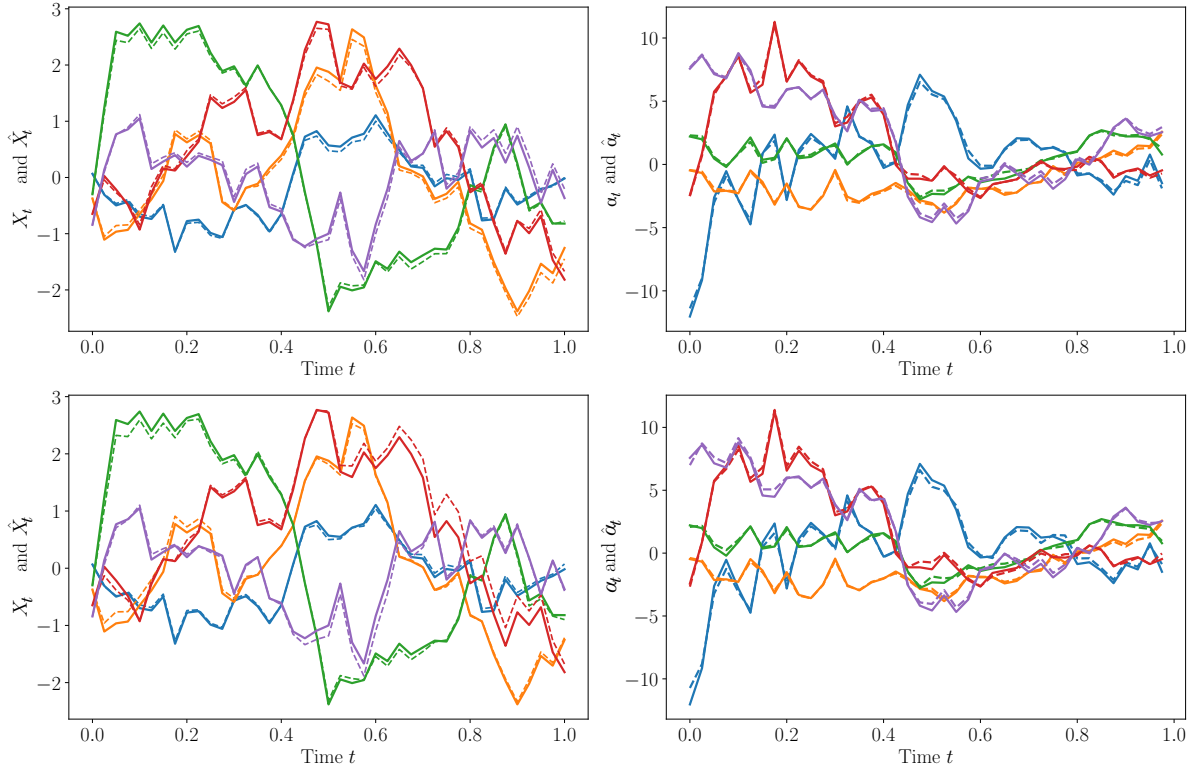


Figure 4: The linear-quadratic regulator problem with delay in Section 2.2.2. A sample path of the first 5 dimensions of the state  $X_t$  and control  $\alpha_t$  obtained from the LSTM (top) model and FNN (top) model. Left: the optimal state process discretized from the analytical solution  $(X_t)_i$  (solid lines) and its approximation  $(\hat{X}_t)_i$  (dashed lines) provided by the approximating control, under the same realized path of Brownian motion. Right: comparisons of the optimal control  $(\alpha_t)_i$  (solid lines) and  $(\hat{\alpha}_t)_i$  (dashed lines).

Compared with standard optimal control, see (2.1), the functions take as an extra input the population distribution.

**Definition 2.7** (MFC optimum). *A feedback control  $\alpha^* \in \mathbb{A}$  is an optimal control for the MFC problem for a given initial distribution  $\mu_0 \in \mathcal{P}_2(\mathbb{R}^d)$  if it minimizes*

$$J(\alpha) : \alpha \mapsto \mathbb{E} \left[ \int_0^T f(t, X_t, \mu_t, \alpha_t) dt + g(X_T, \mu_T) \right],$$

where  $\mu_t$  is the probability distribution of the law of  $X_t$ , under the constraint that the process  $X = (X_t)_{t \geq 0}$  solves the stochastic differential equation of the McKean-Vlasov (MKV) type,

$$dX_t = b(t, X_t, \mu_t, \alpha_t) dt + \sigma(t, X_t, \mu_t, \alpha_t) dW_t, \quad t \geq 0, \quad (2.17)$$

with  $X_0$  having distribution  $\mu_0$ .

Existence and uniqueness results have been studied in the literature and we refer the interested reader to *e.g.* [53] and in particular the assumption ‘‘Control of MKV Dynamics’’ on page 555. Furthermore, under mild conditions there is an optimal control that is Markovian, so it is sufficient to focus on controls that are functions of time and the individual state. The framework can also encompass problems in which the interactions are through the joint distribution of state and actions and not just the distribution of states. Such problems are sometimes referred to as extended MFC problems. Although the numerical method discussed below can be adapted in a rather straightforward way (as illustrated below in an example below), the theoretical framework is more challenging.

To solve the MFC problem using deep learning, one can for example follow the lines of the global approach described in Section 2.2.1 to discretize time and to replace the control by a sequence of neural networks functions of the state. However, in contrast with standard OC problems, here, the costs and the dynamics can depend on mean field terms, so we also need to approximate the distribution of the state. To this end, The simplest approach is to use the empirical distribution of a population of particles.

Following this approach, the original MFC problem is approximated by the following problem: minimize over the neural network parameters  $\theta = (\theta_n)_{n=0, \dots, N_T-1}$

$$\check{J}^N(\theta) : \theta \mapsto \frac{1}{N} \sum_{i=1}^N \mathbb{E} \left[ \sum_{n=0}^{N_T-1} f(t_n, \check{X}_{t_n}^{i,\theta}, \check{\mu}_{t_n}^{N,\theta}, \alpha_{t_n}(\check{X}_{t_n}^{i,\theta}; \theta_n)) \Delta t + g(\check{X}_T^{i,\theta}, \check{\mu}_T^{N,\theta}) \right],$$

subject to

$$\check{X}_{t_{n+1}}^{i,\theta} = \check{X}_{t_n}^{i,\theta} + b(t_n, \check{X}_{t_n}^{i,\theta}, \check{\mu}_{t_n}^{N,\theta}, \alpha_{t_n}(\check{X}_{t_n}^{i,\theta}; \theta_n)) \Delta t + \sigma(t_n, \check{X}_{t_n}^{i,\theta}, \check{\mu}_{t_n}^{N,\theta}, \alpha_{t_n}(\check{X}_{t_n}^{i,\theta}; \theta_n)) \Delta \check{W}_n^i, \quad n = 0, \dots, N_T-1,$$

where the initial positions  $(\check{X}_0^{i,\theta})_{i=1, \dots, N}$  are i.i.d. with distribution  $\mu_0$ , the empirical distribution is denoted by

$$\check{\mu}_{t_n}^{N,\theta} = \frac{1}{N} \sum_{j=1}^N \delta_{\check{X}_{t_n}^{j,\theta}},$$

and  $(\Delta \check{W}_n^i)_{i=1, \dots, N, n=0, \dots, N_T-1}$  denotes i.i.d. random variables with Gaussian distribution  $\mathcal{N}(0, \Delta t)$ . Note that this problem is not equivalent to solving an  $N$ -agent optimal control problem since, in the latter case, the control would in general need to be a function of all the agents' states while here we consider only distributed controls, functions of each agent's state. Intuitively, this approximation is justified by propagation of chaos results [230]: as  $N \rightarrow +\infty$  the particles become independent and the empirical distribution converges to the distribution of the MKV SDE (2.17). See [167] in the context of MFC problems.

This technique was proposed in [56] (with a single neural network function of time and space instead of a sequence of neural networks functions of space online). Although we focus here on a basic setting for which a simple feedforward fully connected architecture performs well, other architectures may yield better results for problems with more complex time dependencies; see *e.g.*, [90, 100] for applications with RNNs. See also [94, 7] and the survey [57] for more details.

**Remark 2.8** (Theoretical analysis). *In [56] Carmona and Laurière provided a proof of convergence of the discrete problem to the original MFC problem in the following sense: under suitable assumptions, the difference between the optimal value of this problem  $\inf_{\theta} \check{J}^N(\theta)$  and the optimal value of the original problem  $\inf_{\alpha} J(\alpha)$  goes to 0 as  $N_T, N$  and the number of parameters in the neural network go to infinity.*

From here, one can use SGD or one of its variants to optimize  $\check{J}^N$  over the parameters. In contrast with the methods discussed previously for standard OC, here one sample corresponds to one population with  $N$  particles. In this context, one sample corresponds to  $\xi = (\check{X}_0^i, (\Delta \check{W}_n^i)_{n=0, \dots, N_T-1})_{i=1, \dots, N}$ , from which we can compute the  $N$  (interacting) trajectories and the total empirical cost:

$$\check{J}^{\xi, N}(\theta) = \frac{1}{N} \sum_{i=1}^N \left[ \sum_{n=0}^{N_T-1} f(\check{X}_{t_n}^{i,\theta,\xi}, \check{\mu}_{t_n}^{N,\theta,\xi}, \alpha_{t_n}(\check{X}_{t_n}^{i,\theta,\xi}; \theta_n)) \Delta t + g(\check{X}_T^{i,\theta,\xi}, \check{\mu}_T^{N,\theta,\xi}) \right].$$

From here, Algorithm 1 in Appendix A.2 can be applied.

### Numerical illustration: a mean-field price impact problem.

We now illustrate the method with a financial application on a problem of optimal execution. The model describes a large group of traders interacting through the price of an asset. The large group of traders has a non-negligible influence on the price, which is referred to price impact. For example when the traders decide to buy at the same moment, the price is driven up, and vice versa when the traders decide to sell simultaneously.

The  $N$ -agent problem was originally solved as a mean-field game (MFG) by Carmona and Lacker in the weak formulation ([54]), and revisited in the book of Carmona and Delarue [52, Sections 1.3.2 and 4.7.1] in the strong formulation. Here, we focus on the mean-field setting. In this model, the inventory representative trader is denoted by  $X_t$ . The control of the trader is denoted by  $\alpha_t$  and corresponds to the trading rate. The dynamics of the inventory are given by

$$dX_t = \alpha_t dt + \sigma dW_t,$$

where  $W$  is a standard Brownian motion, and the cost can be rewritten in terms of  $X$  only as

$$J(\alpha) = \mathbb{E} \left[ \int_0^T \left( c_\alpha(\alpha_t) + c_X(X_t) - \gamma X_t \int_{\mathbb{R}} a d\nu_t^\alpha(a) \right) dt + g(X_T) \right].$$

Following the Almgren-Chriss linear price impact model, we assume that the functions  $c_X$ ,  $c_\alpha$  and  $g$  are quadratic. Thus, the cost is of the form

$$J(\alpha) = \mathbb{E} \left[ \int_0^T \left( \frac{c_\alpha}{2} \alpha_t^2 + \frac{c_X}{2} X_t^2 - \gamma X_t \int_{\mathbb{R}} a d\nu_t^\alpha(a) \right) dt + \frac{c_g}{2} X_T^2 \right]. \quad (2.18)$$

This model has a semi-explicit solution obtained by reducing the problem to a system of ordinary differential equations (ODEs) as explained in [52, Sections 1.3.2 and 4.7.1].

The deep learning method described above can readily be adapted to solve MFC with interactions through the control's distribution by computing the empirical distribution of controls for an interacting system of  $N$  particles. Figure 5 shows the control and the distribution at various time steps. Here we plot the values of the control represented by the neural network evaluated at samples generated by following the  $N$ -interacting particle system. We see that the shape is approximately linear at every time steps, and furthermore that it coincides with the lines corresponding to the theoretical optimal solution. The distribution, represented by histograms computed using the  $N$  particles, starts on the right and moves towards 0, which can be interpreted as the fact that the traders liquidate their portfolios. We used the parameters:  $T = 1$ ,  $c_X = 2$ ,  $c_\alpha = 1$ ,  $c_g = 0.3$ ,  $\sigma = 0.5$  and  $\gamma = 0.2$ . When using a larger value of  $\gamma$ , the collective influence of the traders on the price is higher. As can be seen in Figure 6 obtained with  $\gamma = 1$ , the traders do not liquidate all the time from  $t = 0$  until time  $t = T$ . Instead, they liquidate their portfolio at the beginning and then start buying. We can explain this behavior as follows: since this is a cooperative problem, the traders can use the price impact to drive the price up to increase the value of the stock they own, thus increasing their final reward.

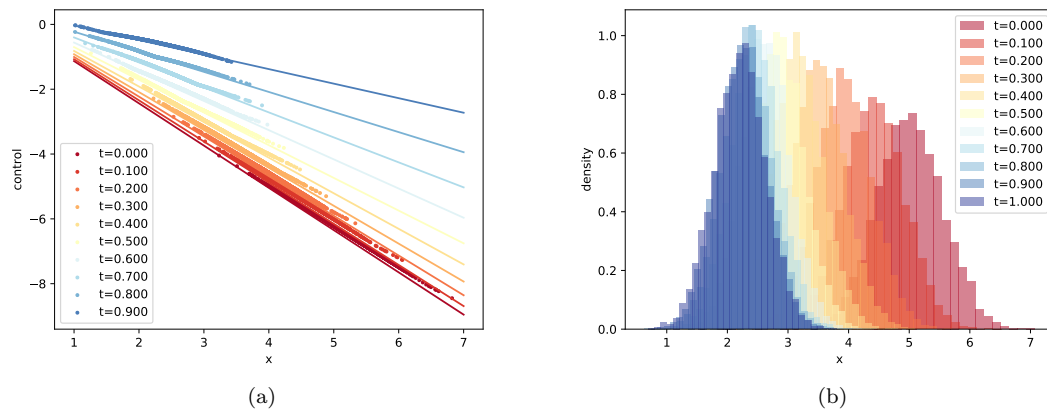


Figure 5: Price impact MFC example in Section 2.2.3 solved by direct method. Left: Control learnt (dots) and exact solution (lines). Right: associated empirical state distribution. Here we take  $\gamma = 0.2$  in (2.18).

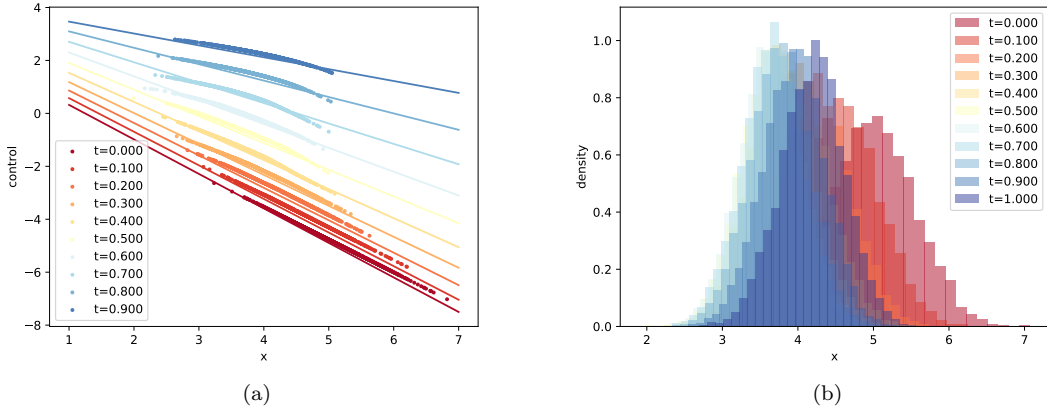


Figure 6: Price impact MFC example in Section 2.2.3 solved by direct method. Left: Control learnt (dots) and exact solution (lines). Right: associated empirical state distribution. Here we take  $\gamma = 1$  in (2.18).

### 2.3 BSDE-based deep learning algorithms

We now turn our attention to an alternative deep learning methods for control problems (2.2)–(2.3), which are based on solving the associated backward stochastic differential equations (BSDEs) (*cf.* (2.6) and (2.7)). To simplify the presentation, we explain the algorithms on a generic BSDE,

$$dY_t = -F(t, X_t, Y_t, Z_t) dt + Z_t^T dW_t, \quad t \in [0, T], \quad Y_T = G(X_T), \quad (2.19)$$

where  $X$  solves the (possibly) coupled forward equation

$$dX_t = B(t, X_t, Y_t, Z_t) dt + \sigma(t, X_t) dW_t, \quad t \in [0, T], \quad X_0 \sim \mu_0. \quad (2.20)$$

As mentioned in Section 2.1, the connection between optimal control and BSDEs (or FBSDEs) can be established in several ways.

#### 2.3.1 Deep backward stochastic differential equation (Deep BSDE) method

The Deep BSDE method was proposed by E, Han and Jentzen in [82, 124], which, to the best of our knowledge, were the first works to use deep learning to solve BSDEs in high dimension and has inspired many followup works. This method relies on a stochastic version of a shooting method that is extensively used to solve ODEs. The strategy has been successfully applied to problems in economic contract theory where it is sometimes referred to as Sannikov's trick; see for example [162, 73, 72]. The idea is to try to guess the initial value  $Y_0$  and the  $(Z_t)_{t \in [0, T]}$  process so as to meet the terminal condition  $Y_T = g(X_T)$ . It has originally been proposed in [82] for decoupled FBSDE systems, and then extended to fully coupled FBSDEs; see *e.g.* [125, 150].

To be precise, solving the system (2.19)–(2.20) is reduced to identifying  $(Y_0, (Z_t)_{t \in [0, T]})$  in (2.19) which is characterized as the solution to the following control problem, *i.e.*, to minimize the cost over  $(y_0, z)$

$$J(y_0, z) = \mathbb{E} [\|Y_T - g(X_T)\|^2],$$

subject to:

$$\begin{cases} dX_t = B(t, X_t, Y_t, z(t, X_t)) dt + \sigma(t, X_t) dW_t, & t \in [0, T], \\ dY_t = -F(t, X_t, Y_t, z(t, X_t)) dt + z(t, X_t)^T dW_t, & t \in [0, T], \\ X_0 \sim \mu_0, \quad Y_0 = y_0(X_0). \end{cases}$$

Then, as in the methods presented above (see Section 2.2), the control functions  $y_0$  and  $z$  are replaced by deep neural networks, say  $y_0(\cdot; \theta^Y)$  and  $z(\cdot; \theta^Z)$  with parameters  $\theta^Y$  and  $\theta^Z$ , respectively. Furthermore,

time is discretized using a uniform grid  $t_0 < t_1 \dots < t_{N_T} = T$ ,  $t_n - t_{n-1} = \Delta t = T/N_T$ . Then the problem becomes to minimize over  $\theta = (\theta^Y, \theta^Z)$  the cost

$$\check{J}(\theta) = \mathbb{E} [\|\check{Y}_T^\theta - g(\check{X}_T^\theta)\|^2],$$

subject to:

$$\begin{cases} \check{X}_{t_{n+1}}^\theta - \check{X}_{t_n}^\theta = B(t_n, \check{X}_{t_n}^\theta, \check{Y}_{t_n}^\theta, z(t_n, \check{X}_{t_n}^\theta); \theta^Z) \Delta t + \sigma(t_n, \check{X}_{t_n}^\theta) \Delta \check{W}_{t_{n+1}}, & n = 0, \dots, N_T - 1, \\ \check{Y}_{t_{n+1}}^\theta - \check{Y}_{t_n}^\theta = -F(t_n, \check{X}_{t_n}^\theta, \check{Y}_{t_n}^\theta, z(t_n, \check{X}_{t_n}^\theta); \theta^Z) \Delta t + z(t_n, \check{X}_{t_n}^\theta; \theta^Z)^\top \Delta \check{W}_{t_{n+1}}, & n = 0, \dots, N_T - 1, \\ \check{X}_0^\theta = X_0 \sim \mu_0, \quad \check{Y}_0^\theta = y_0(\check{X}_0^\theta; \theta^Y), \end{cases}$$

where  $\Delta \check{W}_{t_{n+1}} = \check{W}_{t_{n+1}} - \check{W}_{t_n}$ .

Finally, the optimization can be carried out by applying SGD algorithm (Algorithm 1 in Appendix A.2) with  $L(\theta) = \check{J}(\theta)$  and one sample is  $\xi = (X_0, (\Delta \check{W}_{t_n})_{n=1, \dots, N_T})$ , which is sufficient to simulate  $(\check{X}_{t_n}^\theta, \check{Y}_{t_n}^\theta)_{n=0, \dots, N_T}$ .

**Remark 2.9.** *Instead of using a single neural network for  $z$ , viewed as a function of  $t$  and  $x$ , another possibility is to put a different neural network at each time step, which is a function of  $x$  only. With this approach, each neural network can use fewer parameters since there are fewer inputs. However, possible drawbacks are that: (a) the number of neural networks grows linearly with the number of time steps; and (b) the time dependence is not captured (at least not directly).*

*A possible shortcoming of this method is that the optimization is done globally in time: the loss function is computed only after simulating a whole trajectory, and only then can the parameters be updated. For problems with long time horizons or complicated terminal conditions, the method may have difficulty in converging, as has been pointed out in [145].*

**Remark 2.10** (Theoretical analysis). *A posteriori error bounds for the Deep BSDE method have been proved by Han and Long in [125], extending the results of [27] for uncoupled FBSDEs. They have shown, under suitable conditions, that the numerical error can be bounded by the value of the loss, and that this loss can be made as small as desired provided the approximation capability of the neural network is sufficient. Such results have then been extended to the fully coupled mean-field setting by Reisinger, Stockinger, and Zhang in [217].*

Several variants of the Deep BSDE method have been proposed. For example, [150] considers learning  $Y$  as a feedback of  $X$  or using Picard iterations to learn feedback controls based on  $(X, Y, Z)$ . The Deep BSDE method has been extended to include control problems with mean-field effects [56, Section 4.2] and delay [90, Section 3.2], and generalized to stochastic differential games [122, Section 3.2].

As mentioned in Section 2.1, the solution to a BSDE is closely related to the solution of a semi-linear PDE which could be derived from an uncontrolled volatility problem. In the case of a fully controlled volatility problem, a similar relation exists, and the corresponding deep 2BSDE method is proposed by Beck, E and Jentzen [22]. We also note that several works have refined and extended the Deep BSDE method. For instance [64] improved the performance of the Deep BSDE method with specific architectures and training methods, and illustrated them on several examples of semi-linear PDEs, including an HJB equation.

### 2.3.2 Deep backward dynamic programming (DBDP)

The DBDP method has been proposed by Huré, Pham and Warin in [145], based on ideas similar to the local approach discussed in Section 2.2.1. The main idea is to learn  $\check{Y}_{t_n}$  and  $\check{Z}_{t_n}$  at each  $t_n$  as functions of  $\check{X}_{t_n}$  by backward induction in time. So the resolution of the BSDE is decomposed as a sequence of optimization problems that are solved backward in time. This is in contrast with the Deep BSDE method, which goes forward in time, just like the difference between the two algorithms introduced in Section 2.2.

In DBDP, for each  $n$ ,  $\check{Y}_{t_n}$  and  $\check{Z}_{t_n}$  are replaced by neural networks, say  $y_n(\cdot; \theta_n^Y)$  and  $z_n(\cdot; \theta_n^Z)$ , with possibly different parameters at each time step. Here, one first chooses a sequence of distributions, say  $\mu_{t_n}$  from which  $\check{X}_{t_n}$  can be sampled for each  $t_n$ ,  $n = 0, \dots, N_T$ . The algorithm proceed with a backward induction. First,  $\theta_{N_T}^Y$  is trained such that  $y_{N_T}(\cdot; \theta_{N_T}^Y) \approx g(\cdot)$ , for example by minimizing

$$\check{J}(\theta^Y) = \mathbb{E} [\|y_{N_T}(\check{X}_T; \theta^Y) - g(\check{X}_T)\|^2],$$

where  $\check{X}_T \sim \mu_{N_T}$ . Note that the value of  $\theta_{N_T}^Z$  is not relevant for the result of the method. Then, the neural networks  $y_n(\cdot; \theta_n^Y)$  and  $z_n(\cdot; \theta_n^Z)$  are trained for  $n = N_T - 1, N_T - 2, \dots, 0$ . There are at least two different ways to train these neural networks:

- Version 1:  $\theta_n = (\theta_n^Y, \theta_n^Z)$  is trained to minimize over  $\theta = (\theta^Y, \theta^Z)$ ,

$$\check{J}_n^1(\theta) = \mathbb{E} \left[ \left\| y_{n+1}(\check{X}_{t_{n+1}}^\theta; \theta_{n+1}^Y) - y_n(\check{X}_{t_n}; \theta^Y) + F(t_n, \check{X}_{t_n}, y_n(\check{X}_{t_n}; \theta^Y), z_n(\check{X}_{t_n}; \theta^Z)) \Delta t \right. \right. \\ \left. \left. - z_n(\check{X}_{t_n}; \theta^Z) \cdot \Delta \check{W}_{t_{n+1}} \right\|^2 \right],$$

with

$$\check{X}_{t_{n+1}}^\theta = \check{X}_{t_n} + B(t_n, \check{X}_{t_n}, y_n(\check{X}_{t_n}; \theta^Y), z_n(\check{X}_{t_n}; \theta^Z)) \Delta t + \sigma(t_n, \check{X}_{t_n}) \Delta \check{W}_{t_{n+1}}, \quad \check{X}_{t_n} \sim \mu_{t_n}.$$

- Version 2:  $\theta_n^Y$  is trained to minimize over  $\theta = \theta^Y$ ,

$$\check{J}_n^2(\theta) = \mathbb{E} \left[ \left\| y_{n+1}(\check{X}_{t_{n+1}}^\theta; \theta_{n+1}^Y) - y_n(\check{X}_{t_n}; \theta^Y) + F(t_n, \check{X}_{t_n}, y(\check{X}_{t_n}; \theta^Y), \sigma^T \mathcal{D}_x y_n(\check{X}_{t_n}; \theta^Y)) \Delta t \right. \right. \\ \left. \left. - \mathcal{D}_x y_n(\check{X}_{t_n}; \theta^Y)^T \sigma \Delta \check{W}_{t_{n+1}} \right\|^2 \right],$$

with

$$\check{X}_{t_{n+1}}^\theta = \check{X}_{t_n} + B(t_n, \check{X}_{t_n}, y_n(\check{X}_{t_n}; \theta^Y), \sigma^T \mathcal{D}_x y_n(\check{X}_{t_n}; \theta^Y)) \Delta t + \sigma(t_n, \check{X}_{t_n}) \Delta \check{W}_{t_{n+1}}, \quad \check{X}_{t_n} \sim \mu_{t_n},$$

where the derivative  $\mathcal{D}_x y_n$  represents the numerical differentiation of the neural network  $y_n$ . In this version, the  $Z$  component is directly approximated by the derivative of the neural network for  $Y$ , so we do not use any parameter  $\theta^Z$ .

Then at each time step  $t_n$ , the optimization can be carried out by applying SGD algorithm (see Algorithm 1 in Appendix A.2) to the loss  $\check{J}_n^1(\theta)$  or  $\check{J}_n^2(\theta)$ , and one sample is  $\xi = (\check{X}_{t_n}, \Delta \check{W}_{t_{n+1}})$ . The DBDP method has been used successfully to solve BSDEs associated with semi-linear PDEs and fully non-linear PDEs, see respectively [145] and [211].

**Remark 2.11.** *In [145], the authors also extended this idea to reflected BSDEs that arise in optimal stopping problem and American option pricing in finance [209, Section 6.5]. However, as mentioned in the introduction, we do not discuss optimal stopping problems in this survey for the sake of brevity.*

The difference between the two versions of DBDP is: Version 1 uses independent neural networks for the approximation of  $Y_t$  and  $Z_t$  in (2.19); while Version 2 only approximate  $Y_t$  by neural networks and representing  $Z_t$  through auto-differentiating  $y_n(\cdot; \theta_n^Y)$ . Though the former one has more modeling flexibility, it may also introduce some inconsistency, as in many scenarios, the backward process is a function of time and the forward process  $Y_t = u(t, X_t)$  and the adjoint process is indeed the derivative of this function up to a scaling factor:  $Z_t = \sigma^T(t, X_t) \nabla_x u(t, X_t)$ .

The main advantage of the DBDP method is that it makes use of the time structure of the problem to split it into much simpler problems. Two possible shortcomings of the DBDP method are that: (1) the number of neural networks grows linearly with the number of time steps; and (2) it is not always clear how to choose the sampling distributions  $\mu_{t_n}$ , which have an impact on the way the neural networks are trained.

**Remark 2.12** (Theoretical analysis). Huré, Pham and Warin analyzed in [145] the error due to the time discretization, as well as the impact of different choices of loss functions.

## 2.4 Primal-Dual approaches

The Deep BSDE method presented above tackles directly a BSDE, without making explicit use from the fact that, in our context, the BSDE comes from an optimal control problem. In this context and under suitable assumptions, we can rely on a dual formulation to introduce primal-dual deep learning methods. Such methods have been studied, *e.g.*, in [130, 26, 76] and have applications to several problems in finance.

Recall that the stochastic optimal control we consider is given by (2.2)–(2.3). Using the aforementioned methods (*e.g.*, Deep BSDE or DBDP), it is generally hard to know how close to being optimal the neural network solution is. This is because we do not know *a priori* the minimal cost. However, we are always sure that these methods provide an upper bound since, given any admissible control  $\tilde{\alpha}$  (*e.g.*, in the form of a neural network as in the Deep BSDE method), we can compute  $J(\tilde{\alpha})$  which is at least as large as the infimum  $J^* = \inf_{\alpha} J(\alpha)$ . So to claim that  $\tilde{\alpha}$  is almost optimal, it is enough to exhibit a lower bound on  $J^*$  that is close to  $J(\tilde{\alpha})$ .

Except in special cases, there is no analytical expression for a good lower bound, and traditional numerical methods might be inefficient if the problem is in high dimension. Fortunately, the optimal value can be computed through a dual problem which is formulated as a maximization problem and hence yields a lower bound. We refer to *e.g.* [131] for more details.

Formally, the dual problem can be expressed as

$$\sup_{\varphi} \mathbb{E} \left[ \inf_{\alpha} \Phi^{\varphi, \alpha} \right],$$

where

$$\Phi^{\varphi, \alpha} = g(X_T^{\alpha}) + \int_0^T f(t, X_t^{\alpha}, \alpha_t) dt - \int_0^T \varphi(t, X_t^{\alpha}) \sigma(t, X_t^{\alpha}) dW_t,$$

and the superscript  $\alpha$  in  $X_t^{\alpha}$  emphasizes the dependence on the control  $\alpha$ . Here the infimum over  $\alpha$  is a pathwise optimization since it is inside the expectation. In some cases, it can be solved explicitly. Then we are left with a more standard optimal control problem with feedback control  $\varphi$ . The latter can be solved for instance using ideas similar to the ones presented in the previous sections such as the direct parameterization or the Deep BSDE method, see Sections 2.2 and 2.3. We refer to *e.g.* [130] for more details and numerical examples.

## 2.5 PDE-based algorithms

To conclude this part of the survey, we discuss PDE-based approaches. As discussed in Section 2.1, the optimal control can be identified by solving the corresponding HJB equation (2.4).

The Deep Galerkin Method (DGM) proposed by Sirignano and Spiliopoulos [227] aims at approximating the solution of the parabolic PDE with a deep neural network. In fact, the DGM can tackle PDEs of other (potentially nonlinear) types, with terminal (or initial) condition and boundary conditions. To focus on the main ideas, we present the algorithm for a generic PDE on a spatial domain  $\mathcal{Q} \subseteq \mathbb{R}^d$  and a time interval  $[0, T]$ ,

$$\begin{cases} \partial_t u(t, x) + \mathcal{L}u(t, x) = 0, & (t, x) \in [0, T] \times \mathcal{Q}, \\ u(T, x) = u_T(x), & x \in \mathcal{Q}, \\ u(t, x) = \Gamma(t, x), & x \in [0, T] \times \partial \mathcal{Q}. \end{cases}$$

Here  $\mathcal{L}$  is an operator in  $x$ , possibly nonlinear. A Dirichlet boundary condition is considered although other boundary conditions (Neumann, Robin) can also be treated in this framework.

The DGM algorithm proposes to replace  $u$  by a deep neural network, denoted by  $u(t, x; \theta)$ , and minimizes the following loss function

$$\begin{aligned} J(\theta) = & \eta \|\partial_t u(t, x; \theta) + \mathcal{L}u(t, x; \theta)\|_{L^2([0, T] \times \mathcal{Q}; \mu_1)}^2 + \eta_I \|u(T, x; \theta) - u_T(x)\|_{L^2(\mathcal{Q}; \mu_2)}^2 \\ & + \eta_{BC} \|u(t, x; \theta) - \Gamma(t, x)\|_{L^2([0, T] \times \partial \mathcal{Q}; \mu_3)}^2, \end{aligned} \quad (2.21)$$

where  $\mu_i$ ,  $i = 1, 2, 3$ , are probability distributions on the corresponding domains, and  $\|f(y)\|_{L^2(\mathcal{Y}; \mu)}^2 = \int_{\mathcal{Y}} |f(y)|^2 \mu(dy)$ . The first term is for the PDE residual, the second one is for the terminal condition and the third term is for the boundary condition. The positive constants  $\eta$ ,  $\eta_I$  and  $\eta_{BC}$  give more or less importance to each component. The differential operators  $\partial_t u(t, x; \theta)$  and  $\mathcal{L}u(t, x; \theta)$  can be computed exactly using automatic differentiation. However, most of the time, the second derivatives are computationally costly of  $\mathcal{O}(d^2 \times N_{\text{Batch}})$  and third-order derivatives  $\nabla_{\theta} \text{Hess}_x u(t, x; \theta)$  are also needed for SGD algorithms. A fast computation of second derivatives using a Monte Carlo method was proposed in [227, Section 3]. The

squared  $L^2$  norm of each term in (2.21) is calculated as the average of the squared value evaluated at random points drawn according to respective probability densities. Then we use SGD (see Algorithm 1) to minimize the loss function  $J$  defined in (2.21). One sample is  $\xi = ((t, x), x', x'') \in ([0, T] \times \mathcal{Q}) \times \mathcal{Q} \times \partial \mathcal{Q}$ , picked according to the distribution  $\mu_1 \otimes \mu_2 \otimes \mu_3$ .

When applying the DGM to the HJB equation (2.4) associated with the stochastic control problem (2.2)–(2.3), one uses the terminal condition  $u_T(x) = g(x)$ , and omit the boundary condition if there is not any.

**Remark 2.13.** *The DGM method can, at least in principle, be applied to a large variety of PDEs. Its flexibility is a key advantage. However, many choices need to be made in practice when implementing this method. First, the sampling distributions  $(\mu_i)_{i=1,2,3}$  strongly influences the training process and thus the learned function. Choosing a suitable distribution inside the domain and on its boundary is sometimes not trivial, particularly since one needs to sample from this distribution efficiently. Furthermore, when dealing with a loss function composed of several terms (as e.g. (2.21)), balancing the various terms can be challenging but is important to ensure that no term dominates the loss or is obliterated by the other terms. If some weight is too small, the neural network will tend to neglect the corresponding term. On the other hand, if some weight is much larger than needed, it will obfuscate the other terms. Overall, the choice of suitable coefficients seems important to efficiently guide the neural network towards a good local minimum.*

**Remark 2.14** (Theoretical analysis). *Sirignano and Spiliopoulos showed in [227], assuming that the PDE is quasilinear parabolic and has a smooth enough solution, that for any level  $\epsilon$ , there exists a wide-enough neural network that can make the  $L^2$  error  $J(\theta)$  smaller than  $\epsilon$ . They also shower, under stronger conditions, how we can obtain a sequence of neural networks converging to the PDE solution. To the best of our knowledge, the convergence of this algorithm remains to be studied for more general PDEs.*

The DGM has been extended to deal with path-dependent PDEs in [222], which used an LSTM network to capture the dependence on the path, and then passed this information to a feed-forward network in charge of learning the PDE solution. Other closely related works are the physics-informed neural networks (PINNs) [215], which is introduced to approximate solutions to equations arising in physics; and the deep Ritz method [81] which solves variational problems that arise from PDEs. The key idea is, here again, to look for the solution to the equation among a class of neural networks. The error analysis has been discussed in [232, 195, 77, 78, 79, 194] for various types of PDEs and operators.

### 3 Stochastic Differential Games

The previous section is dedicated to studying how a single agent makes strategic decisions in a random environment. This section will focus on stochastic differential games, which model and analyze the interactions between multiple rational agents in a dynamical random system. In games, an important concept is the so-called Nash equilibrium, which refers to a situation in which no one has an incentive to deviate. Finding a Nash equilibrium is one of the core problems in noncooperative game theory. However, the computation of Nash equilibria is extremely time-consuming and memory demanding for large populations of players [75].

When the number of player  $N$  becomes extremely large, the recently developed theory of mean-field game (MFG) [142, 141, 172, 174] provides an approximation to  $N$ -player Nash equilibria if individuals interact symmetrically [48]. Despite the huge model reduction from modeling  $N$  players to one representative player interacting with the population distribution, the MFG itself is still hard to solve numerically if this representative player's state is in a high-dimensional space, or if its evolution involves delay features, common noise, or complicated constraints.

A rich literature on game theory has been developed to study the consequences of strategies on interactions between a large group of rational “agents”, e.g., system risk caused by inter-bank borrowing and lending [49], price impacts imposed by agents’ optimal liquidation [44], market price from the monopolistic competition, and optimal investment with relative performance concerns [169, 168, 140]. This makes it crucial to develop efficient theory and fast algorithms for computing Nash equilibria of  $N$ -player stochastic differential games and MFGs.

As discussed in the previous sections, deep neural networks with many layers have been shown to solve efficiently stochastic control problems. These deep learning techniques also brought the possibility of computing equilibria in high-dimensional games, although extra difficulties arise since in general Nash equilibria are fixed point problems are not optimization problems.

Next, we review deep learning algorithms for solving stochastic (moderately large)  $N$ -player games, and mean-field games as an approximation for extremely large  $N$ -player games. In particular, the strategy of *deep fictitious play*, which integrates fictitious play (a learning scheme in game theory [36, 37]) into deep neural network designs, will be used frequently to develop parallelizable deep learning algorithms for computing Nash equilibria of stochastic differential games.

### 3.1 $N$ -player stochastic games

We first consider a stochastic differential game with  $N$  players indexed by  $i \in \mathcal{I} = \{1, 2, \dots, N\}$ . Each player has a state process  $X_t^i \in \mathbb{R}^d$  and takes an action  $\alpha_t^i$  in the action set  $\mathcal{A} \subset \mathbb{R}^k$ . In the context of games, we will use interchangeably the terms *control* and *strategy*. The dynamics of the controlled state process  $X^i$  on  $[0, T]$  are given by

$$dX_t^i = b^i(t, \mathbf{X}_t, \boldsymbol{\alpha}_t) dt + \sigma^i(t, \mathbf{X}_t, \boldsymbol{\alpha}_t) dW_t^i + \sigma^0(t, \mathbf{X}_t, \boldsymbol{\alpha}_t) dW_t^0, \quad X_0^i = x^i, \quad i \in \mathcal{I}, \quad (3.1)$$

where  $\mathbf{W} = [W^0, W^1, \dots, W^N]$  are  $(N + 1)$   $m$ -dimensional independent Brownian motions, and we shall call  $W^i$  the individual noises and  $W^0$  the common noise. Although at the  $N$ -player level, adding an extra common noise process is equivalent to choosing  $N$  correlated Brownian motions, the current formulation is more convenient when passing the limit  $N \rightarrow \infty$ .  $(b^i, \sigma^i)$  are deterministic functions:  $[0, T] \times \mathbb{R}^{dN} \times \mathcal{A}^N \rightarrow \mathbb{R}^d \times \mathbb{R}^{d \times m}$ . The  $N$  dynamics are coupled since all states  $\mathbf{X}_t = [X_t^1, \dots, X_t^N]$  and all the controls<sup>1</sup>  $\boldsymbol{\alpha}_t = [\alpha_t^1, \dots, \alpha_t^N]$  affect the drifts  $b^i$  and diffusion coefficients  $\sigma^i$ . Given a set of strategies  $(\boldsymbol{\alpha}_t)_{t \in [0, T]}$ , the cost associated to player  $i$  is of the form

$$J^i(\boldsymbol{\alpha}) = \mathbb{E} \left[ \int_0^T f^i(t, \mathbf{X}_t, \boldsymbol{\alpha}_t) dt + g^i(\mathbf{X}_T) \right], \quad (3.2)$$

where the running cost  $f^i : [0, T] \times \mathbb{R}^{dN} \times \mathcal{A}^N \rightarrow \mathbb{R}$  and terminal cost  $g^i : \mathbb{R}^{dN} \rightarrow \mathbb{R}$  are deterministic measurable functions.

Player  $i$  chooses  $(\alpha_t^i)_{t \in [0, T]}$  to minimize her cost  $J^i(\boldsymbol{\alpha})$  within a set  $\mathbb{A}^i$  of admissible strategies. As in Section 2, the set  $\mathbb{A}^i$  usually describes the measurability and integrability of  $\alpha_t^i$ . Different measurabilities correspond to different information structures available to the players, and they lead to different types of solutions to the game. In the noncooperative setting, the notion of optimality is the so-called *Nash equilibrium* (NE), and the three main types are open-loop NE ( $\mathbf{W}_{[0, t]}$ ), closed-loop NE ( $\mathbf{X}_{[0, t]}$ ), and closed-loop in feedback form NE ( $\mathbf{X}_t$ ) also known as Markovian Nash equilibrium. In this section, we will focus on the open-loop case (Section 3.1.1) and the closed-loop in feedback form case (Section 3.1.2).

Before proceeding to the open-loop case, we first summarize some commonly used notations as below. Given a probability space  $(\Omega, \mathcal{F}, \mathbb{P})$ , we consider

- $\mathbf{W} = [W^0, W^1, \dots, W^N]$ , a  $(N + 1)$ -vector of  $m$ -dimensional independent Brownian motions;
- $\mathbb{F} = \{\mathcal{F}_t, 0 \leq t \leq T\}$ , the augmented filtration generated by  $\mathbf{W}$ ;
- $\mathbb{H}_T^2(\mathbb{R}^d)$ , the space of all progressively measurable  $\mathbb{R}^d$ -valued stochastic processes  $\alpha : [0, T] \times \Omega \rightarrow \mathbb{R}^d$  such that  $\|\alpha\|_2^2 = \mathbb{E}[\int_0^T |\alpha_t|^2 dt] < \infty$ ;
- $\boldsymbol{\alpha} = [\alpha^1, \alpha^2, \dots, \alpha^N]$ , a strategy profile, *i.e.*, a collection of all players' strategies. The notation  $\boldsymbol{\alpha}^{-i} = [\alpha^1, \dots, \alpha^{i-1}, \alpha^{i+1}, \dots, \alpha^N]$  with a negative superscript means the strategies of all players

<sup>1</sup>Although in the literature of financial mathematics, one usually models  $b^i$  and  $\sigma^i$  to only depend on player  $i$ 's own action, it is common in the economics literature that player  $i$ 's state is also influenced by others' actions. For instance,  $\alpha_t^i$  and  $X_t^i$  can be respectively the price set by the company and the quantity it produces. To be general, we include this feature in our model, yielding (3.1). Note that by choosing  $b^i$  and  $\sigma^i$  properly, one can reduce it to the simpler case where each player controls her *private* state through  $\alpha_t^i$ .

excluding player  $i$ 's. If a non-negative superscript  $\mathbf{k}$  appears (e.g.,  $\boldsymbol{\alpha}^{\mathbf{k}}$ ), this  $N$ -tuple stands for the strategies from stage  $\mathbf{k}$ .  $\boldsymbol{\alpha}^{-i,\mathbf{k}} = [\alpha^{1,\mathbf{k}}, \dots, \alpha^{i-1,\mathbf{k}}, \alpha^{i+1,\mathbf{k}}, \dots, \alpha^{N,\mathbf{k}}]$  is a  $(N-1)$ -tuple representing strategies excluding player  $i$  at stage  $\mathbf{k}$ . We use the same notations for other stochastic processes (e.g.,  $\mathbf{X}^{-i}, \mathbf{X}^{\mathbf{k}}$ ).

### 3.1.1 Open-loop Nash equilibrium

We first consider the open-loop structure. In this setting, each player's control  $\alpha^i$  is in the space  $\mathbb{A} = \mathbb{H}_T^2(\mathcal{A})$ .

**Definition 3.1** (Open-loop Nash equilibrium). *A strategy profile  $(\hat{\alpha}_t)_{t \in [0, T]} = (\hat{\alpha}_t^1, \dots, \hat{\alpha}_t^N)_{t \in [0, T]} \in \mathbb{A}^N$  is called an open-loop Nash equilibrium if*

$$\forall i \in \mathcal{I} \text{ and } \beta^i \in \mathbb{A}, \quad J^i(\hat{\alpha}) \leq J^i(\beta^i, \hat{\alpha}^{-i}),$$

where  $\hat{\alpha}^{-i} = [\hat{\alpha}^1, \dots, \hat{\alpha}^{i-1}, \hat{\alpha}^{i+1}, \dots, \hat{\alpha}^N] \in \mathbb{A}^{N-1}$  is the equilibrium strategies of all the players except the  $i$ -th one.

Hu proposed in [139] the idea of deep fictitious play (DFP for short), which consists in decoupling the  $N$ -player game into  $N$  individual decision problems using *fictitious play*, and then solving these  $N$  individual problems using deep neural networks. Fictitious play was firstly introduced by Brown for static games [36, 37], and was recently adapted to the mean-field setting by [43, 114, 35]. It is a simple yet important learning scheme in game theory for finding Nash equilibria. Deep learning provides efficient tools for solving the decoupled yet still high-dimensional optimization problems.

The DFP algorithm starts with an initial strategy profile  $(\boldsymbol{\alpha}_t^0)_{t \in [0, T]} \in \mathbb{A}^N$ , which can be interpreted as the initial belief of all players, and updates  $K$  times:  $\boldsymbol{\alpha}_t^0 \rightarrow \boldsymbol{\alpha}_t^1 \rightarrow \dots \rightarrow \boldsymbol{\alpha}_t^k \rightarrow \dots \rightarrow \boldsymbol{\alpha}_t^K$  or until some stopping criterion is satisfied. At the beginning of stage  $\mathbf{k}+1$ ,  $\boldsymbol{\alpha}^{\mathbf{k}}$  is observable by all players. Player  $i$  then considers that other players are going to reuse the same strategy as they used in the previous iteration, namely  $\boldsymbol{\alpha}^{-i,\mathbf{k}}$ , and looks for a best response. Then, player  $i$  faces an optimization problem

$$\inf_{\beta^i \in \mathbb{A}} J^i(\beta^i; \boldsymbol{\alpha}^{-i,\mathbf{k}}), \quad J^i(\beta^i; \boldsymbol{\alpha}^{-i,\mathbf{k}}) = \mathbb{E} \left[ \int_0^T f^i(t, \mathbf{X}_t^{\boldsymbol{\alpha}}, (\beta^i, \boldsymbol{\alpha}^{-i,\mathbf{k}})) dt + g^i(\mathbf{X}_T^{\boldsymbol{\alpha}}) \right], \quad (3.3)$$

where  $\mathbf{X}_t^{\boldsymbol{\alpha}} = [X_t^{1,\boldsymbol{\alpha}}, X_t^{2,\boldsymbol{\alpha}}, \dots, X_t^{N,\boldsymbol{\alpha}}]$  are state processes controlled by  $(\beta^i, \boldsymbol{\alpha}^{-i,\mathbf{k}})$ ,

$$dX_t^{\ell,\boldsymbol{\alpha}} = b^{\ell}(t, \mathbf{X}_t^{\boldsymbol{\alpha}}, (\beta^i, \boldsymbol{\alpha}^{-i,\mathbf{k}})) dt + \sigma^{\ell}(t, \mathbf{X}_t^{\boldsymbol{\alpha}}, (\beta^i, \boldsymbol{\alpha}^{-i,\mathbf{k}})) dW_t^{\ell} + \sigma^0(t, \mathbf{X}_t^{\boldsymbol{\alpha}}, (\beta^i, \boldsymbol{\alpha}^{-i,\mathbf{k}})) dW_t^0, \quad (3.4)$$

with  $X_0^{\ell,\boldsymbol{\alpha}} = x^{\ell}$ , for all  $\ell \in \mathcal{I}$ . Denote by  $\alpha^{i,\mathbf{k}+1}$  the minimizer in (3.3),

$$\alpha^{i,\mathbf{k}+1} = \arg \min_{\beta^i \in \mathbb{A}^i} J^i(\beta^i; \boldsymbol{\alpha}^{-i,\mathbf{k}}), \quad \forall i \in \mathcal{I}, \mathbf{k} < K. \quad (3.5)$$

We assume  $\alpha^{i,\mathbf{k}+1}$  exists and is unique throughout this section. More precisely,  $\alpha^{i,\mathbf{k}+1}$  is player  $i$ 's optimal strategy at stage  $\mathbf{k}+1$  when the other players' controls are (3.1) evolve according to  $\alpha^{j,\mathbf{k}}$ ,  $j \neq i$ . All players find their best responses simultaneously, which together form  $\boldsymbol{\alpha}^{k+1}$ .

**Remark 3.2.** Note that the above learning process is different than the usual simultaneous fictitious play [36, 37], where the belief is described by the average over strategies played in previous iterations of the algorithm:  $\frac{1}{K} \sum_{k'=1}^K \boldsymbol{\alpha}^{-i,k'}$ .

In general, one can not expect that the players' actions  $\boldsymbol{\alpha}^{\mathbf{k}}$  always converge. However, if the sequence  $\{\boldsymbol{\alpha}^{\mathbf{k}}\}_{\mathbf{k}=1}^{\infty}$  ever admits a limit, denoted by  $\boldsymbol{\alpha}^{\infty}$ , one would expect it to form an open-loop Nash equilibrium under suitable assumptions. Intuitively, in the limiting situation, when all other players are using strategies  $\alpha^{j,\infty}$ ,  $j \neq i$ , by some stability argument, player  $i$ 's optimal strategy to the control problem (3.3) should be  $\alpha^{i,\infty}$ , meaning that she will not deviate from  $\alpha^{i,\infty}$ , which makes  $(\alpha^{i,\infty})_{i=1}^N$  an open-loop equilibrium.

**Remark 3.3** (Theoretical analysis). *In [139], Hu proved that for linear-quadratic games, under appropriate conditions, the family  $\{\boldsymbol{\alpha}^n\}_{n \in \mathbb{N}}$  converges to an open-loop Nash equilibrium of the original problem (3.1)-(3.2). Moreover, the limit, denoted by  $\boldsymbol{\alpha}^{\infty}$ , is independent of the choice of initial belief  $\boldsymbol{\alpha}^0$ .*

When seeking for an open-loop equilibrium, admissible controls in the optimization problem (3.5) for player  $i$  are  $\mathbf{W}$ -adapted. After a time discretization, the control at time  $t_n$  can be expressed as a function of  $\mathbf{W}$  at the previous time steps. So the problem is by nature high-dimensional, which motivates the use of deep neural networks. Similarly to the direct approach reviewed in Section 2.2, Hu [139] solved each player's control problems (3.3) at stage  $\mathbf{k}$  by using a feedforward fully connected network to directly parameterize  $\alpha^{i,\mathbf{k}}$ . When seeking for an open-loop equilibrium, the  $N$  optimization problems (3.5) for  $i = 1, \dots, N$  can be solved in parallel, as  $\alpha^{i,\mathbf{k}}$  are meant to be  $\mathbf{W}$ -adapted thus are not influenced by changes in the other players' states  $\mathbf{X}_t^{-i}$ . More precisely, to solve the optimization problem in (3.5), each  $\beta_{t_n}^{i,\mathbf{k}}$ ,  $n = 0, \dots, N_T - 1$ , is implemented by

$$\beta_{t_n}^{i,\mathbf{k}} \sim \beta_{t_n}^{i,\mathbf{k}}(\check{\mathbf{X}}_0, \check{\mathbf{W}}_{t_1}, \dots, \check{\mathbf{W}}_{t_n}; \theta_n^i), \quad (3.6)$$

which maps  $\mathbb{R}^{N(n+1)}$  to  $\mathbb{R}$ , and the optimal strategy at the  $\mathbf{k}^{th}$  stage, denoted by  $(\alpha_{t_n}^{i,\mathbf{k}}(\cdot; \theta_n^i))_{n=0}^{N_T-1}$ , is determined by minimizing a discretized version of (3.3), *i.e.*,

$$\{\theta_n^i\}_{n=0}^{N_T-1} \in \arg \min_{\{\theta_n^i\}_{n=0}^{N_T-1}} \mathbb{E} \left[ \sum_{n=0}^{N_T-1} f^i(t_n, \check{\mathbf{X}}_{t_n}^\theta, (\beta_{t_n}^{i,\mathbf{k}}(\check{\mathbf{X}}_0, \check{\mathbf{W}}_{t_1}, \dots, \check{\mathbf{W}}_{t_n}; \theta_n^i), \alpha_{t_n}^{-i,\mathbf{k}-1})) \Delta t + g^i(\check{\mathbf{X}}_T^\theta) \right], \quad (3.7)$$

where  $(\check{\mathbf{X}}_{t_n}^\theta)_{n=1}^{N_T}$  follows an Euler scheme corresponding to (3.4) with controls  $(\beta_{t_n}^{i,\mathbf{k}}, \alpha_{t_n}^{-i,\mathbf{k}-1})_{n=0}^{N_T-1}$  being used. The pseudo-code is given in Algorithm 3 in Appendix C.

### Numerical illustration: a linear-quadratic systemic risk problem with 24 players.

We illustrate the DFP algorithm on the LQ systemic risk game presented in Section 1.2 and originally introduced in [49]. For explicit formulas describing the open-loop Nash equilibrium, we refer to [49, Section 3.1].

In the numerical illustration, the number of players is set to be  $N = 24$ , and the time steps is set at  $N_T = 20$ , after observing the maximum relative errors, defined by

$$\max_{i \in \mathcal{I}} \frac{J^i(\alpha^{i,\mathbf{k}}; \alpha^{-i,\mathbf{k}-1}) - J^i(\hat{\alpha})}{J^i(\hat{\alpha})},$$

did not increase too much from  $N_T = 50$  to  $N_T = 20$ . The initial positions for the  $i^{th}$  player is  $x_0^i = 0.5i$ , and results are presented in Figures 7-9. Some key features that have been observed: the maximum of relative error drops below 3% after ten iterations; the average error of estimated trajectories are convex/concave functions of time  $t$ ; the standard deviation of estimated error aggregates from steps to steps. In fact, the convexity/concavity with respect to time  $t$  is caused by two factors: the propagation of errors, which produces an increase in error mean; and the existence of terminal cost, which puts more weight on  $X_T$  than  $X_t$ ,  $t \in (0, T)$ , resulting in a better estimate of  $X_T$  and a decreasing effect.

In the original paper, the author also gave numerical experiments with  $N = 5$  and  $N = 10$  players. To better illustrate that the algorithm can mitigate the curse of dimensionality, the performance comparison is made across different  $N$ . In particular, the author computed the error  $\max_{i \in \mathcal{I}} \max_{n \leq N_T} |X_{t_n}^i - \check{X}_{t_n}^{i,\theta}|$ , where  $X$  denotes the state process following the open-loop Nash equilibrium, while  $\check{X}^\theta$  is the deep fictitious play counterpart. The error is  $1.09 \times 10^{-2}$  for  $N = 5$ ,  $1.49 \times 10^{-2}$  for  $N = 10$  and  $2.08 \times 10^{-2}$  for  $N = 24$ .

#### 3.1.2 Markovian Nash equilibrium

In this subsection, consider closed-loop Nash equilibria and in particular Markovian Nash equilibria. A Markovian strategy for player  $i$  is a measurable functions of  $(t, \mathbf{X}_t)$ . Given a Markovian strategy profile  $\alpha_t$ , (3.1) rewrites as

$$dX_t^i = b^i(t, \mathbf{X}_t, \alpha(t, \mathbf{X}_t)) dt + \sigma^i(t, \mathbf{X}_t, \alpha(t, \mathbf{X}_t)) dW_t^i + \sigma^0(t, \mathbf{X}_t, \alpha(t, \mathbf{X}_t)) dW_t^0, \quad X_0^i = x_0^i, \quad i \in \mathcal{I}.$$

Each player aims to minimize the cost

$$J^i(\alpha) = \mathbb{E} \left[ \int_0^T f^i(t, \mathbf{X}_t, \alpha(t, \mathbf{X}_t)) dt + g^i(\mathbf{X}_T) \right].$$

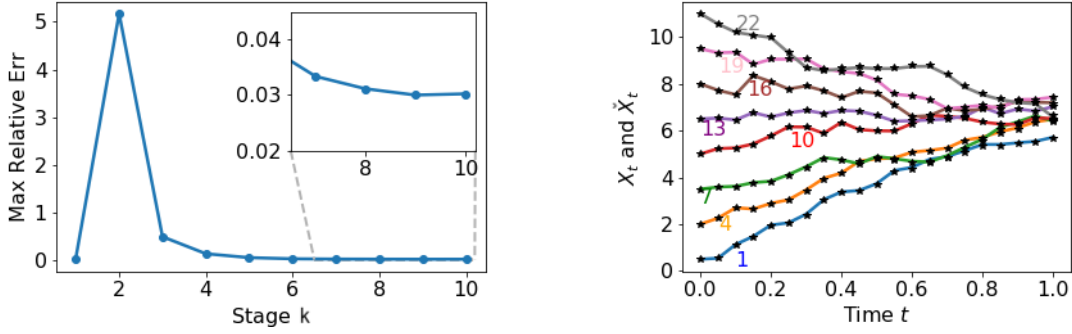


Figure 7: Comparisons of cost functions and optimal trajectories for  $N = 24$  players in the linear quadratic systemic risk problem in Section 3.1.1. Left: the maximum relative errors of the cost functions for 24 players; Right: for a sake of clarity, the comparison of optimal trajectories in only presented for the 1<sup>st</sup>, 4<sup>th</sup>, 7<sup>th</sup>, 10<sup>th</sup>, 13<sup>th</sup>, 16<sup>th</sup>, 19<sup>th</sup> and 22<sup>th</sup> players, where the solid lines are given by the closed-form solution and the stars are computed by deep fictitious play.

The dependence of  $b^i$  and  $\sigma^i$  on  $\alpha$  leads to a problem with stronger coupling than the open-loop setting. The problem is thus harder to solve, both theoretically and numerically.

**Definition 3.4.** A strategy profile  $\hat{\alpha} = (\hat{\alpha}^1, \dots, \hat{\alpha}^N)$  consisting of Markovian strategies is called a Markovian Nash equilibrium, if

$$\forall i \in \mathcal{I}, \text{ and any Markovian strategy } \beta^i, \quad J^i(\hat{\alpha}) \leq J^i(\hat{\alpha}^1, \dots, \hat{\alpha}^{i-1}, \beta^i, \hat{\alpha}^{i+1}, \dots, \hat{\alpha}^N),$$

where on the right-hand side,  $(\hat{\alpha}^1, \dots, \hat{\alpha}^{i-1}, \beta^i, \hat{\alpha}^{i+1}, \dots, \hat{\alpha}^N)(t, \mathbf{X}_t)$  is used in (3.1) to solve for  $\mathbf{X}_t$ .

In this case, due to the fact that each player's control is a function of the other players' states, any change in  $\mathbf{X}_t$  will cause a change in  $\alpha_t$ . As a consequence, merely adapting the algorithm in Section 3.1.1 will not be efficient nor parallelizable. In the Markovian setting, finding a Nash equilibrium can be reduced to solving  $N$  coupled HJB equations. To this end, we define  $u^i(t, \mathbf{x})$  as the value function of player  $i$ . For the sake of notation clarity, we present the discussion based on the “vectorized” system,

$$d\mathbf{X}_t = b(t, \mathbf{X}_t, \alpha(t, \mathbf{X}_t)) dt + \Sigma(t, \mathbf{X}_t, \alpha(t, \mathbf{X}_t)) d\mathbf{W}_t, \quad \mathbf{X}_0 = \mathbf{x}_0, \quad (3.8)$$

where  $\mathbf{X}$ ,  $b(t, \mathbf{x}, \alpha(t, \mathbf{x}))$  and  $\mathbf{W}$  are vectorizations of  $X^i$ ,  $b^i$ ,  $W^i$  respectively, and  $\Sigma(t, \mathbf{x}, \alpha(t, \mathbf{x}))$  is matrix-valued given by

$$\mathbf{X}_t = \begin{bmatrix} X_t^1 \\ X_t^2 \\ \vdots \\ X_t^N \end{bmatrix}, \quad b = \begin{bmatrix} b^1 \\ b^2 \\ \vdots \\ b^N \end{bmatrix}, \quad \mathbf{W}_t = \begin{bmatrix} W_t^0 \\ W_t^1 \\ \vdots \\ W_t^N \end{bmatrix}, \quad \Sigma = \begin{bmatrix} \sigma^0 & \sigma^1 \\ \sigma^0 & \sigma^2 \\ \vdots & \vdots \\ \sigma^0 & \sigma^N \end{bmatrix}.$$

Using the dynamic programming principle, the HJB system reads

$$\begin{cases} \partial_t u^i(t, \mathbf{x}) + G^i(t, \mathbf{x}, \hat{\alpha}(t, \mathbf{x}), \nabla_{\mathbf{x}} u^i(t, \mathbf{x}), \text{Hess}_{\mathbf{x}} u^i(t, \mathbf{x})) = 0, \\ u^i(T, \mathbf{x}) = g^i(\mathbf{x}), \quad i \in \mathcal{I}, \\ \hat{\alpha}^i(t, \mathbf{x}) = \inf_{\alpha^i \in \mathcal{A}} G^i(t, \mathbf{x}, (\alpha^i, \hat{\alpha}^{-i}(t, \mathbf{x})), \nabla_{\mathbf{x}} u^i(t, \mathbf{x}), \text{Hess}_{\mathbf{x}} u^i(t, \mathbf{x})), \end{cases} \quad (3.9)$$

where  $G^i$  is given by

$$G^i = G^i(t, \mathbf{x}, \alpha, p, q) = b(t, \mathbf{x}, \alpha) \cdot p + f^i(t, \mathbf{x}, \alpha) + \frac{1}{2} \text{Tr}(\Sigma \Sigma^T(t, \mathbf{x}, \alpha) q). \quad (3.10)$$

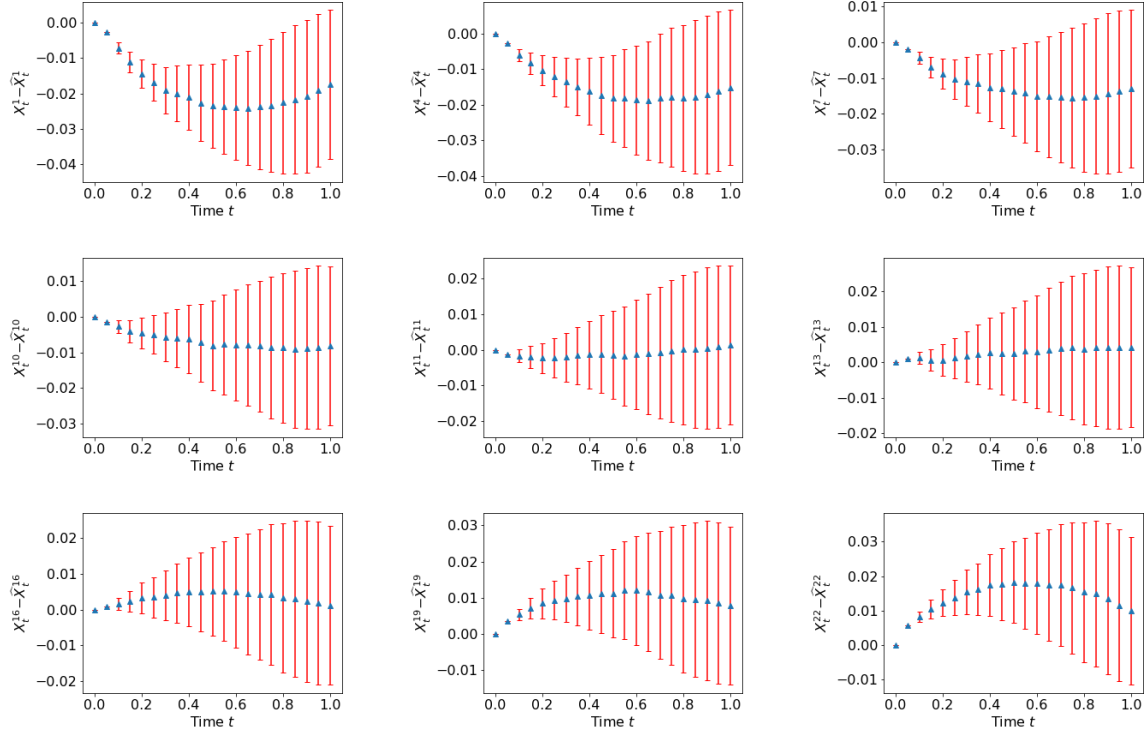


Figure 8: Comparisons of trajectories for  $N = 24$  players in the linear quadratic game in Section 3.1.1 using the learnt equilibrium strategy profile. For the sake of clarity, we only show the mean (blue triangles) and standard deviation (red bars) of trajectories errors for the 1<sup>st</sup>, 4<sup>th</sup>, 7<sup>th</sup>, 10<sup>th</sup>, 11<sup>th</sup>, 13<sup>th</sup>, 16<sup>th</sup>, 19<sup>th</sup> and 22<sup>th</sup> player, respectively. The results are based on a total of 65536 sample paths. They show that deep fictitious play provides a relatively uniformly good accuracy.

Note that when  $N = 1$ ,  $G^i$  coincides with the  $H$  function defined in (2.5). When  $N > 1$ , the equation for  $u^i$  in (3.9) depends on the equilibrium controls of the other players, which themselves depend on the value functions of these players. Hence the  $N$  equations are coupled.

Han and Hu proposed in [122] a version of the DFP algorithm for finding Markovian NE. Similar to ideas reviewed in Section 3.1.1, the optimization problems for the  $N$  players are decoupled by fictitious play in the following sense. Starting with a guess of the solution  $\boldsymbol{\alpha}^0 \in \mathbb{A}$ , the algorithm iteratively updates  $\boldsymbol{\alpha}^{k+1}$ : at iteration  $k + 1$ ,  $\boldsymbol{\alpha}^k$  is observed by all players, and player  $i$ 's decision problem is

$$\inf_{\alpha^i \in \mathbb{A}^i} J^i(\alpha^i; \boldsymbol{\alpha}^{-i, k}), \quad (3.11)$$

where  $J^i$  is defined in (3.2), and the state process  $\mathbf{X}_t$  is given in (3.8) with  $\boldsymbol{\alpha}$  replaced by  $(\alpha^i, \boldsymbol{\alpha}^{-i, k})$ . This problem is decoupled from the problems solved by the other players at the same iteration. The optimal strategy, assuming it exists, is denoted by  $\alpha^{i, k+1}$ . Problems (3.11) for all  $i \in \mathcal{I}$  are solved simultaneously using  $\boldsymbol{\alpha}^{-i, k}$ , and the optimal responses together form  $\boldsymbol{\alpha}^{k+1}$ . Thanks to the Markovian structure, problem (3.11) corresponds to solving the HJB equation

$$\partial_t u^{i, k+1} + \inf_{\alpha^i \in \mathcal{A}^i} G^i(t, \mathbf{x}, (\alpha^i, \boldsymbol{\alpha}^{-i, k}(t, \mathbf{x})), \nabla_{\mathbf{x}} u^{i, k+1}, \text{Hess}_{\mathbf{x}} u^{i, k+1}, u^{i, k+1}) = 0, \quad (3.12)$$

with the terminal condition  $u^{i, k+1}(T, \mathbf{x}) = g^i(\mathbf{x})$ . In the uncontrolled volatility problem (as *e.g.* in [122]),  $G^i$  does not depend on the  $q$  variable and hence the PDE is semi-linear. Let us assume that the minimizer  $\arg \min_{\alpha^i \in \mathcal{A}^i} G^i(t, \mathbf{x}, \boldsymbol{\alpha}, p, s)$  exists, is unique, and can be computed as an explicit function of other arguments:  $(t, \mathbf{x}, (\alpha^j)_{j \neq i}, p, s) \mapsto \alpha^{i, k+1, *}(t, \mathbf{x}, (\alpha^j)_{j \neq i}, p, s)$ . Then, the new control for player  $i$  is given by:

$$\alpha^{i, k+1}(t, \mathbf{x}) = \alpha^{i, k+1, *}(t, \mathbf{x}, \boldsymbol{\alpha}^{-i, k}(t, \mathbf{x}), \nabla_{\mathbf{x}} u^{i, k+1}(t, \mathbf{x}), u^{i, k+1}(t, \mathbf{x})). \quad (3.13)$$

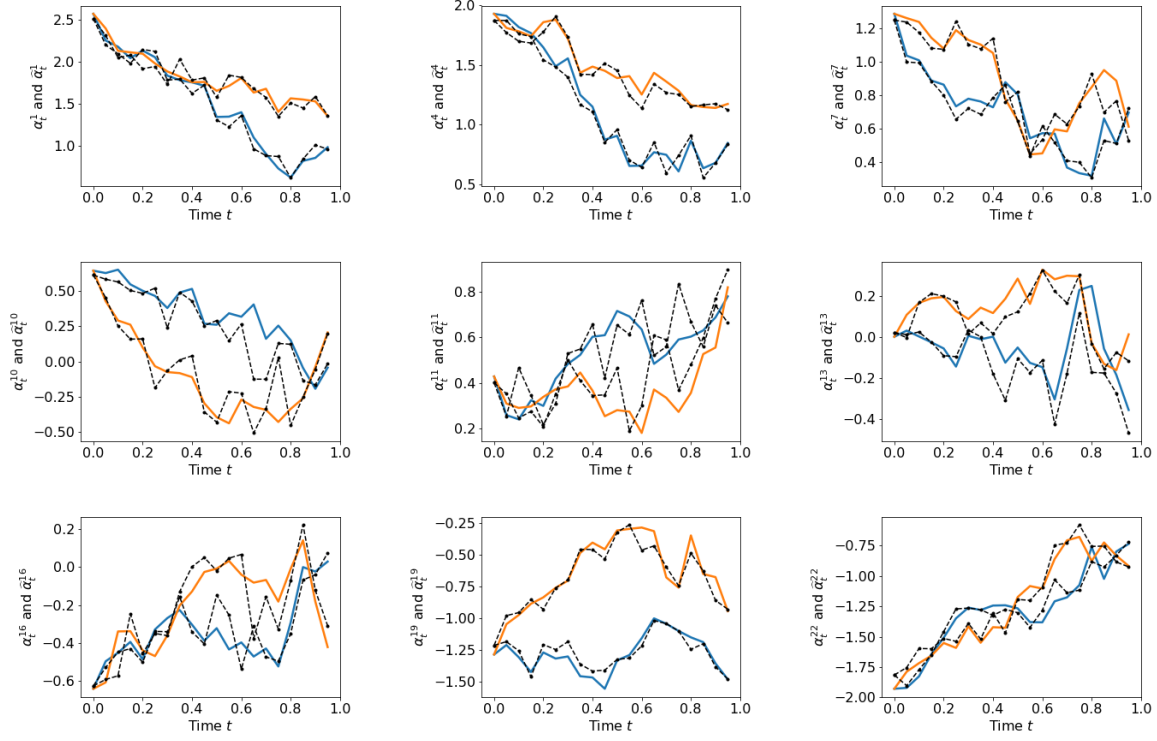


Figure 9: Comparisons of optimal controls for  $N = 24$  players in the linear quadratic game in Section 3.1.1. For clarity, we only show two sample paths of optimal controls for the 1<sup>st</sup>, 4<sup>th</sup>, 7<sup>th</sup>, 10<sup>th</sup>, 11<sup>th</sup>, 13<sup>th</sup>, 16<sup>th</sup>, 19<sup>th</sup> and 22<sup>th</sup> player, respectively. The solid lines are optimal controls given by the closed-form solution, and the dotted dash lines are computed by deep fictitious play.

Solving (3.12) for all  $i \in \mathcal{I}$  completes one stage in the loop of fictitious play.

To solve numerically the  $N$  decoupled semi-linear PDEs, one can for example interpret their solution through BSDEs via the non-linear Feynman-Kac formula (2.6):

$$\begin{cases} \mathbf{X}_t^{i,k+1} = \mathbf{x}_0 + \int_0^t \tilde{b}^i(s, \mathbf{X}_s^{i,k+1}; \boldsymbol{\alpha}^{-i,k}(s, \mathbf{X}_s^{i,k+1})) ds + \int_0^t \Sigma(s, \mathbf{X}_s^{i,k+1}) d\mathbf{W}_s, \\ Y_t^{i,k+1} = g^i(\mathbf{X}_T^{i,k+1}) \\ \quad + \int_t^T h^i(s, \mathbf{X}_s^{i,k+1}, Y_s^{i,k+1}, \mathbf{Z}_s^{i,k+1}; \boldsymbol{\alpha}^{-i,k}(s, \mathbf{X}_s^{i,k+1})) ds - \int_t^T (\mathbf{Z}_s^{i,k+1})^T d\mathbf{W}_s, \end{cases} \quad (3.14)$$

with  $Y_t^{i,k+1} = u^{i,k+1}(t, \mathbf{X}_t^{i,k+1})$  and  $\mathbf{Z}_t^{i,k+1} = \Sigma(t, \mathbf{X}_t^{i,k+1})^T \nabla_{\mathbf{x}} u^{i,k+1}(t, \mathbf{X}_t^{i,k+1})$ , where  $\tilde{b}^i$  and  $h^i$  are functions such that (3.12) can be rewritten as

$$\begin{aligned} \partial_t u^{i,k+1} + \frac{1}{2} \text{Tr}(\Sigma^T \text{Hess}_{\mathbf{x}} u^{i,k+1} \Sigma) + \tilde{b}^i(t, \mathbf{x}; \boldsymbol{\alpha}^{-i,k}) \cdot \nabla_{\mathbf{x}} u^{i,k+1} \\ + h^i(t, \mathbf{x}, u^{i,k+1}, \Sigma^T \nabla_{\mathbf{x}} u^{i,k+1}; \boldsymbol{\alpha}^{-i,k}) = 0. \end{aligned} \quad (3.16)$$

We stress once again that  $\boldsymbol{\alpha}^{-i,k}$  are known functions when solving the BSDE, which is why the BSDEs for  $i \in \mathcal{I}$  are decoupled. They can thus be solved in parallel, for example using the deep BSDE algorithm (see Section 2.3.1).

For each player  $i$ , the BSDE (3.14)–(3.15) is then solved using the deep BSDE algorithm (see Section 2.3.1). More precisely, let us consider the minimization problem (for less cumbersome notations, the subscript  $t_n$  in  $\mathbf{X}, \mathbf{Y}, \mathbf{Z}$  has been replaced by  $n$ , and the superscript  $k$  that denotes the index of fictitious

play is dropped for simplicity),

$$\inf_{\psi_0 \in \mathcal{N}_0^{i'}, \{\phi_n \in \mathcal{N}_n^i\}_{n=0}^{N_T-1}} \mathbb{E} |g^i(\check{\mathbf{X}}_{N_T}^i) - \check{\mathbf{Y}}_{N_T}^i|^2, \quad (3.17)$$

$$\begin{aligned} s.t. \quad & \check{\mathbf{X}}_0^i = \mathbf{x}_0, \quad \check{\mathbf{Y}}_0^i = \psi_0(\check{\mathbf{X}}_0^i), \quad \check{\mathbf{Z}}_n^i = \phi_n(\check{\mathbf{X}}_n^i), \quad n = 0, \dots, N_T - 1 \\ & \check{\mathbf{X}}_{n+1}^i = \check{\mathbf{X}}_n^i + \tilde{b}^i(t_n, \check{\mathbf{X}}_n^i; \boldsymbol{\alpha}^{-i}(t_n, \check{\mathbf{X}}_n^i)) \Delta t + \Sigma(t_n, \check{\mathbf{X}}_n^i) \Delta \mathbf{W}_{t_n}, \\ & \check{\mathbf{Y}}_{n+1}^i = \check{\mathbf{Y}}_n^i - h^i(t_n, \check{\mathbf{X}}_n^i, \check{\mathbf{Y}}_n^i, \check{\mathbf{Z}}_n^i; \boldsymbol{\alpha}^{-i}(t_n, \check{\mathbf{X}}_n^i)) \Delta t + (\check{\mathbf{Z}}_n^i)^T \Delta \mathbf{W}_{t_n}, \end{aligned} \quad (3.18)$$

where we recall that  $\Delta t = t_{n+1} - t_n$ ,  $\Delta \mathbf{W}_{t_n} = \mathbf{W}_{t_{n+1}} - \mathbf{W}_{t_n}$ . Here  $\mathcal{N}_0^{i'}$  and  $\{\mathcal{N}_n^i\}_{n=0}^{N_T-1}$  are hypothesis spaces of player  $i$  related to deep neural networks. The goal of the optimization is to find optimal deterministic maps  $\psi_0^{i,*}, \{\phi_n^{i,*}\}_{n=0}^{N_T-1}$  such that the loss function is small. The pseudo-code of the proposed deep fictitious play algorithm is summarized in Algorithm 4 in Appendix C.

**Remark 3.5.** In addition to the cost functional considered in (3.2), in [122] Han and Hu also considered the risk-sensitive minimization problem,

$$J^i(\boldsymbol{\alpha}) = \mathbb{E} \left[ \xi_i \exp \left\{ \xi_i \left( \int_0^T f^i(t, \mathbf{X}_t, \boldsymbol{\alpha}(t, \mathbf{X}_s)) dt + g^i(\mathbf{X}_T) \right) \right\} \right],$$

where  $\xi_i$  is a parameter characterizing how risk-averse or risk-seeking player  $i$  is. This flexibility allows one to model much broader classes of games that accommodate the players' attitudes to risk. In this case, the  $G^i$  function defined in (3.10) becomes

$$G^i = G^i(t, \mathbf{x}, \boldsymbol{\alpha}, p, q, s) = b(t, \mathbf{x}, \boldsymbol{\alpha}) \cdot p + \xi_i s f^i(t, \mathbf{x}, \boldsymbol{\alpha}) + \frac{1}{2} \text{Tr}(\Sigma \Sigma^T(t, \mathbf{x}, \boldsymbol{\alpha}) q).$$

Numerical examples on risk-sensitive problems are also presented therein.

**Remark 3.6** (Theoretical analysis). In [119], Han, Hu and Long provided a theoretical foundation for the DFP algorithm for Markovian Nash equilibria with the objective (3.2). They proved the convergence to the true Nash equilibrium if the decoupled sub-problems (3.11)–(3.12) are solved exactly and repeatedly. They also gave an a posteriori error bound on the numerical error on the deep BSDE algorithm, identified the  $\epsilon$ -Nash equilibrium produced by DFP, and analyzed the numerical performance of the algorithm on the original game.

The DFP algorithm has then been extended in [67] with the Scaled Deep Fictitious Play (SDFP) algorithm. There, the authors integrated the importance sampling and invariant layer embedding into DFP. Then focusing on the homogeneous agent problem, they utilized the symmetry and showed numerical experiments with up to  $N = 3,000$  agents. Along with the idea of combining fictitious play and deep learning, [126] recently studied the heterogeneous agent model in macroeconomics. In addition to parameterizing the control (as proposed in [121]), they also use neural networks to approximate the value function to reduce further the computational complexity of evaluating expectations of the type (3.7).

### Numerical illustration: the linear-quadratic systemic risk example revisited.

Here we revisit the example introduced in Section 1.2 and studied in Section 3.1.1, but focus on the Markovian Nash equilibrium.

To describe the model in the form of (3.8), we concatenate the log-monetary reserves  $X_t^i$  of  $N$  banks to form  $\mathbf{X}_t = [X_t^1, \dots, X_t^N]^T$ . The associated drift term and diffusion term are defined as

$$b(t, \mathbf{x}, \boldsymbol{\alpha}) = [a(\bar{x} - x^1) + \alpha^1, \dots, a(\bar{x} - x^N) + \alpha^N]^T \in \mathbb{R}^{N \times 1}, \quad \bar{x} = \frac{1}{N} \sum_{i=1}^N x^i, \quad (3.19)$$

$$\Sigma(t, \mathbf{x}) = \begin{bmatrix} \sigma \rho & \sigma \sqrt{1 - \rho^2} & 0 & \cdots & 0 \\ \sigma \rho & 0 & \sigma \sqrt{1 - \rho^2} & \cdots & 0 \\ \vdots & \vdots & \vdots & \ddots & \vdots \\ \sigma \rho & 0 & 0 & \cdots & \sigma \sqrt{1 - \rho^2} \end{bmatrix} \in \mathbb{R}^{N \times (N+1)}, \quad (3.20)$$

and  $\mathbf{W}_t = (W_t^0, \dots, W_t^N)$  is  $(N+1)$ -dimensional. Recall the running and terminal costs that player  $i$  aims to minimize

$$f^i(t, \mathbf{x}, \boldsymbol{\alpha}) = \frac{1}{2}(\alpha^i)^2 - q\alpha^i(\bar{x} - x^i) + \frac{\epsilon}{2}(\bar{x} - x^i)^2, \quad g^i(\mathbf{x}) = \frac{c}{2}(\bar{x} - x^i)^2.$$

The closed-form Nash equilibrium is detailed in [49, Sections 3.2-3.3].

The coupled HJB system corresponding to this game reads

$$\partial_t u^i + \inf_{\alpha^i} \left\{ \sum_{j=1}^N [a(\bar{x} - x^j) + \alpha^j] \partial_{x^j} u^i + \frac{(\alpha^i)^2}{2} - q\alpha^i(\bar{x} - x^i) + \frac{\epsilon}{2}(\bar{x} - x^i)^2 \right\} + \frac{1}{2} \text{Tr}(\Sigma^T \text{Hess}_{\mathbf{x}} u^i \Sigma) = 0,$$

with the terminal condition  $u^i(T, \mathbf{x}) = \frac{c}{2}(\bar{x} - x^i)^2$ ,  $i \in \mathcal{I}$ . The minimizer in the infimum gives a candidate of the optimal control for player  $i$ :  $\alpha^i(t, \mathbf{x}) = q(\bar{x} - x^i) - \partial_{x^i} u^i(t, \mathbf{x})$ . Plugging it back into the  $i^{th}$  equation yields a PDE of form (3.16),

$$\begin{aligned} \partial_t u^i + \frac{1}{2} \text{Tr}(\Sigma^T \text{Hess}_{\mathbf{x}} u^i \Sigma) + a(\bar{x} - x^i) \partial_{x^i} u^i + \sum_{j \neq i} [a(\bar{x} - x^j) + \alpha^j(t, \mathbf{x})] \partial_{x^j} u^i \\ + \frac{\epsilon}{2}(\bar{x} - x^i)^2 - \frac{1}{2}(q(\bar{x} - x^i) - \partial_{x^i} u^i)^2 = 0, \end{aligned}$$

where  $\alpha^j$  with  $j \neq i$  are considered exogenous for player  $i$ 's problem, and are given by the best responses of the other players from the previous stage. To be precise,  $\tilde{b}^i$  and  $h^i$  in (3.16) are defined as

$$\begin{aligned} \tilde{b}^i(t, \mathbf{x}; \boldsymbol{\alpha}^{-i}) &= [a(\bar{x} - x^1) + \alpha^1, \dots, a(\bar{x} - x^i), \dots, a(\bar{x} - x^N) + \alpha^N]^T, \\ h^i(t, \mathbf{x}, y, \mathbf{z}; \boldsymbol{\alpha}^{-i}) &= \frac{\epsilon}{2}(\bar{x} - x^i)^2 - \frac{1}{2}(q(\bar{x} - x^i) - \frac{z^i}{\sigma\sqrt{1-\rho^2}})^2, \end{aligned}$$

where  $\mathbf{z} = (z^0, z^1, \dots, z^N) \in \mathbb{R}^{N+1}$ .

Figures 10–11 show the performance of the DFP algorithm on a ten-player game, using the parameter,

$$a = 0.1, \quad q = 0.1, \quad c = 0.5, \quad \epsilon = 0.5, \quad \rho = 0.2, \quad \sigma = 1, \quad T = 1.$$

The relative squared error (RSE) is defined by

$$\text{RSE} = \frac{\sum_{\substack{i \in \mathcal{I} \\ 1 \leq j \leq J}} \left( u^i(0, \mathbf{x}_{t_0}^{(j)}) - \hat{u}^i(0, \mathbf{x}_{t_0}^{(j)}) \right)^2}{\sum_{\substack{i \in \mathcal{I} \\ 1 \leq j \leq J}} \left( u^i(0, \mathbf{x}_{t_0}^{(j)}) - \bar{u}^i \right)^2}, \text{ or } \text{RSE} = \frac{\sum_{\substack{0 \leq n \leq N_T-1 \\ 1 \leq j \leq J}} \left( \nabla_{\mathbf{x}} u^i(t_n, \mathbf{x}_{t_n}^{(j)}) - \nabla_{\mathbf{x}} \hat{u}^i(t_n, \mathbf{x}_{t_n}^{(j)}) \right)^2}{\sum_{\substack{0 \leq n \leq N_T-1 \\ 1 \leq j \leq J}} \left( \nabla_{\mathbf{x}} u^i(t_n, \mathbf{x}_{t_n}^{(j)}) - \bar{\nabla}_{\mathbf{x}} u^i \right)^2},$$

where  $\hat{u}^i$  is the prediction from the neural networks, and  $\bar{u}^i$  (resp.  $\bar{\nabla}_{\mathbf{x}} u^i$ ) is the average of  $u^i$  (resp.  $\nabla_{\mathbf{x}} u^i$ ) evaluated at all the indices  $j, n$ . To compute the relative error,  $J = 256$  ground truth sample paths  $\{\mathbf{x}_{t_n}^{(j)}\}_{n=0}^{N_T-1}$  are generated using an Euler scheme based on (3.8)(3.19)(3.20) and the true optimal strategy. Note that the superscript  $(j)$  here does not mean the player index, but the  $j^{th}$  path for all players.

In particular, Figure 10 compares the relative squared error as  $N_{\text{SGD\_per\_stage}}$  varies from 10 to 400. The convergence of the learning curves with small  $N_{\text{SGD\_per\_stage}}$  asserts that each individual problem does not need to be solved so accurately. Furthermore, the fact that the performances are similar under different  $N_{\text{SGD\_per\_stage}}$  with the same total budget of SGD updates suggest that the algorithm is insensitive to the choice of this hyperparameter. The final relative squared errors of  $u$  and  $\nabla u$  averaged from three independent runs of deep fictitious play are 4.6% and 0.2%, respectively. Figure 11 presents one sample path for each player of the optimal state process  $X_t^i$  and the optimal control  $\alpha_t^i$  vs. their approximations  $\hat{X}_t^i, \hat{\alpha}_t^i$  provided by the optimized neural networks.

### 3.2 Mean-field games

Mean-field games, introduced independently by Lasry and Lions in [172, 173, 174] and by Huang, Malhamé and Caines in [142, 141], provide a paradigm to approximate the solutions of stochastic games with very

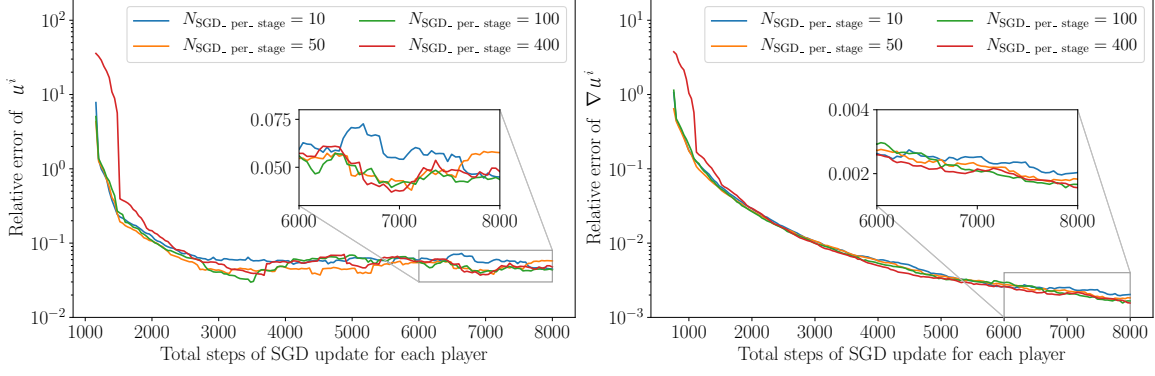


Figure 10: Linear-quadratic systemic risk example in Section 3.1.2. The relative squared errors of  $u^i$  (left) and  $\nabla u^i$  (right) along the training process of deep fictitious play for the inter-bank game. The relative squared errors of  $u^i(0, \hat{\mathbf{X}}_0^i)$  and  $\{\nabla u^i(t_n, \hat{\mathbf{X}}_n^i)\}_{n=0}^{N_T-1}$  are evaluated. The error is computed every 400 SGD updates, averaged over all the players. A smoothed moving average with window size 3 is applied in the final plots.

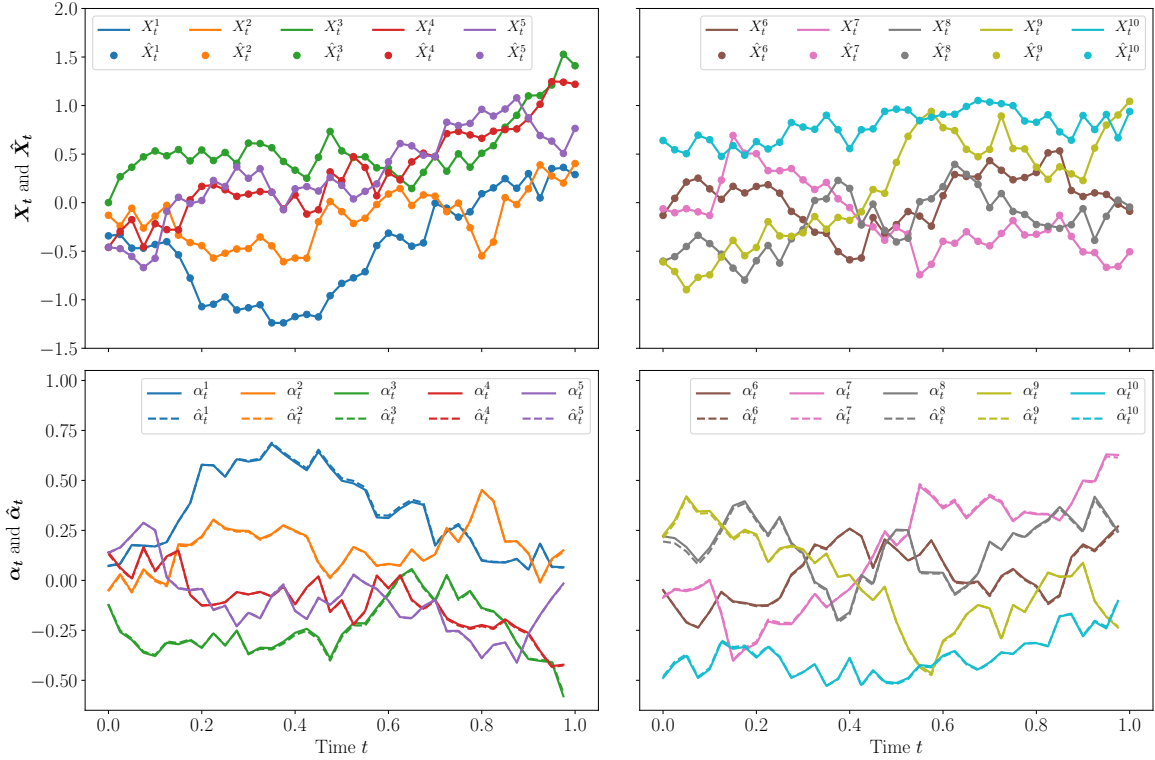


Figure 11: Linear-quadratic systemic risk example in Section 3.1.2. A sample path for each player of the inter-bank game with  $N = 10$ . Top: the optimal state process  $X_t^i$  (solid lines) and its approximation  $\hat{X}_t^i$  (circles) provided by the optimized neural networks, under the same realized path of Brownian motion. Bottom: comparisons of the strategies  $\alpha_t^i$  and  $\hat{\alpha}_t^i$  (dashed lines).

large number of players. The approximation relies on two main assumptions: anonymity, which means that the players interact only through the population's empirical distribution, and indistinguishability, which means that  $(b^i, \sigma^i, f^i, g^i)$  are the same for all  $i$ . Then, one can pass (at least formally) to the limit by letting the number of players grow to infinity. In the asymptotic problem, the influence of each individual player on

the rest of the population vanishes and the Nash equilibrium can be characterized by studying the problem posed to a representative player. Under suitable assumptions, it can be shown that solving this limiting problem provides an approximate equilibrium for the finite-player game. We refer to the notes [41] and the books [28, 52, 53] as well as the references therein for further background on mean-field games. Numerical methods for such games have been developed using mostly traditional techniques such as finite difference schemes [3, 2], semi-Lagrangian schemes [45, 46], or methods based on probabilistic approaches [66, 13]. See, *e.g.*, [5, 176] for recent surveys. However, similarly to control problems or finite-player games, these methods do not scale well in terms of dimensionality, and in particular, they are not very suitable for problems with delay or with common noise. This motivates the development of deep learning methods, some of which are described in [57]. In the sequel, we describe the theoretical framework of mean field games and then survey recent deep learning methods.

### 3.2.1 Theoretical background

We start by defining the notion of MFG, and then we discuss how equilibria can be characterized in terms of PDEs, BSDEs, and the so-called master equation.

#### 3.2.1.1 Definition of the problem

Going back to problem (3.2), let us assume that  $b^i, \sigma^0, \sigma^i, f^i, g^i$  depend on the rest of the population's states and actions in an anonymous way, *i.e.*, there exists functions  $b, \sigma^0, \sigma, f, g$  such that:  $b^i(t, \mathbf{X}_t, \boldsymbol{\alpha}_t) = b(t, X_t^i, \nu_t^N, \alpha_t^i)$ ,  $\sigma^0(t, \mathbf{X}_t, \boldsymbol{\alpha}_t) = \sigma^0(t, X_t^i, \nu_t^N, \alpha_t^i)$ ,  $\sigma^i(t, \mathbf{X}_t, \boldsymbol{\alpha}_t) = \sigma(t, X_t^i, \nu_t^N, \alpha_t^i)$ ,  $f^i(t, \mathbf{X}_t, \boldsymbol{\alpha}_t) = f(t, X_t^i, \nu_t^N, \alpha_t^i)$  and  $g^i(\mathbf{X}_T) = g(X_T^i, \mu_T^N)$ , where  $\nu_t^N = \frac{1}{N} \sum_{j=1}^N \delta_{(X_t^j, \alpha_t^j)}$  is the empirical state-action distribution of the population and  $\mu_t^N = \frac{1}{N} \sum_{j=1}^N \delta_{X_t^j}$  is its first marginal, which corresponds to the state distribution. We keep the same notation  $\sigma^0$  for simplicity, with a slight abuse of notation.

Then the cost associated to a strategy profile  $\boldsymbol{\alpha}$  is defined as

$$J^i(\boldsymbol{\alpha}) = \mathbb{E} \left[ \int_0^T f(t, X_t^i, \nu_t^N, \alpha_t^i) dt + g(X_T^i, \mu_T^N) \right], \quad (3.21)$$

where the processes  $X^j$ ,  $j = 1, \dots, N$ , solve the SDE system

$$dX_t^j = b(t, X_t^j, \nu_t^N, \alpha_t^j) dt + \sigma(t, X_t^j, \nu_t^N, \alpha_t^j) dW_t^j + \sigma^0(t, X_t^j, \nu_t^N, \alpha_t^j) dW_t^0, \quad X_0^j \sim \mu_0, \quad j \in \mathcal{I},$$

where the initial positions are i.i.d., with  $\nu$  and  $\mu$  being as above the flows of empirical state-action and empirical state distributions. The influence of a given player on the dynamics and the cost of another player occurs only through the empirical distribution flow  $\nu^N$ . So when  $N$  increases, the influence of each player decreases. By symmetry, we can expect that in the limit it is sufficient to study the problem for a single representative player.

To formulate the MFG, let  $\nu = (\nu_t)_{0 \leq t \leq T}$  be a stochastic distribution flow adapted to the filtration generated by  $W^0$ , which is interpreted at the evolution of the population's state-action configuration. Let  $\alpha$  be an open-loop control. A representative player's dynamics are given by,

$$\begin{cases} dX_t^{\nu, \alpha} = b(t, X_t^{\nu, \alpha}, \nu_t, \alpha_t) dt \\ \quad + \sigma(t, X_t^{\nu, \alpha}, \nu_t, \alpha_t) dW_t + \sigma^0(t, X_t^{\nu, \alpha}, \nu_t, \alpha_t) dW_t^0, \quad t \geq 0 \\ X_0^{\nu, \alpha} \sim \mu_0, \end{cases} \quad (3.22)$$

where  $W$  is a standard  $m$ -dimensional Brownian motion independent of  $W^0$ . For a representative player, the cost associated to using the control  $\alpha$  when the population is given by the distribution flow  $\nu = (\nu_t)_{0 \leq t \leq T}$  is defined as

$$J^{MFG}(\alpha; \nu) = \mathbb{E} \left[ \int_0^T f(t, X_t^{\nu, \alpha}, \nu_t, \alpha_t) dt + g(X_T^{\nu, \alpha}, \mu_T) \right], \quad (3.23)$$

under the constraint that the process  $X^{\nu, \alpha} = (X_t^{\nu, \alpha})_{t \geq 0}$  solves the SDE (3.22).

**Definition 3.7** (mean field Nash equilibrium). *Consider the MFG problem introduced above. A pair  $(\hat{\nu}, \hat{\alpha})$  consisting of a stochastic flow  $\hat{\nu} = (\hat{\nu}_t)_{0 \leq t \leq T}$  of probability measures in  $\mathcal{P}_2(\mathbb{R}^d)$  adapted to the common noise filtration and an open-loop control  $\hat{\alpha} = (\hat{\alpha}_t)_{t \in [0, T]}$  is a mean field Nash equilibrium if it satisfies the following two conditions*

1.  $\hat{\alpha}$  minimizes  $J^{MFG}(\cdot; \hat{\nu})$ ;
2. For all  $t \in [0, T]$ ,  $\hat{\nu}_t$  is the probability distribution of  $(X_t^{\hat{\nu}, \hat{\alpha}}, \hat{\alpha}_t)$  conditioned on  $W^0$ .

Note that, in the first condition,  $\hat{\nu}$  is fixed when an infinitesimal agent performs their optimization. The second condition ensures that if all the players use the control  $\hat{\alpha}$ , the law of their individual states and actions is indeed  $\hat{\nu}$ . The original formulation of MFGs [175] considers interactions through the state distribution only. MFGs with interactions through the joint distribution of state and actions, as presented in the above definition, are sometimes referred to as extended MFGs or MFGs of controls, see *e.g.*, [98, 99, 44, 159, 179].

Next, we review several ways to characterize the mean field Nash equilibrium concept using analytical and probabilistic techniques.

### 3.2.1.2 PDE system

For simplicity, let us assume that there is no common noise. We assume that there exists an equilibrium and we denote by  $\hat{\nu} = (\hat{\nu}_t)_{t \geq 0}$  the associated mean-field flow of distributions. When considering Markovian controls, one can define the value function  $u$  by

$$u(t, x) = \inf_{\alpha} \mathbb{E} \left[ \int_t^T f(s, X_s, \hat{\nu}_s, \alpha_s) ds + g(X_T, \hat{\mu}_T) | X_t = x \right].$$

As in standard OC problems, under suitable conditions,  $u(t, x)$  solves the HJB equation:

$$\begin{cases} \partial_t u(t, x) + \min_{\alpha \in \mathcal{A}} H(t, x, \hat{\nu}_t, \nabla_x u(t, x), \text{Hess}_x u(t, x), \alpha) = 0, \\ u(T, x) = g(x, \hat{\mu}_T), \end{cases} \quad (3.24)$$

where

$$H(t, x, \nu, p, q, \alpha) = b(t, x, \nu, \alpha) \cdot p + \frac{1}{2} \text{Tr}(\sigma(t, x, \nu, \alpha) \sigma(t, x, \nu, \alpha)^T q) + f(t, x, \nu, \alpha). \quad (3.25)$$

If (3.24) has a classical solution, then the optimal control is given by

$$\hat{\alpha}(t, x) = \alpha(t, x, \hat{\nu}_t, \nabla_x u(t, x), \text{Hess}_x u(t, x)),$$

where

$$\alpha(t, x, \nu, p, q) = \arg \min_{\alpha \in \mathcal{A}} H(t, x, \nu, p, q, \alpha).$$

The consistency condition for the equilibrium mean-field flow is equivalent to: the state distribution flow  $\hat{\mu} = (\hat{\mu}_t)_{t \geq 0}$  solves the following Kolmogorov-Fokker-Planck (KFP) PDE

$$\begin{cases} \partial_t \hat{\mu}(t, x) - \sum_{i,j} \frac{\partial^2}{\partial x_i \partial x_j} \left( \hat{D}_{i,j}(t, x) \hat{\mu}(t, x) \right) + \text{div} \left( \hat{\mu}(t, x) \hat{b}(t, x) \right) = 0, \\ \hat{\mu}(0) = \mu_0, \end{cases} \quad (3.26)$$

where

$$\hat{D}(t, x) = \frac{1}{2} \sigma(t, x, \hat{\nu}_t, \hat{\alpha}(t, x)) \sigma(t, x, \hat{\nu}_t, \hat{\alpha}(t, x))^T, \quad \hat{b}(t, x) = b(t, x, \hat{\nu}_t, \hat{\alpha}(t, x)),$$

and the state-action distribution  $\hat{\nu}_t$  at time  $t$  is the push forward of  $\hat{\mu}_t$  by  $(I_d, \hat{\alpha}(t, \cdot))$ , which we will denote by  $\hat{\nu}_t = \hat{\mu}_t \circ (I_d, \hat{\alpha}(t, \cdot))^{-1}$ . The forward-backward PDE system (3.25)–(3.26) characterizes the mean field Nash equilibrium. We refer to *e.g.*, [159] for the existence of classical solutions to such PDE systems under suitable assumptions.

**Remark 3.8.** *MFC problems also give rise to analogous forward-backward PDE systems, except that the solution  $u$  of the backward equation is not interpreted as a value function of an optimal control problem but rather as an adjoint state. We refer to [28, 4] for more details. The KFP equation remains the same, but the HJB equation has one extra term reflecting the fact that the whole population performs the optimization simultaneously.*

In the presence of common noise, the HJB and KFP equations become stochastic. We will not discuss this system in the sequel, and refer the interested readers to [206] for the derivation of stochastic HJB equations and [51, 42] for stochastic HJB-KFP systems arising in MFG (with the state distribution only).

### 3.2.1.3 FBSDE system

We now review the characterization of MFG equilibria using BSDEs. As for standard OC (see Section 2.1), BSDEs can be used to characterize the value function or its gradient. For simplicity, we assume that there is no common noise. We further assume that the volatility of the idiosyncratic noise is uncontrolled, in which case  $\hat{\alpha}$  is independent of  $\text{Hess}_x u(t, x)$  and the PDE (3.24) becomes semi-linear:

$$\begin{aligned} \partial_t u(t, x) + \frac{1}{2} \text{Tr}(\sigma(t, x, \hat{\nu}_t) \sigma(t, x, \hat{\nu}_t)^T \text{Hess}_x u(t, x)) + b(t, x, \hat{\nu}_t, \hat{\alpha}(t, x, \hat{\nu}_t, \nabla_x u(t, x))) \cdot \nabla_x u(t, x) \\ + f(t, x, \hat{\alpha}(t, x, \hat{\nu}_t, \nabla_x u(t, x))) = 0. \end{aligned}$$

Suppose that there exist functions  $\mu(t, \nu, x)$  and  $h(t, x, \nu, z)$  such that

$$\begin{aligned} \tilde{b}(t, \hat{\nu}_t, x) \cdot \nabla_x u(t, x) + h(t, x, \hat{\nu}_t, \sigma(t, x)^T \nabla_x u(t, x)) \\ = b(t, x, \hat{\nu}_t, \hat{\alpha}(t, x, \hat{\nu}_t, \nabla_x u(t, x))) \cdot \nabla_x u(t, x) + f(t, x, \hat{\nu}_t, \hat{\alpha}(t, x, \nabla_x u(t, x))). \end{aligned}$$

Then the non-linear Feynman-Kac formula (see [204]) gives the following BSDE interpretation of  $u(t, x)$ :

$$\begin{cases} d\mathcal{X}_t = \tilde{b}(t, \hat{\nu}_t, \mathcal{X}_t) dt + \sigma(t, \hat{\nu}_t, \mathcal{X}_t) dW_t, & \mathcal{X}_0 \sim \mu_0, \\ d\mathcal{Y}_t = -h(t, \hat{\nu}_t, \mathcal{X}_t, \mathcal{Z}_t) dt + \mathcal{Z}_t dW_t, & \mathcal{Y}_T = g(\mathcal{X}_T, \hat{\mu}_T), \end{cases}$$

by the relation

$$\mathcal{Y}_t = u(t, \mathcal{X}_t), \quad \mathcal{Z}_t = \sigma(t, \hat{\nu}_t, \mathcal{X}_t)^T \nabla_x u(t, \mathcal{X}_t).$$

Moreover, the optimal value is given by  $\mathbb{E}[\mathcal{Y}_0] = \mathbb{E}[u(0, \mathcal{X}_0)]$ . This BSDE characterizes the value function for a representative player given the mean field flow  $\hat{\nu}$ . Then consistency condition reads:

$$\hat{\nu}_t = \mathcal{L}(\mathcal{X}_t, \hat{\alpha}(t, \mathcal{X}_t, \hat{\nu}_t, (\sigma(t, \hat{\nu}_t, \mathcal{X}_t)^T)^{-1} \mathcal{Z}_t)).$$

In the controlled volatility case, the PDE (3.24) is fully nonlinear, and its solution is connected to a solution of the 2BSDE, see [69] and Section 2.1.

The Pontryagin stochastic maximum principle provides the connection to the FBSDE. Define the generalized Hamiltonian  $\mathcal{H}$  by

$$\mathcal{H}(t, x, \nu, y, z, \alpha) = b(t, x, \nu, \alpha)y + \text{Tr}(\sigma^T(t, x, \nu, \alpha)z) + f(t, x, \nu, \alpha). \quad (3.27)$$

If the Hamiltonian  $\mathcal{H}$  is convex in  $(x, \alpha)$ , and  $(X_t, Y_t, Z_t)$  solve

$$\begin{cases} dX_t = b(t, X_t, \hat{\nu}_t, \hat{\alpha}_t) dt + \sigma(t, X_t, \hat{\nu}_t, \hat{\alpha}_t) dW_t, & X_0 \sim \mu_0, \\ dY_t = -\nabla_x \mathcal{H}(t, X_t, \hat{\nu}_t, Y_t, Z_t, \hat{\alpha}_t) dt + Z_t dW_t, & Y_T = \partial_x g(X_T, \hat{\mu}_T), \end{cases}$$

such that  $\hat{\alpha}$  minimizes  $\mathcal{H}$  along  $(X_t, \hat{\nu}_t, Y_t, Z_t)$ , then  $\hat{\alpha}$  is the optimal control. If the value function is smooth enough, then

$$Y_t = \nabla_x u(t, X_t), \quad Z_t = \sigma(t, X_t, \hat{\nu}_t, \hat{\alpha})^T \text{Hess}_x u(t, X_t).$$

In this case, the consistency condition for the equilibrium mean field flow  $\hat{\nu}$  reads

$$\hat{\nu}_t = \mathcal{L}(X_t, \hat{\alpha}(t, X_t, \hat{\nu}_t, (\sigma(t, \hat{\nu}_t, X_t)^T)^{-1} Y_t, Z_t)).$$

When there is common noise, the FBSDE system becomes

$$\begin{cases} dX_t = b(t, X_t, \hat{\nu}_t, \hat{\alpha}_t) dt + \sigma(t, X_t, \hat{\nu}_t, \hat{\alpha}_t) dW_t + \sigma^0(t, X_t, \hat{\nu}_t, \hat{\alpha}_t) dW_t^0, & X_0 \sim \mu_0, \\ dY_t = -\nabla_x \mathcal{H}(t, X_t, \hat{\nu}_t, Y_t, Z_t, Z_t^0, \hat{\alpha}_t) dt + Z_t dW_t + Z_t^0 dW_t^0, & Y_T = \partial_x g(X_T, \hat{\mu}_T), \end{cases}$$

where, compared with (3.27), the definition of  $\mathcal{H}$  includes an extra term  $\text{Tr}(\sigma^{0T}(t, x, \nu, \alpha) z^0)$ .

**Remark 3.9.** *MFC problems also lead to analogous FBSDE systems. In the absence of common noise, Pontryagin's maximum principle is derived for instance in [50] and [1] when the interactions are through the state or the state-action distributions respectively. This leads to a BSDE with an extra term accounting for the variation of the distribution during the optimization of the control.*

All the above systems are particular cases of the following generic system of FBSDEs of McKean-Vlasov type (MKV FBSDE for short)

$$\begin{cases} dX_t = B(t, X_t, \mathcal{L}(X_t, Y_t, Z_t | W^0), Y_t, Z_t, Z_t^0) dt \\ \quad + \sigma(t, X_t, \mathcal{L}(X_t, Y_t, Z_t | W^0), Y_t, Z_t, Z_t^0) dW_t \\ \quad + \sigma^0(t, X_t, \mathcal{L}(X_t, Y_t, Z_t | W^0), Y_t, Z_t, Z_t^0) dW_t^0, \\ dY_t = -F(t, X_t, \mathcal{L}(X_t, Y_t, Z_t | W^0), Y_t, \sigma^T(t, X_t, \mathcal{L}(X_t, Y_t, Z_t | W^0), Y_t, Z_t, Z_t^0) Z_t, \\ \quad \sigma^{0T}(t, X_t, \mathcal{L}(X_t, Y_t, Z_t | W^0), Y_t, Z_t, Z_t^0) Z_t^0) dt \\ \quad + Z_t dW_t + Z_t^0 dW_t^0, \\ \mathcal{L}(X_0) = \mu_0, \quad Y_T = G(X_T, \mathcal{L}(X_T | W^0)). \end{cases}$$

**Remark 3.10.** *When there is no common noise,  $W^0$  and  $Z^0$  are dropped and the system becomes*

$$\begin{cases} dX_t = B(t, X_t, \mathcal{L}(X_t, Y_t, Z_t), Y_t, Z_t) dt + \sigma(t, X_t, \mathcal{L}(X_t, Y_t, Z_t), Y_t, Z_t) dW_t, \\ dY_t = -F(t, X_t, \mathcal{L}(X_t, Y_t, Z_t), Y_t, \sigma^T(t, X_t, \mathcal{L}(X_t, Y_t, Z_t), Y_t, Z_t) Z_t) dt + Z_t dW_t, \\ \mathcal{L}(X_0) = \mu_0, \quad Y_T = G(X_T, \mathcal{L}(X_T)). \end{cases} \quad (3.28)$$

*When the interactions are not through the state-action distribution but through the state distribution only,  $\mathcal{L}(X_t, Y_t, Z_t)$  is reduced to  $\mathcal{L}(X_t)$ .*

### 3.2.1.4 Master equation

As mentioned earlier, in the PDE system (3.24)–(3.26),  $u$  plays the role of the value function of a representative player when the rest of the population is at equilibrium. This function depends explicitly on  $t$  and  $x$  but, intuitively, a player's value function can also depend on the population distribution. When there is no common noise, this distribution evolves in a deterministic way, so knowing  $\mu_0$  and  $t$  as well as the control used by the population (which is the equilibrium control  $\hat{\alpha}$ , assuming the population is at equilibrium) is enough to recover  $\hat{\mu}(t)$ , *e.g.*, by solving the corresponding KFP equation (3.26). However, we can make this dependence explicit by considering a function  $\mathcal{U} : [0, T] \times \mathbb{R}^d \times \mathcal{P}(\mathbb{R}^d) \rightarrow \mathbb{R}$  such that

$$\mathcal{U}(t, x, \hat{\mu}(t)) = u(t, x), \quad (3.29)$$

where  $\hat{\mu} = (\hat{\mu}(t))_t$  is the mean-field equilibrium distribution flow. This correspondence is even more useful when common noise influences the dynamics of the players. In this case,  $u(t, x)$  is a random variable whereas  $\mathcal{U}$  is still a deterministic function and the lefthand side of (3.29) is random only due to  $\hat{\mu}(t)$ . This function  $\mathcal{U}$  has been instrumental in proving the convergence of finite-player Nash equilibria towards mean field Nash equilibria, see [42] for more details.

It turns out that, under suitable conditions,  $\mathcal{U}$  satisfies the a PDE that we will present below, introduced by Pierre-Louis Lions and called the Master equation. It involves partial derivatives with respect to the

probability measure argument in  $\mathcal{U}$ . We say that a function  $F : \mathcal{P}(\mathbb{R}^d) \rightarrow \mathbb{R}$  is  $\mathcal{C}^1$  if there exists a continuous map  $\frac{\delta F}{\delta \mu} : \mathcal{P}(\mathbb{R}^d) \times \mathbb{R}^d \rightarrow \mathbb{R}$  such that, for any  $\mu, \mu' \in \mathcal{P}(\mathbb{R}^d)$ ,

$$\lim_{s \rightarrow 0^+} \frac{F((1-s)\mu + s\mu') - F(\mu)}{s} = \int_{\mathbb{R}^d} \frac{\delta F}{\delta \mu}(\mu, y) d(\mu' - \mu)(y).$$

The derivative  $\frac{\delta F}{\delta \mu}$  is sometimes referred to as the flat derivative. If  $\frac{\delta F}{\delta \mu}$  is of class  $\mathcal{C}^1$  with respect to the second variable, the intrinsic derivative  $\partial_\mu F : \mathcal{P}(\mathbb{R}^d) \times \mathbb{R}^d \rightarrow \mathbb{R}$  is defined by

$$\partial_\mu F(\mu, y) = \partial_y \frac{\delta F}{\delta \mu}(\mu, y).$$

We will write  $\partial_\mu F(\mu)(y)$  instead of  $\partial_\mu F(\mu, y)$ . For more details, we refer to the lectures of Pierre-Louis Lions [188], as well as [41] and [52, Chapter 5].

We can now present the Master equation. To the best of our knowledge, the theory has not yet been developed for the general MFG model described above. We thus consider the case in which the volatility is not controlled and the interactions are only through the state distribution instead of the state-action distribution. For the sake of brevity, we omit the derivation and refer to *e.g.* [53, Section 4.4]. The Master equation is the following backward PDE, posed on the space  $[0, T] \times \mathbb{R}^d \times \mathcal{P}_2(\mathbb{R}^d)$ ,

$$\begin{aligned} & \partial_t \mathcal{U}(t, x, \mu) \\ & + b(t, x, \mu, \hat{\alpha}(t, x, \mu, \partial_x \mathcal{U}(t, x, \mu))) \cdot \partial_x \mathcal{U}(t, x, \mu) \\ & + \int_{\mathbb{R}^d} b(t, v, \mu, \hat{\alpha}(t, v, \partial_x \mathcal{U}(t, v, \mu))) \cdot \partial_\mu \mathcal{U}(t, x, \mu)(v) d\mu(v) \\ & + \frac{1}{2} \text{Tr} [(\sigma \sigma^T + \sigma^0 (\sigma^0)^T)(t, x, \mu) \partial_{xx}^2 \mathcal{U}(t, x, \mu)] \\ & + \frac{1}{2} \int_{\mathbb{R}^d} \text{Tr} [(\sigma \sigma^T + \sigma^0 (\sigma^0)^T)(t, v, \mu) \partial_v \partial_\mu \mathcal{U}(t, x, \mu)(v)] d\mu(v) \\ & + \frac{1}{2} \int_{\mathbb{R}^{2d}} \text{Tr} [(\sigma \sigma^T + \sigma^0 (\sigma^0)^T)(t, v, \mu) \partial_\mu^2 \mathcal{U}(t, x, \mu)(v, v')] d\mu(v) d\mu(v') \\ & + \int_{\mathbb{R}^d} \text{Tr} [(\sigma^0(t, x, \mu) (\sigma^0)^T)(t, v, \mu) \partial_x \partial_\mu \mathcal{U}(t, x, \mu)(v)] d\mu(v) \\ & + f(t, x, \mu, \hat{\alpha}(t, x, \mu, \partial_x \mathcal{U}(t, x, \mu))) = 0, \end{aligned}$$

for  $t \in [0, T]$ ,  $x \in \mathbb{R}^d$  and  $\mu \in \mathcal{P}_2(\mathbb{R}^d)$ , and with the terminal condition: for every  $x \in \mathbb{R}^d$  and  $\mu \in \mathcal{P}_2(\mathbb{R}^d)$ ,

$$\mathcal{U}(T, x, \mu) = g(x, \mu).$$

For more details on the analysis of this PDE, we refer the interested reader to the monographs [42], [53], Chapters 4 to 7], and [65] concerning the existence of classical solutions under suitable conditions.

### 3.2.2 The Sig-DFP algorithm for mean-field games with common noise

As seen in Definition 3.7, a mean-field equilibrium is a standard control problem (corresponding to the first item in the definition) plus a fixed point problem (corresponding to the second item). Motivated by MFG models with common noise, Min and Hu [193] proposed an algorithm called Sig-DFP utilizing the concept of signature in rough path theory [191] and fictitious play from game theory [36, 37]. Signature is used to accurately represent the conditional distribution of the state given the common noise, and fictitious play is used to solve the fixed-point problem and identify the equilibrium [43].

For a path  $x : [0, T] \rightarrow \mathbb{R}^d$ , the  $p$ -variation is defined by

$$\|x\|_p = \left( \sup_{D \subset [0, T]} \sum_{n=0}^{r-1} \|x_{t_{n+1}} - x_{t_n}\|^p \right)^{1/p},$$

where  $D \subset [0, T]$  denotes a partition  $0 \leq t_0 < t_1 < \dots < t_r \leq T$ . Let  $T((\mathbb{R}^d)) = \bigoplus_{k=0}^{\infty} (\mathbb{R}^d)^{\otimes k}$  be the tensor algebra. Let  $\mathcal{V}^p([0, T], \mathbb{R}^d)$  be the space of continuous mappings from  $[0, T]$  to  $\mathbb{R}^d$  with finite  $p$ -variation, equipped with norm  $\|\cdot\|_{\mathcal{V}^p} = \|\cdot\|_{\infty} + \|\cdot\|_p$ .

**Definition 3.11** (Signature). *Let  $X \in \mathcal{V}^p([0, T], \mathbb{R}^d)$  such that the following integral is well defined. The signature of  $X$ , denoted by  $S(X)$ , is the element of  $T((\mathbb{R}^d))$  defined by  $S(X) = (1, X^1, \dots, X^k, \dots)$  with*

$$X^k = \int_{0 < t_1 < t_2 < \dots < t_k < T} dX_{t_1} \otimes \dots \otimes dX_{t_k}. \quad (3.30)$$

Denoting by  $S^M(X)$  the truncated signature of  $X$  of depth  $M$ , i.e.,  $S^M(X) = (1, X^1, \dots, X^M)$  which has the dimension  $\frac{d^{M+1}-1}{d-1}$ .

In the current setting,  $X$  is a semi-martingale, thus equation (3.30) is understood in the Stratonovich sense. The signature has many nice properties, including the following ones. First, it characterizes paths uniquely up to the tree-like equivalence, and the equivalence is removed if at least one dimension of the path is strictly increasing [32]. Therefore, in practice one usually augments the original path  $X_t$  with the time dimension, i.e., working with  $\hat{X}_t = (t, X_t)$  since  $S(\hat{X})$  characterizes paths  $\hat{X}$  uniquely. Second, terms in the signature present a factorial decay property [190], which implies that a path can be well approximated with just a few terms in the signature (i.e., a small  $M$ ). Last, As a feature map of sequential data, the signature has a universality property [33], which is summarized below.

Let  $p \geq 1$  and  $f : \mathcal{V}^p([0, T], \mathbb{R}^d) \rightarrow \mathbb{R}$  be a continuous function. For any compact set  $K \subset \mathcal{V}^p([0, T], \mathbb{R}^d)$ , if  $S(x)$  is a geometric rough path (see [191, Definition 3.13] for a detailed definition) for any  $x \in K$ , then for any  $\epsilon > 0$ , there exists a linear functional  $l$  in the dual space of  $T((\mathbb{R}^d))$  such that

$$\sup_{x \in K} |f(x) - \langle l, S(x) \rangle| < \epsilon.$$

Motivated by the unique characterization of  $(W_s^0)_{s \in [0, t]}$  by  $S(\hat{W}_t^0)$  and the factorial decay property, one can approximate

$$\nu_t \equiv \mathcal{L}(X_t, \alpha_t | \mathcal{F}_t^0) = \mathcal{L}(X_t, \alpha_t | S(\hat{W}_t^0)),$$

by  $\mathcal{L}(X_t, \alpha_t | S^M(\hat{W}_t^0))$ , for  $\hat{W}_t^0 = (t, W_t^0)$ . In particular, if the mean-field interaction is through moments  $\bar{\nu}_t = \mathbb{E}[\iota(X_t, \alpha_t) | \mathcal{F}_t^0]$ , for some measurable function  $\iota$ , the approximation can be arbitrarily accurate for sufficiently large  $M$ , see [193, Lemma 4.1]. Then [193] proposed to use the approximation

$$\bar{\nu}_t \approx \langle \tilde{l}, S^M(\hat{W}_t^0) \rangle, \quad \text{where } \tilde{l} = \arg \min_{\beta} \|\mathbf{y} - \mathbf{X}\beta\|^2, \quad \mathbf{y} = \{\iota(X_t(\omega_i), \alpha_t(\omega_i))\}_{i=1}^N, \quad \mathbf{X} = \{S^M(\hat{W}_t^0(\omega_i))\}_{i=1}^N, \quad (3.31)$$

where  $\omega_i$  denotes the  $i^{th}$  sample path. The rational behind this approximation is the universality of signatures and the interpretation of ordinary linear regression: the least square minimization gives the best possible prediction of  $\mathbb{E}[\mathbf{y} | \mathbf{X}]$  using linear relations. Once  $\tilde{l}$  is obtained, the prediction on an unseen common noise is efficient:  $\bar{\nu}_t(\tilde{\omega}) \approx \langle \tilde{l}, S^M(\hat{W}_t^0(\tilde{\omega})) \rangle$  for any  $\tilde{\omega}$  and  $t$ .

Then finding the mean-field equilibrium is broken down into the following steps. We start with an initial value  $\bar{\nu}^{(0)}$ . Then, we solve the standard control problem given  $\bar{\nu}^{(0)}$  in (3.23) in the spirit of [121]. From here, we approximate  $\bar{\nu}^{(1)}$  via signature using (3.31), i.e., compute  $\tilde{l}^{(1)}$ . These steps are repeated until convergence. The update of  $\bar{\nu}_t$  from step to step is done by averaging  $\tilde{l}^{(n)}$ . The Sig-DFP algorithm consists of repeatedly solving (3.22)–(3.23) for a given  $\bar{\nu}$  using deep learning in the spirit of [121], and passing the obtained  $\bar{\nu}$  to the next iteration by using signatures. A flowchart illustrating the ideas is given in Figure 12.

More precisely, at each step, given a proxy  $\hat{\nu}^{(k-1)}$  of the equilibrium distribution  $\hat{\nu}$ , the problem (3.22)–(3.23) becomes a standard stochastic control and is solved by using the direct parameterization approach reviewed in Section 2.2.1: the loss function will be the discretized version of (3.23),  $\check{X}$  will be follow the Euler scheme of (3.22) with  $\nu$  replaced by  $\hat{\nu}^{(k-1)}$  and so do  $f$  and  $g$ , and the control  $\alpha_{t_n}$  is parameterized by a neural network of the following form

$$\alpha_{t_n} = \alpha(t_n, \check{X}_{t_n}, \hat{\nu}_{t_n}^{(k-1)}; \theta),$$

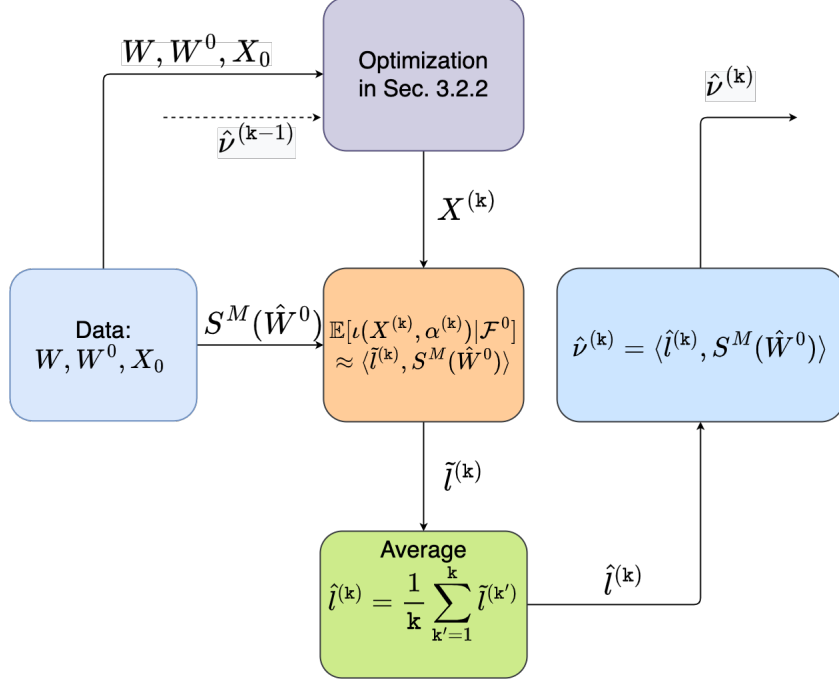


Figure 12: Flowchart of one iteration in the Sig-DFP Algorithm. Input: idiosyncratic noise  $W$ , common noise  $W^0$ , initial position  $X_0$  and vector  $\hat{\nu}^{(k-1)}$  from the last iteration. Output: vector  $\hat{\nu}^{(k)}$  for the next iteration.

which takes  $\hat{\nu}_{t_n}^{(k-1)}$  as an extra input on top of  $(t_n, \tilde{X}_{t_n})$ . The optimizer  $\theta^*$  obtained in this way gives  $\alpha_{t_n}^{(k)}$ , with which the optimized state process paths are simulated. The conditional law, denoted by  $\nu^{(k)}$ , is approximated using signatures via (3.31). This finishes one iteration of fictitious play. Denote by  $\tilde{\nu}^{(k)}$  the approximation of  $\nu^{(k)}$ , we then pass  $\tilde{\nu}^{(k)}$  to the next iteration via updating  $\hat{\nu}^{(k)} = \frac{1}{k} \tilde{\nu}^{(k)} + \frac{k-1}{k} \hat{\nu}^{(k-1)}$  by averaging the coefficients obtained in (3.31). We summarize it in Algorithm 5 in Appendix C; see [193, Appendix B] for the implementation details.

**Remark 3.12** (Theoretical analysis). *In [193] Min and Hu provided a proof of convergence of this algorithm showing that, under suitable assumptions, the difference between the  $k^{th}$  iteration solution and the mean-field equilibrium can be made arbitrarily small, provided that  $k$  is sufficient large and  $\nu^{(k)}$  can be approximated sufficiently well by truncated signatures.*

#### Numerical illustration: MFG of optimal consumption and investment.

We consider an extended heterogeneous MFG proposed by [168], where agents interact via both states and controls. The setup is similar to [169] except for including consumption and using power utilities. Each agent's type is characterized by a random vector  $\zeta = (\xi, \delta, \theta, b, \sigma, \sigma^0, \epsilon)$ , and the optimization problem reads

$$\sup_{\pi, c} \mathbb{E} \left[ \int_0^T U(c_t X_t (\Gamma_t m_t)^{-\theta}; \delta) dt + \epsilon U(X_T m_T^{-\theta}; \delta) \right],$$

where  $U(x; \delta) = \frac{1}{1-\frac{1}{\delta}} x^{1-\frac{1}{\delta}}$ ,  $\delta \neq 1$ , is the power utility function,  $X_t$  follows

$$dX_t = \pi_t X_t (b dt + \sigma dW_t + \sigma^0 dW_t^0) - c_t X_t dt, \quad (3.32)$$

and  $X_0 = \xi$ . The processes  $\Gamma_t = \exp \mathbb{E}[\log c_t | \mathcal{F}_t^0]$  and  $m_t = \exp \mathbb{E}[\log X_t | \mathcal{F}_t^0]$  are the mean-field interactions from the control and state processes. Two constraints are posed:  $X_t \geq 0$ ,  $c_t \geq 0$ .

The interpretation of this problem is as follows. There are infinitely many agents trade in a common investment horizon  $[0, T]$ , each invests between a bond (with constant return rate  $r$ ) and a private stock with dynamics  $dS_t/S_t = b dt + \sigma dW_t + \sigma^0 dW_t^0$ , and consume  $c_t$  of his wealth at time  $t$ . The portion of wealth into  $S_t$  is denoted by  $\pi_t$ . Assuming  $r \equiv 0$  without loss of generality, the wealth process reads (3.32). Then each agent aims to maximize his utility of consumption plus his terminal wealth compared to his peers' averages  $\Gamma_t$  and  $m_t$ . To relate it to the formulation (3.22)–(3.23),  $\alpha \equiv (\alpha^1, \alpha^2) = (\pi, c)$  will be a 2D control with the constraint  $\alpha_t^2 \geq 0$ ,  $b(t, x, \nu, \alpha) = ba^1 x - \alpha^2 x$ ,  $\sigma(t, x, \nu, \alpha) = \sigma a^1 x$ ,  $\sigma^0(t, x, \nu, \alpha) = \sigma^0 a^1 x$ ,  $f = -U$  and  $g = -U$ . The explicit solutions is derived in [168] and also summarized in [193, Appendix D].

For this experiment, we use truncated signatures of depth  $M = 4$ . The optimal controls  $(\pi_t, c_t)_{0 \leq t \leq 1}$  are parameterized by two neural networks  $\pi(\cdot; \theta)$  and  $c(\cdot; \theta)$ , each with three hidden layers of size 64 and taking  $(\zeta, t, X_t, m_t, \Gamma_t)$  as inputs due to the nature of heterogeneous extended MFG. Due to the extended mean-field interaction term  $\Gamma_t$ , we will propagate two conditional distribution flows, *i.e.*, two linear functionals  $\hat{l}^{(k)}, \hat{l}_c^{(k)}$  during each iteration of fictitious play. Instead of estimating  $m_t, \Gamma_t$  directly, we estimate  $\mathbb{E}[\log X_t | \mathcal{F}_t^0], \mathbb{E}[\log c_t | \mathcal{F}_t^0]$  by  $\langle \hat{l}^{(k)}, S^4(W_t^0) \rangle, \langle \hat{l}_c^{(k)}, S^4(W_t^0) \rangle$  and then take exponential to get  $m_t, \Gamma_t$ . To ensure the non-negativity condition of  $X_t$ , we evolve  $\log X_t$  and then take exponential to get  $X_t$ . For optimal consumption,  $c(\cdot; \theta)$  is used to predicted  $\log c_t$  and thus  $\exp c(\cdot; \theta)$  gives the predicted  $c_t$ . With 600 iterations of fictitious play and a learning rate of 0.1 decaying by a factor of 5 for every 200 iterations, the relative  $L^2$  errors for  $\pi_t, c_t, m_t, \Gamma_t$  are 0.1126, 0.0614, 0.0279, 0.0121, respectively. Figure 13 compares  $X$  and  $m$  to their approximations, and plots the maximized utilities. Further comparison with the existing literature, different choices of truncation  $M$ , and the ability to deal with higher  $m_0$  are also discussed in [193].

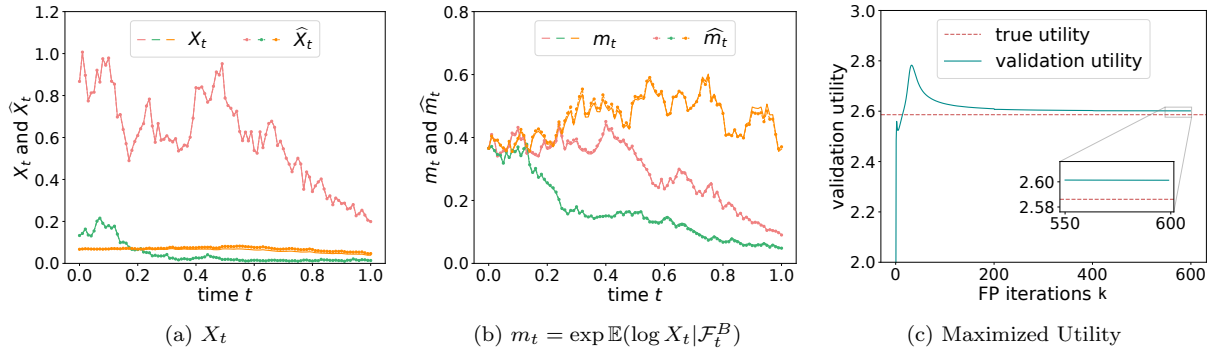


Figure 13: MFG of optimal consumption and investment in Section 3.2.2. Panels (a) and (b) give three trajectories of  $X_t$  and  $m_t = \exp(\mathbb{E}[\log X_t | \mathcal{F}_t^0])$  (solid lines) and their approximations  $\hat{X}_t$  and  $\hat{m}_t$  (dashed lines) using different  $(X_0, W, W^0)$  from validation data. Panel (c) shows the maximized utility computed using validation data over fictitious play iterations. Parameter choices are:  $\delta \sim U(2, 2.5)$ ,  $b \sim U(0.25, 0.35)$ ,  $\sigma \sim U(0.2, 0.4)$ ,  $\theta, \xi \sim U(0, 1)$ ,  $\sigma^0 \sim U(0.2, 0.4)$ ,  $\epsilon \sim U(0.5, 1)$ .

### 3.2.3 Deep learning for mean-field PDE systems

We now consider the PDE systems describing the equilibrium or social optimum in MFG or MFC, respectively. The Deep Galerkin Method (DGM) introduced in [227] and reviewed in Section 2.5 has been adapted to solve such PDE systems, see [8, 55, 221, 40, 187, 176]. We recall that the principle of the method is, for a single PDE, to replace the unknown function by a neural network and to optimize the parameters so as to minimize the residual of the PDE.

For the sake of the presentation, we consider the MFG PDE system (3.24)–(3.26). In line with the DGM method described in section 2.5, we proceed as follows. First, the MFG PDE system is rewritten as a minimization problem over the pair consisting of the density and the value function. The loss function is the sum of the two PDE residuals, as well as penalization terms for the initial and terminal conditions.

Instead of the whole state space  $\mathbb{R}^d$ , we focus on a compact subset  $\tilde{\mathcal{Q}} \subset \mathbb{R}^d$ . If needed, extra penalization terms taking into account the boundary conditions can be added in the loss function. To be specific, we introduce the following loss function

$$L(\mu, u) = L^{(\text{KFP})}(\mu, u) + L^{(\text{HJB})}(\mu, u),$$

which is composed of one term for each PDE of the MFG system (3.24)–(3.26). Each term is itself split into two terms: one for the residual inside the domain and one for the initial or terminal condition. The KFP loss function is

$$L^{(\text{KFP})}(\mu, u) = C^{(\text{KFP})} \left\| \partial_t \mu - \sum_{i,j} \frac{\partial^2}{\partial x_i \partial x_j} (D_{i,j} \mu) + \text{div}(\mu b) \right\|_{L^2([0,T] \times \tilde{\mathcal{Q}})}^2 + C_0^{(\text{KFP})} \|\mu(0) - \mu_0\|_{L^2(\tilde{\mathcal{Q}})}^2,$$

with  $\nu_t = \mu_t \circ (I_d, \alpha(t, \cdot))^{-1}$  where  $\alpha(t, x) = \alpha(t, x, \nu_t, \nabla_x u(t, x), \text{Hess}_x u(t, x))$ , and  $D$  and  $b$  are defined as:

$$D(t, x) = \frac{1}{2} \sigma(t, x, \nu_t, \alpha(t, x)) \sigma(t, x, \nu_t, \alpha(t, x))^T, \quad b(t, x) = b(t, x, \nu_t, \alpha(t, x)).$$

The HJB loss function is

$$L^{(\text{HJB})}(\mu, u) = C^{(\text{HJB})} \left\| \partial_t u + \min_{\alpha \in \mathcal{A}} H(\cdot, \cdot, \nu, \nabla_x u, \text{Hess}_x u, \alpha) \right\|_{L^2([0,T] \times \tilde{\mathcal{Q}})}^2 + C_T^{(\text{HJB})} \|u(T) - g(\cdot, \mu(T))\|_{L^2(\tilde{\mathcal{Q}})}^2,$$

with  $H$  defined by (3.25). The weights  $C^{(\text{KFP})}$ ,  $C_0^{(\text{KFP})}$ ,  $C^{(\text{HJB})}$ , and  $C_T^{(\text{HJB})}$  are positive constants that are used to tune the importance of each component relatively to the other components. If  $(\mu, u)$  is a smooth enough solution to the PDE system (3.24)–(3.26), then  $L(\mu, u) = 0$ . From here, the same strategy as in the DGM can be applied: one can look for an approximate solution using a class of parameterized functions for  $\mu$  and  $u$ , replace the  $L^2$  norms by integrals, and use samples to get Monte Carlo estimates; see [227] and Section 2.5 for more details.

**Remark 3.13.** *The same ideas can be applied to tackle the PDE systems arising in MFC, or other settings such as ergodic MFG. In this latter case, the initial and terminal conditions are replaced by normalization conditions; see [174]. Furthermore, if the PDE system was initially posed on a bounded domain and the solution had to satisfy boundary conditions, then these extra conditions could be dealt with by adding more penalty terms. See e.g., [55] for more details on these settings. For MFC with nonsmooth costs, Reisinger, Stockinger and Zhang [216] developed an iterative algorithm incorporating the gradient information and the proximal map of the nonsmooth cost.*

### Numerical illustration: a mean-field model of optimal execution.

We now present an example based on a model of optimal execution. This model is similar to the one studied in Subsection 2.2.3. We consider a population of traders in which each trader wants to liquidate  $Q_0$  shares of a given stock by a fixed time horizon  $T$ . At time  $t \in [0, T]$ , we denote by  $S_t$  the price of the stock, by  $Q_t$  the inventory (i.e., number of shares) held by the representative trader, and by  $X_t$  their wealth. These state variables are subject to the following dynamics

$$\begin{cases} dS_t = \gamma \bar{\mu}_t dt + \sigma dW_t, \\ dQ_t = \alpha_t dt, \\ dX_t = -\alpha_t (S_t + \kappa \alpha_t) dt. \end{cases}$$

The evolution of the price  $S$  is stochastic, representing that it can not be predicted with certainty. The randomness, scaled by  $\sigma$ , comes in through a standard Wiener process  $W$ . Furthermore, the drift of  $S$  captures the permanent price impact  $\gamma \bar{\mu}_t$  at time  $t$ . Here  $\gamma > 0$  is a multiplicative constant and  $\bar{\mu}_t$  is the aggregate trading rate of all the traders. The control  $\alpha_t$  at time  $t$  corresponds to the individual rate of trading of the representative trader. Last,  $\kappa > 0$  is a constant that represents a quadratic transaction cost.

We assume that the representative agent tries to maximize the following quantity, in which the first two terms reflect their payoff while the last two terms captures their risk aversion

$$\mathbb{E} \left[ X_T + Q_T S_T - A|Q_T|^2 - \phi \int_0^T |Q_t|^2 dt \right].$$

The constants  $\phi > 0$  and  $A > 0$  give weights to penalties for holding inventory through time and at the terminal time, respectively.

**Remark 3.14.** *Except for the fact that  $\bar{\mu}_t$  is here endogenous, this is the model considered in [61], to which a deep learning method has been applied in [180] to approximate the optimal control on real data.*

In contrast with the model studied in Subsection 2.2.3, the model considered here is not linear-quadratic and the inventory is not directly subject to random shocks. We refer the interested reader to [60] and [59] for more details and variants of these models.

Although this problem is formulated with three state variables, we can actually reduce the complexity of the problem in the following way. When  $(\bar{\mu}_t)_{0 \leq t \leq T}$  is given, the optimal control of the representative agent can be found by solving an HJB equation. Following [61], the value function  $V(t, x, s, q)$  can be decomposed as  $V(t, x, s, q) = x + qs + v(t, q)$  for some function  $v$  which is a solution to

$$-\gamma \bar{\mu} q = \partial_t v - \phi q^2 + \sup_{\alpha} \{\alpha \partial_q v - \kappa \alpha^2\},$$

with terminal condition  $v(T, q) = -Aq^2$ . The maximizer in the supremum leads to the optimal control, which can be expressed as:  $\alpha_t^*(q) = \frac{\partial_q v(t, q)}{2\kappa}$ . Based on this and going back to the consistency condition yields that, at equilibrium, the aggregate trading rate is

$$\bar{\mu}_t = \int \alpha_t^*(q) \mu(t, dq) = \int \frac{\partial_q v(t, q)}{2\kappa} \mu(t, dq),$$

where  $\mu(t, \cdot)$  is the distribution of inventories at time  $t$  satisfying the KFP PDE:

$$\partial_t \mu + \partial_q \left( \mu \frac{\partial_q v(t, q)}{2\kappa} \right) = 0, t \geq 0, \quad \mu(0, \cdot) = \mu_0.$$

As a consequence, the equilibrium solution of the MFG satisfies

$$\begin{cases} -\gamma \bar{\mu} q = \partial_t v - \phi q^2 + \frac{|\partial_q v(t, q)|^2}{4\kappa}, \\ \partial_t \mu + \partial_q \left( \mu \frac{\partial_q v(t, q)}{2\kappa} \right) = 0, \\ \bar{\mu}_t = \int \frac{\partial_q v(t, q)}{2\kappa} \mu(t, dq), \\ \mu(0, \cdot) = \mu_0, v(T, q) = -Aq^2. \end{cases} \quad (3.33)$$

The mean-field coupling between the two equations is non-local since it involves  $\bar{\mu}_t$ , and it combines the population distribution with the HJB solution. The value function, the associated control, and the mean of the distribution can be computed by solving a system of ODEs, which provides a benchmark to test numerical methods. We refer to [44] for more details.

Moreover, [8] proposed a further change of variables to simplify the numerical computations and then used the DGM to approximate the solution of the transformed PDE system. Here, to simplify the presentation, we stick to the above PDE system (3.33) and solve it directly using DGM. The initial and terminal conditions are imposed by penalization. For the non-local term  $\bar{\mu}_t$ , we use Monte Carlo samples to estimate the integral. In the implementation, we used the following values for the parameters:  $T = 1$ ,  $\sigma = 0.3$ ,  $A = 1$ ,  $\phi = 1$ ,  $\kappa = 1$ ,  $\gamma = 1$ , and a Gaussian initial distribution with mean 4 and variance 0.3. To ensure that the neural network for the distribution always outputs positive values, we used on the last layer the exponential function as an activation function. Figure 14 shows the evolution of the distribution  $m$ . Figure 15 shows the control obtained from the neural network approximating the HJB solution. The final distribution is concentrated near 0, which is consistent with the intuition that the traders need to liquidate. Furthermore, the learnt control coincides with the theoretical optimal control that can be computed by solving an ODE system [44].

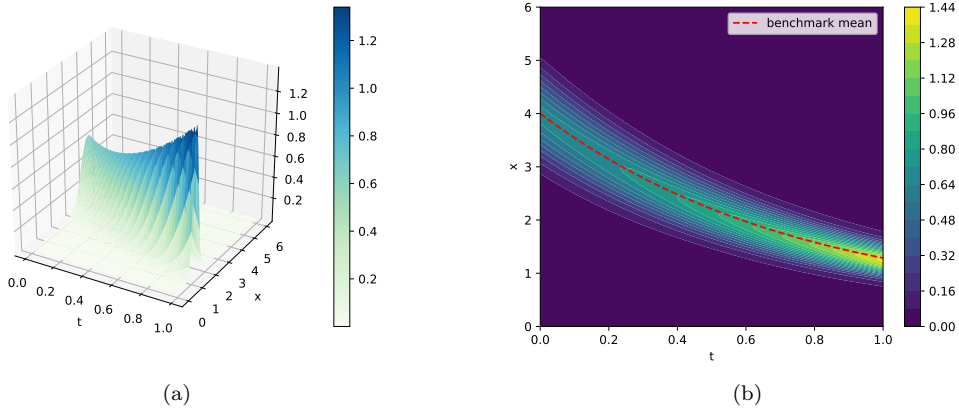


Figure 14: Trade crowding MFG example in Section 3.2.3 solved by DGM. Evolution of the distribution  $m$ . Left: surface with the horizontal axes representing time and space and the vertical axis representing the value of the density. Right: contour plot of the density with a dashed red line corresponding to the mean of the density computed by the semi-explicit formula.

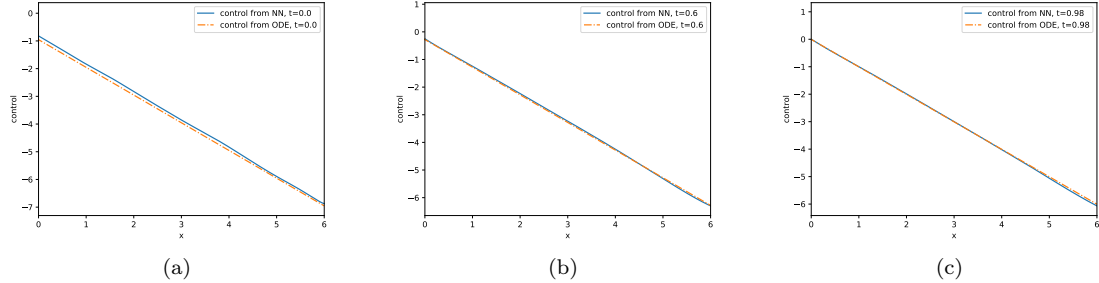


Figure 15: Trade crowding MFG example in Section 3.2.3 solved by DGM. Each plot corresponds to the control at a different time step: Optimal control  $\alpha^*$  (dashed line) and learnt control (full line).

### 3.2.4 Deep learning for McKean-Vlasov FBSDE systems

We now explain how to adapt the Deep BSDE method introduced in [82] and reviewed in Section 2.3.1 to mean-field FBSDEs. We recall that the principle of the method is to use neural networks to approximate  $Y_0$  and  $(Z_t)_{t \in [0, T]}$  and to train the neural network parameters by relying on Monte Carlo samples until the terminal condition is approximately matched. In the mean-field setting, the same idea can be used to solve forward-backward systems of McKean-Vlasov (MKV) SDEs; see [90, 56, 94, 120].

Let us consider the FBSDE (3.28) in the absence of common noise, with interactions through the state distribution only, and uncontrolled volatility. We rewrite the problem as: minimize over  $y_0 : \mathbb{R}^d \rightarrow \mathbb{R}^d$  and  $z : \mathbb{R}_+ \times \mathbb{R}^d \rightarrow \mathbb{R}^{d \times m}$  the cost functional

$$J(y_0, z) = \mathbb{E} \left[ |Y_T^{y_0, z} - G(X_T^{y_0, z}, \mathcal{L}(X_T^{y_0, z}))|^2 \right],$$

where  $(X^{y_0, z}, Y^{y_0, z})$  solves

$$\begin{cases} dX_t^{y_0, z} = B(t, X_t^{y_0, z}, \mathcal{L}(X_t^{y_0, z}), Y_t^{y_0, z}) dt + \sigma(t, X_t) dW_t, & t \geq 0, \\ dY_t^{y_0, z} = -F(t, X_t^{y_0, z}, \mathcal{L}(X_t^{y_0, z}), Y_t^{y_0, z}, \sigma^T(t, X_t) z(t, X_t^{y_0, z})) dt + z(t, X_t^{y_0, z}) dW_t, & t \geq 0, \\ X_0^{y_0, z} \sim \mu_0, \quad Y_0^{y_0, z} = y_0(X_0^{y_0, z}). \end{cases}$$

The above problem is an MFC problem if we view  $(X_t^{y_0, z}, Y_t^{y_0, z})$  as state and  $(y_0, z)$  as control. Under suitable conditions, the optimally controlled process  $(X, Y)$  solves the MKV FBSDE system (3.28) and vice versa.

Then, to be able to implement this method, we can proceed similarly to the method described in Section 2.2.3. The mean field distribution can be approximated by an empirical distribution based on a finite population of interacting particles. Furthermore, the controls  $y_0$  and  $z$  can be replaced by neural networks, say  $y_\theta$  and  $z_\omega$  with parameters  $\theta$  and  $\omega$  respectively. Time can be discretized using for instance an Euler-Maruyama scheme. We thus obtain a new optimization problem over finite-dimensional parameters that can be adjusted using SGD.

**Remark 3.15** (Theoretical analysis). *Motivated by numerical schemes and in particular the above adaptation of the deep BSDE method [82, 124] to MKV FBSDEs, Reisinger, Stockinger and Zhang in [217] analyzed a posteriori error for approximate solutions based on a discrete time scheme and a finite population of interacting particles. [120] proposed a deep learning method for computing MKV FBSDEs with a general form of mean-field interactions, and proved that the convergence of the proposed method is free of the curse of dimensionality by using a special class of integral probability metrics previously developed in [118].*

Although we focus here on the continuous-state space setting, the same strategy can be applied to finite-state MFGs; see, e.g., [16, 15].

#### Numerical illustration: linear-quadratic mean-field game in systemic risk problems.

We now consider the MFG version of the systemic risk model introduced in Section 1.2 which has been studied in Section 3.1.1 and revisited in Section 3.1.2. This MFG mean-field game has been analyzed in [49]. Given a mean-field flow  $\mu = (\mu_t)_{t \in [0, T]}$ , the log-monetary reserves of a typical bank evolves according to the dynamics:

$$dX_t = [a(\bar{\mu}_t - X_t) + \alpha_t] dt + \sigma \left( \rho dW_t^0 + \sqrt{1 - \rho^2} dW_t \right).$$

The standard Brownian motions  $W^0$  and  $W$  are independent, in which  $W$  stands for the idiosyncratic noises and  $W^0$  denotes the systemic shock, which is an example of common noise (see also Section 3.2.2).

The cost functions  $f$  and  $g$  appearing in (3.21) takes the following form:

$$f(t, x, \nu, \alpha) = \frac{1}{2} \alpha^2 - q\alpha(\bar{\mu} - x) + \frac{\epsilon}{2}(\bar{\mu} - x)^2, \quad g(x, \nu) = \frac{c}{2}(\bar{\mu} - x)^2,$$

which depend only on the mean  $\bar{\mu} = \mathbb{E}_{X \sim \mu}[X]$  of the first marginal of the state-action distribution  $\nu$ . It has been shown in [49] that, in the MFG setting, the open-loop equilibrium is the same as the closed-loop Nash equilibrium, and it admit an explicit solution. Furthermore, it can be characterized using an MKV FBSDE system, that we omit for brevity; see [49] for the details. If  $\rho = 0$ , then one can apply directly the method described above, with  $y_0$  a function of  $X_0$  and  $z$  a function of  $(t, X_t)$ . When  $\rho > 0$ , two changes need to be made: first, there is an extra process  $Z^0$  to be learned, for which we use a neural network approximation as for  $Z$ ; second, we expect the random variables  $Z_t$  and  $Z_t^0$  to depend not only on  $X_t$  but also on the past of the common noise. In general, this would mean learning functions of the common noise's trajectory. However, in the present case, it is enough to rely on finite-dimensional information. Here, we add  $\bar{\mu}_t$  as an input to the neural networks playing the roles of  $Z_t$  and  $Z_t^0$ , and this is sufficient to learn the optimal solution, see [49].

Figure 16 displays three sample trajectories of  $X$  and  $Y$ , obtained after training the neural networks for  $Y_0, Z$  and  $Z^0$ , by simulating in a forward fashion the trajectories of  $X$  and  $Y$  using Monte Carlo samples and the same Euler-Maruyama scheme used in the numerical method. One can see that the approximation is better for  $X$  than for  $Y$ , particularly towards the end of the time interval. This is probably because the BSDE is solved by guessing the initial point instead of starting from a terminal point, resulting in errors accumulated over time. Furthermore, [56] shows that the results improve as the number of time steps, particles, and units in the neural network increase. In the numerical experiments presented here, we used the following parameters:  $\sigma = 0.5, \rho = 0.5, q = 0.5, \epsilon = q^2 + 0.5 = 0.75, a = 1, c = 1.0$  and  $T = 0.5$ .

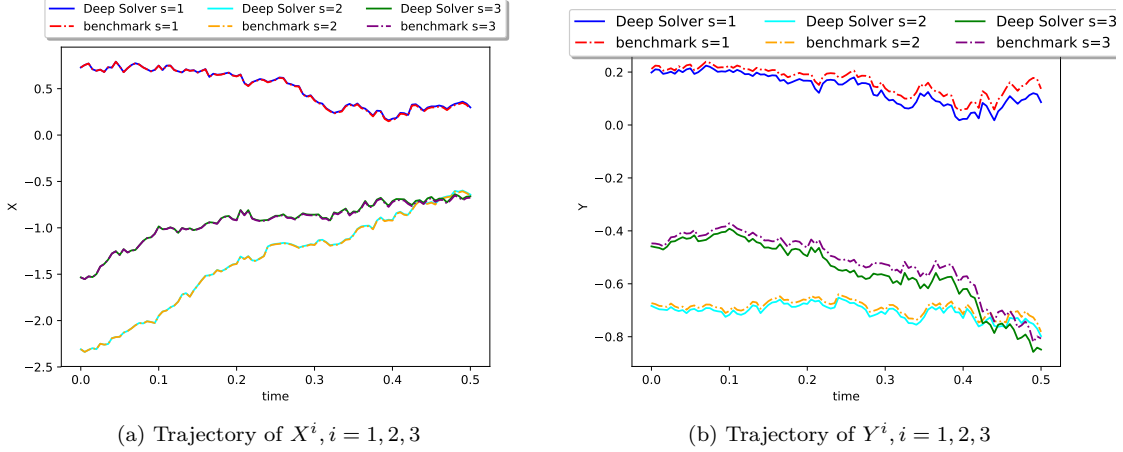


Figure 16: Systemic risk MFG example solved by the algorithm described in Section 3.2.4. Left: three sample trajectories of  $X$  using the neural network approach ('Deep Solver' with full lines, in cyan, blue, and green) or using the analytical formula ('benchmark' with dashed lines, in orange, red and purple). Right: three sample trajectories of  $Y$  (similar labels and colors). Note that the analytical formula satisfies the true terminal condition, whereas the solution computed by neural networks satisfies it only approximately since the trajectories are generated in a forward way starting from the learnt initial condition.

### 3.2.5 Deep learning for mean-field master equation

We now turn our attention to the question of solving the MFG master equation (Section 3.2.1.4). Intuitively, the main motivation is to be able to approximate the value function of a representative player for any population distribution. This is in contrast with the methods presented above, which are based on controls that are fully decentralized in the sense that they are functions of the time and the state of the agent only. The fact that they do not depend on the population distribution is an advantage in that it simplifies the implementation, but it is also a limitation since the agent is not able to react to new distributions. For example, if the initial distribution is not known, the agent is not able to solve the forward equation and hence she is not able to anticipate the distribution at future times. The presence of common noise in the dynamics poses a similar challenge. For these reasons, being able to approximately solve the master equation is interesting for applications. When the state space is continuous, the distribution is an infinite dimensional object which is hard to approximate. For simplicity, we will thus focus here on a finite-state setting, in which case the distribution is simply a histogram. The convergence of finite-state MFGs to continuous-state MFGs has been studied for instance in [115]. Even though assuming the state space to be finite resolves the question of approximating the distribution, the master equation is posed on a high-dimensional space if the number of states is large. We will hence rely once again on neural networks to approximate the solution to this equation.

#### Master equation for finite state MFG.

We consider a finite-state MFG model based on the presentation of such models in [52, Section 7.2]. We consider a finite state space  $\mathcal{E} = \{e_1, \dots, e_d\}$  and an action space  $\mathcal{A} \subseteq \mathbb{R}^k$ , which can be discrete or continuous. The states can be viewed as one-hot vectors, *i.e.*, as the elements of a canonical basis of  $\mathbb{R}^d$ . Then, the set of probability distributions on  $\mathcal{E}$  is the simplex  $\{m \in \mathbb{R}^d \mid \sum_{i=1}^d m_i = 1\}$ , and we will sometimes write  $m(x)$  instead of  $m(\{x\})$ . The running cost and the terminal cost are denoted by  $f : \mathcal{E} \times \mathcal{P}(\mathcal{E}) \times \mathcal{A} \rightarrow \mathbb{R}$  and  $g : \mathcal{E} \times \mathcal{P}(\mathcal{E}) \rightarrow \mathbb{R}$ . The dynamics are given by a jump rate function denoted by  $\lambda : \mathcal{E} \times \mathcal{P}(\mathcal{E}) \times \mathcal{A} \rightarrow \mathbb{R}$ . We denote by  $\mathbb{R}^{\mathcal{E}}$  the set of functions from  $\mathcal{E}$  to  $\mathbb{R}$ .

In this context, a finite state MFG equilibrium is a pair  $(\hat{m}, \hat{\alpha})$  with  $\hat{m} : [0, T] \times \mathcal{E} \rightarrow \mathbb{R}$  and  $\hat{\alpha} : [0, T] \times \mathcal{E} \rightarrow \mathcal{A}$  such that

1.  $\hat{\alpha}$  minimizes

$$J_{\hat{m}}^{MFG} : \alpha \mapsto \mathbb{E} \left[ \int_0^T f(X_t^{\hat{m}, \alpha}, \hat{m}(t, \cdot), \alpha(t, X_t^{\hat{m}, \alpha})) dt + g(X_T^{\hat{m}, \alpha}, \hat{m}(T, \cdot)) \right],$$

subject to:  $X^{\hat{m}, \alpha} = (X_t^{\hat{m}, \alpha})_{t \geq 0}$  is a nonhomogeneous  $\mathcal{E}$ -valued Markov chain with transition probabilities determined by the  $Q$ -matrix of rates  $q^{\hat{m}, \alpha} : [0, T] \times \mathcal{E} \times \mathcal{E} \rightarrow \mathbb{R}$  given by

$$q^{\hat{m}, \alpha}(t, x, x') = \lambda(x, x', \hat{m}(t, \cdot), \alpha(t, \cdot)), \quad (t, x, x') \in [0, T] \times \mathcal{E} \times \mathcal{E},$$

and  $X_0^{\hat{m}, \alpha}$  has distribution with density  $m_0$ ;

2. For all  $t \in [0, T]$ ,  $\hat{m}(t, \cdot)$  is the law of  $X_t^{\hat{m}, \hat{\alpha}}$ .

The Hamiltonian of the problem is defined as

$$H(x, m, h) = \sup_{\alpha \in \mathcal{A}} -L(x, m, h, \alpha)$$

where  $L : \mathcal{E} \times \mathcal{P}(\mathcal{E}) \times \mathbb{R}^\mathcal{E} \times \mathcal{A} \rightarrow \mathbb{R}$  denotes the Lagrangian

$$L(x, m, h, \alpha) = \sum_{x' \in \mathcal{E}} \lambda(x, x', m, \alpha) h(x') + f(x, m, \alpha).$$

Under suitable assumptions on the model, the supremum in the definition of  $H$  admits a unique maximizer for every  $(x, m, h) \in \mathcal{E} \times \mathcal{P}(\mathcal{E}) \times \mathbb{R}^\mathcal{E}$ , that we denote by

$$\alpha^*(x, m, h) = \arg \max_{\alpha \in \mathcal{A}} -L(x, m, h, \alpha). \quad (3.34)$$

The coefficients of the rates of the  $Q$ -matrix when using the optimal control are denoted by

$$q^*(x, x', m, h) = \lambda(x, x', m, \alpha^*(x, m, h)),$$

where  $q^* : \mathcal{E} \times \mathcal{E} \times \mathcal{P}(\mathcal{E}) \times \mathbb{R}^\mathcal{E} \rightarrow \mathbb{R}$ .

Similarly to the continuous setting (see Section 3.2.1) the mean field Nash equilibrium can be characterized using a forward-backward system of deterministic or stochastic equations. Using the deterministic approach, the optimal conditions take the form of an ODE system (instead of a PDE system as in the continuous space case). The system is composed of a forward ODE for the mean field  $m : [0, T] \times \mathcal{E} \rightarrow \mathbb{R}$  and a backward ODE for the value function  $u : [0, T] \times \mathcal{E} \rightarrow \mathbb{R}$ . Under suitable assumptions (see, *e.g.*, [52, section 7.2]), there is a unique MFG equilibrium  $(\hat{m}, \hat{\alpha})$ , which is characterized by:

$$\hat{\alpha}(t, x) = \alpha^*(x, \hat{m}(t, \cdot), \hat{u}(t, \cdot)),$$

where  $\alpha^*$  is defined by (3.34) and  $(u, m)$  solves the forward-backward system

$$\begin{cases} 0 = -\partial_t \hat{u}(t, x) + H(x, \hat{m}(t, \cdot), \hat{u}(t, \cdot)), & (t, x) \in [0, T] \times \mathcal{E}, \\ 0 = \partial_t \hat{m}(t, x) - \sum_{x' \in \mathcal{E}} \hat{m}(t, x') q^*(x', x, \hat{m}(t, \cdot), \hat{u}(t, \cdot)), & (t, x) \in (0, T] \times \mathcal{E}, \\ \hat{u}(T, x) = g(x, \hat{m}(T, \cdot)), & \hat{m}(0, x) = m_0(x), \quad x \in \mathcal{E}. \end{cases}$$

This ODE system can be solved using for example techniques discussed in previous sections for forward-backward PDE or SDE systems. However, this assumes that the initial distribution  $m_0$  is known and when it is unknown, new techniques are required. We thus consider the master equation.

As in the continuous space case described in Section 3.2.1.4, the solution to the master equation makes the dependence of  $\hat{u}$  and  $\hat{m}$  completely explicit. In the present discrete space setting, the master equation can be written as follows (see, *e.g.*, [52, section 7.2])

$$-\partial_t \mathcal{U}(t, x, m) + H(x, m, \mathcal{U}(t, \cdot, m)) - \sum_{x' \in \mathcal{E}} h^*(m, \mathcal{U}(t, \cdot, m))(x') \frac{\partial \mathcal{U}(t, x, m)}{\partial m(x')} = 0, \quad (3.35)$$

for  $(t, x, m) \in [0, T] \times \mathcal{E} \times \mathcal{P}(\mathcal{E})$ , with the terminal condition  $\mathcal{U}(T, x, m) = g(x, m)$ , for  $(x, m) \in \mathcal{E} \times \mathcal{P}(\mathcal{E})$ . The function  $h^* : [0, T] \times \mathcal{P}(\mathcal{E}) \times \mathbb{R}^{\mathcal{E}} \times \mathcal{E} \rightarrow \mathbb{R}$  is defined as

$$h^*(m, u)(x') = \sum_{x \in \mathcal{E}} \lambda(x, x', m, \alpha^*(x, m, u))m(x).$$

Besides a simple representation of probability distributions, the fact that the state space is finite has another advantage: we do not need to involve the notions of derivative with respect to a measure discussed in Section 3.2.1.4. Instead, we can rely on standard partial derivatives with respect to the finite-dimensional inputs of  $\mathcal{U}$ . As a matter of fact, in the above equation,  $\frac{\partial \mathcal{U}(t, x, m)}{\partial m(x')}$  denotes the standard partial derivative of  $\mathbb{R}^d \ni m \mapsto \mathcal{U}(t, x, m)$  with respect to the coordinate corresponding to  $x'$  (recall that  $m$  is viewed as a vector of dimension  $d$ ). The analog of (3.29) in the continuous case is

$$\mathcal{U}(t, x, \hat{m}(t)) = \hat{u}(t, x), \quad (3.36)$$

where  $\hat{m} = (\hat{m}(t))_t$  is the mean-field equilibrium distribution flow. Notice that both  $\hat{m}$  and  $\hat{u}$  implicitly depend on the initial distribution  $m_0$ , but  $\mathcal{U}$  does not.

The master equation (3.35) is posed on a possibly high dimensional space since the number  $d$  of states can be large. To numerically solve this equation, we can thus rely on deep learning methods for high-dimensional PDEs, such as the DGM introduced in [227] and already discussed above in Sections 2.5 and 3.2.3. For the sake of completeness, let us mention that this technique boils down to approximating  $\mathcal{U}$  by a neural network, say  $\mathcal{U}_\theta$  with parameters  $\theta$ , and using SGD to adjust the parameters  $\theta$  such that the residual of (3.35) is minimized and the terminal condition is satisfied. SGD as described in Algorithm 1 in Appendix A.2 is used, where a sample is  $\xi = (t, x, m) \in [0, T] \times \mathcal{E} \times \mathcal{P}(\mathcal{E})$  and the loss function is

$$\mathcal{L}(\mathcal{U}_\theta, \xi) = \left| \partial_t \mathcal{U}_\theta(t, x, m) - H(x, m, \mathcal{U}_\theta(t, x, m)) + \sum_{x' \in \mathcal{E}} h^*(m, \mathcal{U}_\theta(t, x, m))(x') \frac{\partial \mathcal{U}_\theta(t, x, m)}{\partial m(x')} \right|^2.$$

**Remark 3.16.** *We have discussed here how to solve the master equation arising in finite-state MFGs. This yields an approach to solving the continuous space master equation described in Section 3.2.1.4 by first introducing a finite-state model that approximates the continuous model and then using the DGM method. Other methods could be investigated, such as the one proposed in [93]: a combination of dynamic programming, Monte Carlo simulations and symmetric neural networks is used to solve the Bellman equation arising in a continuous space MFG problem.*

### Numerical illustration: A Cybersecurity model.

Here we present an example of application of the above method. We consider the cybersecurity introduced in [164]; see also [52, Section 7.2.3]. Each player owns a computer and her goal is to avoid being infected by a malware. The state space is denoted by  $\mathcal{E} = \{DI, DS, UI, US\}$ , which represents the four possible states in which a computer can be depending on its protection level – defended (D) or undefended (U) – and on its infection status – infected (I) or susceptible (S) of infection. The player can choose to switch its protection level between D and U. The change is not instantaneous so the player can only influence the transition rate. We represent by “1” the fact that the player has the intention to change its level of protection (be it from D to U or from U to D). On the other hand, “0” corresponds to the situation where the player does not try to change her protection level. So the set of possible actions is  $\mathcal{A} = \{0, 1\}$ . When the action is equal to 1, the change of level of protection takes place at a rate  $\rho > 0$ . A computer in states DS or US might get infected either directly by a hacker or by getting the virus from an infected computer. We denote by  $v_H q_{inf}^D$  (resp.  $v_H q_{inf}^U$ ) the rate of infection from a hacker if the computer is defended (resp. undefended). We denote by  $\beta_{UU}\mu(\{UI\})$  (resp.  $\beta_{UD}\mu(\{UI\})$ ) the rate of infection from an undefended infected computer if the computer under consideration is undefended (resp. defended). Likewise, we denote by  $\beta_{DU}\mu(\{DI\})$  (resp.  $\beta_{DD}\mu(\{DI\})$ ) the rate of infection from a defended infected computer if the computer under consideration is undefended (resp. defended). Note that these rates involve the distribution since the probability of getting infected should increase with the number of infected computers in the rest of the population. Last, an

infected computer can recover and switch to the susceptible state at rate  $q_{rec}^D$  or  $q_{rec}^U$  depending on whether it is defended or not. These transition rates can be summarized in a matrix form: for  $m \in \mathcal{P}(\mathcal{E})$ ,  $a \in \mathcal{A}$ ,

$$\lambda(\cdot, \cdot, m, a) = (\lambda(x, x', m, a))_{x, x' \in \mathcal{E}} = \begin{pmatrix} \dots & P_{DS \rightarrow DI}^{m, a} & \rho a & 0 \\ q_{rec}^D & \dots & 0 & \rho a \\ \rho a & 0 & \dots & P_{US \rightarrow UI}^{m, a} \\ 0 & \rho a & q_{rec}^U & \dots \end{pmatrix},$$

where

$$\begin{aligned} P_{DS \rightarrow DI}^{m, a} &= v_H q_{inf}^D + \beta_{DD} m(\{DI\}) + \beta_{UD} m(\{UI\}), \\ P_{US \rightarrow UI}^{m, a} &= v_H q_{inf}^U + \beta_{UU} m(\{UI\}) + \beta_{DU} m(\{DI\}). \end{aligned}$$

The dots ( $\dots$ ) on each row stand for the value such that the sum of the coefficients on this row equals 0.

We assume that each player wants to avoid seeing her computer being infected, but protecting a computer costs some resources. So the running cost is of the form

$$f(t, x, \nu, \alpha) = -[k_D \mathbf{1}_{\{DI, DS\}}(x) + k_I \mathbf{1}_{\{DI, UI\}}(x)],$$

where  $k_D > 0$  is a protection cost to be paid whenever the computer is defended, and  $k_I > 0$  is a penalty incurred if the computer is infected. We consider  $g \equiv 0$  (no terminal cost).

By using the DGM, we train a neural network  $\mathcal{U}_\theta$  to approximate the solution  $\mathcal{U}$  to the master equation. Equation (3.36) provides us with a way to check how accurate this approximation is: we can fix an initial distribution, solve the forward-backward ODE system (which is easy given the initial condition), and then compare the value of the neural network  $\mathcal{U}_\theta$  evaluated along the equilibrium flow of distributions with the solution to the backward ODE for the value function. To be specific, for every  $m_0$ , we first compute the equilibrium value function  $\hat{u}^{m_0}$  and the equilibrium flow of distributions  $\hat{m}^{m_0}$ . We then evaluate  $\mathcal{U}_\theta(t, x, \hat{m}^{m_0}(t, \cdot))$  for all  $t \in [0, T]$  and check how close it is to  $\hat{u}^{m_0}(t, x)$  for each of the four possible states  $x$ . Figures 17–19 show that the two curves (for each state) coincide for at least three different initial conditions. This means that, using the DGM, we managed to train a neural network that accurately represent the value function of a representative player for various distributions at once. In the numerical experiments, we used the following values for the parameters

$$\begin{aligned} \beta_{UU} &= 0.3, \beta_{UD} = 0.4, \beta_{DU} = 0.3, \beta_{DD} = 0.4, & v_H &= 0.2, \lambda = 0.5, \\ q_{rec}^D &= 0.1, q_{rec}^U = 0.65, q_{inf}^D = 0.4, q_{inf}^U = 0.3, & k_D &= 0.3, k_I = 0.5. \end{aligned}$$

## 4 Reinforcement Learning

All the previous methods rely, in one way or another, on the fact that the cost functions  $f$  and  $g$  as well as the drift  $b$  and the volatility  $\sigma$  (cf. (2.2)–(2.3)) are known. However, in many applications, coming up with a realistic and accurate model is a daunting task. It is sometimes impossible to guess the form of the dynamics, or the way the costs are incurred. This has motivated the development of so-called model-free methods. The reinforcement learning (RL) theory provides a framework for studying such problems. Intuitively, an agent evolving in an environment can take actions and observe the consequences of her actions: the state of the environment (or her own state) changes, and a cost is incurred to the agent. The agent does not know how the new state and the cost are computed. The goal for the agent is then to learn an optimal behavior by trial and error.

Numerous algorithms have been developed under the topic of RL; see, *e.g.*, the surveys and books [154, 39, 185, 229, 117]. Most of them focus on RL itself, with state-of-the-art methods in single-agent or multi-agent problems and some provide theoretical guarantees of numerical performances. We aim to review its connections to stochastic control and games, as well as the mean-field setting. We shall start by discussing how problems in Section 2 are formulated as single-agent RL<sup>2</sup>. Although we here focus on the

<sup>2</sup>The terminology RL is from the perspective of artificial intelligence/computer science. In the operation research community, it is often called approximate dynamic programming (ADP) [213].

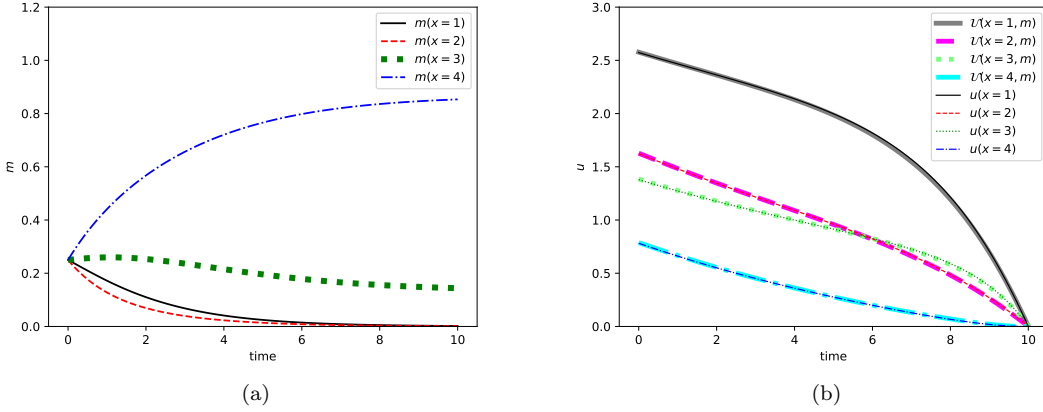


Figure 17: MFG Cybersecurity example in Section 3.2.5. Test case 1: Evolution of the distribution  $m^{m_0}$  (left) and the value function  $u^{m_0}$  and  $U(\cdot, \cdot, m^{m_0}(\cdot))$  (right) for  $m_0 = (1/4, 1/4, 1/4, 1/4)$ . First published in [176] by the American Mathematical Society.

traditional presentation of RL in discrete time, let us mention that a continuous-time stochastic optimal control viewpoint on RL has been also been studied, see *e.g.*, [200] for a policy gradient algorithm, and [235, 234] for a mean-variance portfolio problem and for generic continuous time and space problems. It has also been extended in several directions, such as variance reduction techniques [160], risk-aware problems [148] and mean-field games [113] and [88].

## 4.1 Reinforcement learning for stochastic control problems

Recall the stochastic control problems studied in Section 2, see (2.3)–(2.2). In this section, we will assume that the agent can not directly access  $b, \sigma, f$  and  $g$ , but can observe the “next step” information given the current state and control. We consider the time discretized problem

$$\check{X}_{t_{n+1}} = \check{X}_{t_n} + b(t_n, \check{X}_{t_n}, \alpha_{t_n})\Delta t + \sigma(t_n, \check{X}_{t_n}, \alpha_{t_n})\Delta \check{W}_{t_n}, \quad (4.1)$$

$$\min_{(\alpha_{t_n})_{n=0, \dots, N_T-1}} \mathbb{E} \left[ \sum_{n=0}^{N_T-1} f(t_n, \check{X}_{t_n}, \alpha_{t_n})\Delta t + g(\check{X}_T) \right], \quad (4.2)$$

where

$$0 = t_0 < t_1 < \dots < t_{N_T} = T, \text{ with } t_n - t_{n-1} = \Delta t = T/N_T,$$

is the temporal discretization on  $[0, T]$  as before. By doing so, the system is Markovian, and can be viewed as a Markov decision process (MDP).

### 4.1.1 Markov decision processes

Problem (4.1)–(4.2) can be recast as an MDP, which is a tuple  $(\mathcal{X}, \mathcal{A}, p, f, g, N_T)$ , where

- $\mathcal{X}$  is the set of states called the state space;
- $\mathcal{A}$  is the set of actions called the action space;
- $N_T < +\infty$  is the time horizon;
- $p : \mathcal{X} \times \mathcal{A} \times \{0, \Delta t, 2\Delta t, \dots, T\} \rightarrow \mathcal{P}(\mathcal{X})$  is the transition kernel, and  $p(\cdot|x, a, t_n)$  is a probability density function;
- $f : \{0, \Delta t, 2\Delta t, \dots, T\} \times \mathcal{X} \times \mathcal{A} \rightarrow \mathbb{R}$  is the one-step cost function, and  $f(t_n, x, a)$  is the immediate cost at time  $t_n$  at state  $x$  due to action  $a$ ;

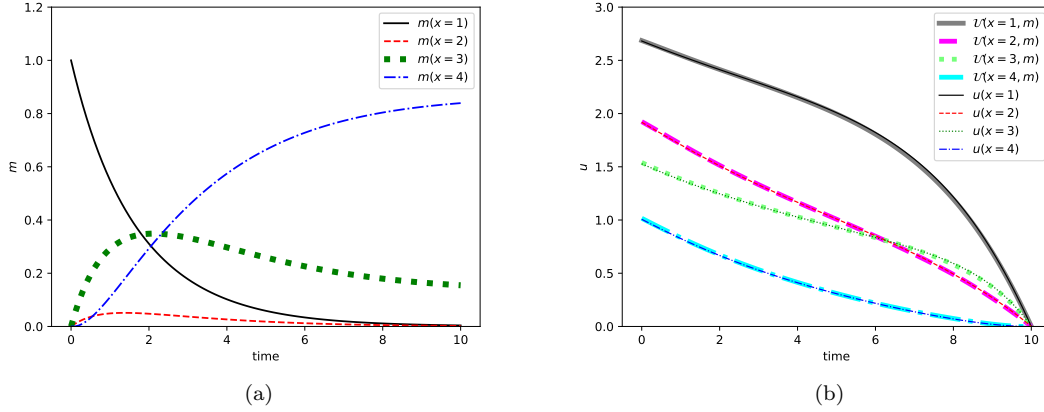


Figure 18: MFG Cybersecurity example in Section 3.2.5. Test case 2: Evolution of the distribution  $m^{m_0}$  (left) and the value function  $u^{m_0}$  and  $U(\cdot, \cdot, m^{m_0}(\cdot))$  (right) for  $m_0 = (1, 0, 0, 0)$ . First published in [176] by the American Mathematical Society.

- $g : \mathcal{X} \rightarrow \mathbb{R}$  is the terminal cost function, and  $g(x)$  is the terminal cost at the final time  $N_T$ .

A large part of the RL literature focuses on the infinite horizon setting with discounted cost. Furthermore, the state space is often discrete, in which case  $p(x'|x, a, t_n) = \mathbb{P}(X_{t_{n+1}} = x' | X_{t_n} = x, \alpha_{t_n} = a)$  is the probability to go to state  $x'$  at time  $t_{n+1}$  if at time  $t_n$  the state  $x$  and the action is  $a$ . However, for the sake of consistency with the previous sections and the literature on optimal control, we stick to the finite horizon and continuous space setting in this section.

In model-free RL, the agent typically uses multiple episodes to learn the control that optimizes (4.1) with a simulator. In one episode of learning, the agent-environment interaction is as follows: Starting with  $X_0 \in \mathcal{X}$ , the agent chooses  $\alpha_0 \in \mathcal{A}$ , pays a one-step cost  $f(0, X_0, \alpha_0)\Delta t$  and finds herself in a new state  $X_{t_1}$ ; the process continues, forming a sequence:

$$X_0, \alpha_0, f(0, X_0, \alpha_0)\Delta t, X_{t_1}, \alpha_{t_1}, f(t_1, X_{t_1}, \alpha_{t_1})\Delta t, \dots, X_T, g(X_T).$$

Under the Euler scheme (4.1), given the state-action pair  $(\check{X}_{t_n}, \alpha_{t_n}) = (x, a)$  at time  $t_n$ ,  $X_{t_{n+1}}$  follows a normal distribution  $\mathcal{N}(x + b(t_n, x, a)\Delta t, \sigma^2(t_n, x, a)\Delta t)$ .

In RL, there are four main components: policy, reward signal, value function, and optionally, a model of the environment. The MDP provides a mathematical framework to describe the agent-environment interface. A *policy*  $\pi : \{0, \Delta t, 2\Delta t, \dots, T\} \times \mathcal{X} \rightarrow \mathcal{P}(\mathcal{A})$  is a mapping from the state space to the probability space of the action space, and  $\pi_t(a|x)$  describes the probability of choosing action  $a$  at state  $x$ , which is in general random.

The *value function* associated to a specific policy  $\pi$  is denoted by  $V_t^\pi$  and defined as the expected cost when starting from  $x$  at time  $t$  and following  $\pi$  thereafter, *i.e.*,

$$V_{t_n}^\pi(x) = \mathbb{E}^\pi \left[ \sum_{j=n}^{N_T-1} f(t_j, X_{t_j}, \alpha_{t_j})\Delta t + g(X_T) | X_{t_n} = x \right],$$

where the superscript  $\pi$  over the expectation means that, at each time step, the action is sampled according to  $\pi$ . Similarly, the *action-value function*  $Q_t^\pi$  associated to  $\pi$  is defined as the expected cost when starting from  $x$  at time  $t$ , taking the action  $a$  and then following  $\pi$ , *i.e.*,

$$Q_{t_n}^\pi(x, a) = \mathbb{E}^\pi \left[ \sum_{j=n}^{N_T-1} f(t_j, X_{t_j}, \alpha_{t_j})\Delta t + g(X_T) | X_{t_n} = x, \alpha_{t_n} = a \right].$$

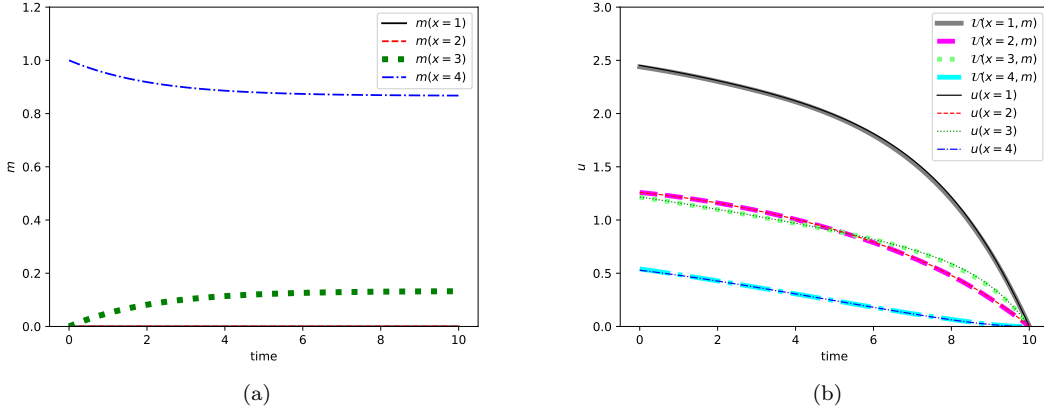


Figure 19: MFG Cybersecurity example in Section 3.2.5. Test case 3: Evolution of the distribution  $m^{m_0}$  (left) and the value function  $u^{m_0}$  and  $U(\cdot, \cdot, m^{m_0}(\cdot))$  (right) for  $m_0 = (0, 0, 0, 1)$ . First published in [176] by the American Mathematical Society.

Both functions satisfy the dynamic programming equations (also called Bellman equations),

$$V_{t_n}^\pi(x) = \int_{a \in \mathcal{A}} \pi_{t_n}(a|x) \int_{x' \in \mathcal{X}} p(x'|x, a, t_n) [f(t_n, x, a) \Delta t + V_{t_{n+1}}^\pi(x')] dx' da,$$

$$Q_{t_n}^\pi(x, a) = \int_{x' \in \mathcal{X}} p(x'|x, a, t_n) [f(t_n, x, a) \Delta t + V_{t_{n+1}}^\pi(x')] dx',$$

with terminal conditions  $V_T^\pi(x) = Q_T^\pi(x, a) = g(x)$ , where we have simplified the subscript  $t_{N_T} = T$ . The goal of RL is to identify the optimal  $\pi^* = (\pi_t^*)_t$  that minimizes  $V_t^\pi(x)$  for every  $t$  and  $x \in \mathcal{X}$ .

To this end, one also works with the *optimal value function*  $V_t^*(x) = \inf_\pi V_t^\pi(x)$  and the *optimal action-value function* defined as  $Q_t^*(x, a) = \inf_\pi Q_t^\pi(x, a)$ , which satisfy and the optimal Bellman equation reads,

$$V_{t_n}^*(x) = \inf_{a \in \mathcal{A}} \int_{x' \in \mathcal{X}} p(x'|x, a, t_n) [f(t_n, x, a) \Delta t + V_{t_{n+1}}^*(x')] dx',$$

$$Q_{t_n}^*(x, a) = f(t_n, x, a) \Delta t + \int_{x' \in \mathcal{X}} p(x'|x, a, t_n) \inf_{a' \in \mathcal{A}} Q_{t_{n+1}}^*(x', a') dx',$$

with terminal conditions  $V_T^*(x) = Q_T^*(x, a) = g(x)$ .

Model-free RL aims at computing  $\pi^*$  without using the knowledge of the transition probability kernel  $p$ , and by instead relying on samples of transitions  $X_{t_{n+1}} \sim p(x'|x, a, t_n)$ . There are primarily two categories of learning methods: value-based methods and policy gradient methods. In the continuous time framework, the connection between policy evaluation in value-based methods and policy gradient methods has been developed in [151, 152].

#### 4.1.1.1 Value-based methods

For value-based methods, the workflow can be summarized as follows: starting with an arbitrary policy  $\pi$ , evaluate its value, improve the policy, and repeat until convergence:

$$\pi_0 \rightarrow V^{\pi_0} \rightarrow \pi_1 \rightarrow V^{\pi_1} \rightarrow \dots \pi_* \rightarrow V^*.$$

The symbol  $\pi_k \rightarrow V^{\pi_k}$  denotes a *policy evaluation*, and the symbol  $\pi_k \rightarrow V^{\pi_{k+1}}$  denotes a *policy improvement*. Evaluating a given policy  $\pi_k \rightarrow V^{\pi_k}$  exactly is not possible since we assume that  $p(\cdot|x, a, t_n)$

is unknown. The Temporal-Difference (TD) learning is remedy this issue by updating  $V_{t_n}^\pi(x)$  with one sample drawn according to  $X_{t_{n+1}} \sim p(x'|x, a, t_n)$ ,

$$V_{t_n}^\pi(X_{t_n}) \leftarrow V_{t_n}^\pi(X_{t_n}) + \beta[f(t_n, X_{t_n}, \alpha_{t_n})\Delta t + V_{t_{n+1}}^\pi(X_{t_{n+1}}) - V_{t_n}^\pi(X_{t_n})],$$

where  $\beta > 0$  is a learning rate. This is the simplest TD method, usually denoted by TD(0). To unify TD methods and MC methods, one can view the later as updating  $V_{t_n}^\pi$  using the entire sequence of observed cost from time  $t_n$  until the end of the episode  $T$ . The  $n$ -step TD method lies in between and consists in simulating  $n$  Monte Carlo samples to update  $V^\pi$ .

TD learning can also be applied to action-value function, for example by using the update rule:

$$Q_{t_n}^\pi(X_{t_n}, \alpha_{t_n}) \leftarrow Q_{t_n}^\pi(X_{t_n}, \alpha_{t_n}) + \beta[f(t_n, X_{t_n}, \alpha_{t_n})\Delta t + Q_{t_{n+1}}^\pi(X_{t_{n+1}}, \alpha_{t_{n+1}}) - Q_{t_n}^\pi(X_{t_n}, \alpha_{t_n})],$$

where  $X_{t_{n+1}}, \alpha_{t_{n+1}}$  are random samples from (4.1) and from  $Q$  plus some randomization using for instance the  $\epsilon$ -greedy policy, which picks the currently optimal action with probability  $1 - \epsilon$  and, with probability  $\epsilon$ , picks an action uniformly at random. This approach is called SARSA. Then the optimal action-value function  $Q^*$  can be learnt as follows: choose  $\alpha_{t_n}$  according to  $Q$  plus  $\epsilon$ -greedy for some exploration, then update  $Q$  using SARSA. This method falls into the category of *on-policy* algorithms since it evaluates or improves the policy that is used to make decisions. In fact, it uses an  $\epsilon$ -greedy policy to balance between learning an optimal behavior and behaving non-optimally for exploration, so it learns the value function for a sub-optimal policy that still explores. *Off-policy* methods, on the contrary, uses different policies for evaluation and data generation. *Q-learning* may be the earliest well known off-policy algorithm, which directly approximates  $Q^*$  using the update rule:

$$Q_{t_n}^\pi(X_{t_n}, \alpha_{t_n}) \leftarrow Q_{t_n}^\pi(X_{t_n}, \alpha_{t_n}) + \beta[f(t_n, X_{t_n}, \alpha_{t_n})\Delta t + \max_a Q_{t_{n+1}}^\pi(X_{t_{n+1}}, a) - Q_{t_n}^\pi(X_{t_n}, \alpha_{t_n})].$$

#### 4.1.1.2 Policy gradient methods

This section describes some methods that aim at directly learning an optimal policy without deducing it from the value function. The use a parameterized class of policies. We denote by  $\pi_t(a|x; \theta)$  the probability of taking action  $a$  at state  $x$  with parameter  $\theta$ . In practice, this can be a linear function  $\theta^T f(x, a)$  where  $f(x, a)$  is called feature vector, or a neural network taking  $x$  as input and outputting a probability distribution over actions. Policy gradient methods update the policy parameter  $\theta$  based on the gradient of some performance measure  $L(\theta)$ , with updates of the form

$$\theta \leftarrow \theta - \beta \widehat{\nabla L(\theta)},$$

where  $\widehat{\nabla L(\theta)}$  denotes an estimation of  $\nabla L(\theta)$  based on Monte Carlo samples. A natural choice of  $L(\theta)$  is the value function  $V^{\pi_\theta}$  we aim to minimize. According to the policy gradient theorem,

$$\nabla V_{t_n}^{\pi_\theta}(x) = \mathbb{E}_\pi \left[ \int_{\mathcal{A}} Q_{t_n}^\pi(x, a) \nabla \pi_{t_n}(a|x; \theta) da \right].$$

Multiplying the first term by  $\pi_{t_n}(a|x; \theta)$ , dividing the second term by  $\pi_{t_n}(a|x; \theta)$ , replacing  $a$  by a sample  $\alpha_{t_n}$ , and using  $\mathbb{E}_\pi[G_{t_n}|x, a] = Q_{t_n}^\pi(x, a)$  leads to the REINFORCE algorithm [237],

$$\theta \leftarrow \theta - \beta G_{t_n} \frac{\nabla_\theta \pi_{t_n}(\alpha_{t_n}|X_{t_n}; \theta)}{\pi_{t_n}(\alpha_{t_n}|X_{t_n}; \theta)},$$

where  $G_{t_n} = \sum_{n'=n+1}^{N_T-1} f(t_{n'}, \tilde{X}_{t_{n'}}, \alpha_{t_{n'}})\Delta t + g(\tilde{X}_T)$  denotes the cumulated cost from time  $t_{n+1}$  to  $T$ .

**Remark 4.1** (Theoretical analysis). *Convergence of policy gradient has been studied in various settings. As for the model-based framework, LQ problems have attracted a particular interest since the optimal control can be written as a linear function of the state. Global convergence in in the infinite horizon setting has been proved by Fazel et al. in [86]. This result has been extended in various directions, such as the finite horizon setting in [116], the neural setting [236], or problems with entropy regularization [63], to cite just a few examples.*

With an additional parameterized value function  $V_{t_n}(x; \theta')$ , this leads to the actor-critic algorithm (see, *e.g.*, [229, Section 13.5] or [80]),

$$\begin{aligned}\delta_{t_n} &= f(t_n, X_{t_n}, \alpha_{t_n})\Delta t + V_{t_{n+1}}(X_{t_{n+1}}; \theta') - V_{t_n}(X_{t_n}; \theta'), \\ \theta' &\leftarrow \theta' - \beta' \delta_{t_n} \nabla_{\theta'} V_{t_n}(X_{t_n}; \theta'), \\ \theta &\leftarrow \theta - \beta \delta_{t_n} \nabla_{\theta} \ln \pi_{t_n}(\alpha_{t_n} | X_{t_n}; \theta).\end{aligned}$$

Both REINFORCE and actor-critic methods mentioned above stochastically select an action  $a$  when in state  $x$  according to the parameter  $\theta$ , *i.e.*,  $a \sim \pi_{t_n}(\cdot | x, \theta)$ . For some problems, it is more appropriate to look for a deterministic policy  $\alpha_{t_n}(x; \theta) \in \mathcal{A}$ . To ensure exploration, one can use an off-policy approach: a stochastic policy  $\tilde{\pi}_{t_n}(a|x)$  is used to choose the action, and a deterministic policy  $\alpha_{t_n}(x; \theta)$  is learned to approximate the optimal one. An example of such method is the deterministic policy gradient (DPG) [226], which is an off-policy actor-critic algorithm that learns a deterministic target policy  $\alpha_{t_n}(x; \theta)$  from an exploratory behavior policy  $\tilde{\pi}_{t_n}(a|x)$ . In particular, a differentiable critic  $Q(x, a; \theta')$  is used to approximate  $Q^{\alpha(\cdot; \theta)}(x, a)$  and is updated via Q-learning: at each step we sample  $\alpha_{t_n}$  from  $\tilde{\pi}_{t_n}(a|x)$  and

$$\begin{aligned}\delta_{t_n} &= f(t_n, X_{t_n}, \alpha_{t_n})\Delta t + Q_{t_{n+1}}(X_{t_{n+1}}, \alpha_{t_{n+1}}(X_{t_{n+1}}; \theta); \theta') - Q_{t_n}(X_{t_n}, \alpha_{t_n}; \theta'), \\ \theta' &\leftarrow \theta' - \beta' \delta_{t_n} \nabla_{\theta'} Q_{t_n}(X_{t_n}, \alpha_{t_n}; \theta'), \\ \theta &\leftarrow \theta - \beta \delta_{t_n} \nabla_{\theta} \alpha_{t_n}(X_{t_n}; \theta) \nabla_a Q(X_{t_n}, \alpha_{t_n}; \theta')|_{a=\alpha_{t_n}(X_{t_n}; \theta)}.\end{aligned}$$

When using neural networks to approximate  $Q^{\alpha(\cdot; \theta)}$  and the deterministic policy  $\alpha_{t_n}(x; \theta)$ , one can use the Deep DPG (DDPG) algorithm [186], which is based on the same intuition as DPG. For the sake of robustness it uses the “replay-buffer” idea borrowed from the Deep Q Network (DQN) algorithm, see [196]: the network parameters are learnt in mini-batches rather than online by using a replay buffer, so that correlation between samples are kept minimal. Another pair of networks  $Q'(x, a; \hat{\theta}')$  and  $\alpha'_{t_n}(x; \hat{\theta})$  are copied from  $Q(x, a; \theta')$  and  $\alpha_{t_n}(x; \theta)$  for calculating the target value in order to improve the stability. At each step, an action  $\alpha_{t_n}$  is sampled from  $\alpha_{t_n}(X_{t_n}; \theta) + \mathcal{N}_t$  where  $\mathcal{N}_t$  is a noise process for exploration; then the cost  $f(t_n, X_{t_n}, \alpha_{t_n})\Delta t$  and the new state  $X_{t_{n+1}}$  are observed and saved to the buffer. A mini-batch of  $N$  transitions  $(X_{t_n}, \alpha_{t_n}, f, X_{t_{n+1}})$  are sampled from the buffer, acting as supervised learning data for the critic  $Q(x, a; \theta')$ . The loss to be minimized is the mean-squared error of  $Q_{t_n}(X_{t_n}, \alpha_{t_n}; \theta')$  and  $f(t_n, X_{t_n}, \alpha_{t_n})\Delta t + Q'_{t_{n+1}}(X_{t_{n+1}}, \alpha'_{t_{n+1}}(X_{t_{n+1}}; \hat{\theta}); \hat{\theta}')$ . The actor network and both copies are updated via

$$\begin{aligned}\theta &\leftarrow \theta - \beta \frac{1}{N} \sum_i \nabla_a Q_{t_n}(x, a; \theta')|_{x=X_{t_n}^i, a=\alpha_{t_n}(X_{t_n}^i; \theta)} \nabla_{\theta} \alpha_{t_n}(X_{t_n}; \theta), \\ \hat{\theta}' &\leftarrow \tau \theta' + (1 - \tau) \hat{\theta}', \quad \hat{\theta} \leftarrow \tau \theta + (1 - \tau) \hat{\theta},\end{aligned}$$

where the superscript  $i$  indicates the  $i^{th}$  sample from the mini-batch, and  $\tau \ll 1$  is used to slowly track the learnt counterparts  $\theta$  and  $\theta'$ .

#### 4.1.2 Mean-field MDP and reinforcement learning for mean-field control problems

We now consider the MFC setting discussed in Section 2.2.3 as an extension of standard OC and we present an RL framework for this setting. MFC can be viewed as an optimal control problem in which a “state” is a population configuration. However an “action” is not a finite-dimensional object but rather a function providing a control for every individual state. Intuitively, in discrete time, this yields an MDP of the form  $(\mathcal{P}(\mathcal{X}), \mathcal{F}_{\mathcal{A}}, \bar{p}, \bar{f}, \bar{g}, N_T)$ , where

- The state space is the set  $\mathcal{P}(\mathcal{X})$  of probability measures on  $\mathcal{X}$ ;
- The action space  $\mathcal{F}_{\mathcal{A}}$  is a suitable subset of  $\mathcal{A}^{\mathcal{X}}$ , the set of functions from  $\mathcal{X}$  to  $\mathcal{A}$ ;
- The transition kernel is given by

$$\bar{p} : \{t_0, t_1, \dots, T\} \times \mathcal{P}(\mathcal{X}) \times \mathcal{F}_{\mathcal{A}} \rightarrow \mathcal{P}(\mathcal{P}(\mathcal{X})), \quad \bar{p}(\cdot | t, \mu, \bar{a}) = \delta_{f_p(\cdot | t, x, \mu, \bar{a}(x))\mu(x)dx},$$

meaning that with probability one, the new mean field state is given by one transition of the population distribution. Here  $\mu$  represents a population distribution,  $\bar{a}$  is an action at the population level, and  $\bar{p}(\cdot|t, \mu, \bar{a})$  is the distribution of the next population distribution, which is a Dirac mass at the next population distribution since there is no common noise in the present model;

- The running and terminal cost functions are given by

$$\bar{f} : \{t_0, t_1, \dots, T\} \times \mathcal{P}(\mathcal{X}) \times \mathcal{F}_{\mathcal{A}} \rightarrow \mathbb{R}, \quad \bar{f}(t, \mu, \bar{a}) = \int_x f(t, x, \mu, \bar{a}(x)) \mu(x) dx,$$

and

$$\bar{g} : \mathcal{P}(\mathcal{X}) \rightarrow \mathbb{R}, \quad \bar{g}(\mu) = \int_x g(x, \mu) \mu(x) dx.$$

Such MDPs have been referred to as mean field MDPs (MFMDP for short) in the literature [92, 58, 109, 110, 199, 20]. These MDPs can be rigorously studied using the tools developed for instance by Bertsekas and Shreve in [30]. Since this problem fits in the framework of MDPs, one can directly apply RL methods in principle. For instance, the Q-function of the MDP naturally satisfies a dynamic programming principle; see [58, 109, 110, 199]. Note that, if there is no common noise (as in the setting presented above), the evolution of the population distribution is purely deterministic.

To implement RL methods for MFC, the main difficulties are related to handling the distribution and the class of controls. In particular, we note that

- If  $\mathcal{X}$  is finite, then the state of the MDP, namely  $\mu$ , is a finite dimensional vector; if  $\mathcal{A}$  is also finite, then  $\mathcal{F}_{\mathcal{A}}$  can simply be taken as  $\mathcal{A}^{\mathcal{X}}$ , which is a finite set as well;
- If  $\mathcal{X}$  is not finite, then  $\mu$  is infinite-dimensional and likewise for the elements of  $\mathcal{A}^{\mathcal{X}}$ .

One simple approach is to discretize  $\mathcal{P}(\mathcal{X})$  and  $\mathcal{A}^{\mathcal{X}}$ , and then use standard RL techniques for finite state, finite action MDPs, such as the ones described in Section 4.1.1. For instance tabular Q-learning has been used *e.g.* in [58, 110] in the first case above by identifying  $\mathcal{P}(\mathcal{X})$  with the simplex  $\Delta_{\mathcal{X}}$  in dimension  $|\mathcal{X}|$  and by approximating the latter with an  $\epsilon$ -net. However, this approach does not scale well when the number of states is large or when  $\mathcal{X}$  is continuous. In this case, one can use RL methods for continuous state space, such as deep RL methods, see for instance [58].

For the sake of illustration, we provide an example in a setting where  $\mathcal{X}$  is finite. Let  $d = |\mathcal{X}|$  be the number of states. As mentioned above, we view  $\mathcal{P}(\mathcal{X})$  as the  $d$ -dimensional simplex  $\Delta_{\mathcal{X}}$ . In this case, the MFMDP is an MDP over a finite-dimensional continuous state space. To avoid discretizing the space, deep RL methods rely on neural networks to efficiently approximate the value function or the policy.

### Numerical illustration: A Cybersecurity model revisited.

We consider the cybersecurity model introduced in [164] (see also [52, Section 7.2.3]) and that we already discussed in Section 3.2.5. We revisit this problem from the point of view of MFC, meaning that the players cooperate to jointly minimize the social cost.

To be able to tackle this problem using RL, we discrete time using a mesh  $\{t_n = n\Delta t, n = 0, 1, 2, \dots, N_T\}$  where  $\Delta t = T/N_T > 0$ . The total cost for the whole population is

$$J(\alpha) = \sum_{n=0}^{N_T-1} \bar{f}(\mu_{t_n}, \alpha(t_n, \cdot)) \Delta t,$$

under the constraint that the evolution of distribution is given by

$$\mu_{t_{n+1}} = \bar{p}(\mu_{t_n}, \alpha(t_n, \cdot)) = (\mu_{t_n})^T (I + P^{\alpha(t_n, \cdot), \mu_{t_n}} \Delta t), \quad n = 0, 1, \dots, N_T - 1, \quad (4.3)$$

with a given initial condition  $\mu_0$ . The population-wise cost function  $\bar{f} : \mathcal{P}(\mathcal{X}) \times \mathcal{A}^{\mathcal{X}} \rightarrow \mathbb{R}$  is defined based on the individual cost function  $f$  by

$$\bar{f}(m, \alpha) = \sum_{x \in \mathcal{X}} f(x, m, \alpha(x)) m(x), \quad (m, \alpha) \in \mathcal{P}(\mathcal{X}) \times \mathcal{A}^{\mathcal{X}},$$

and  $P^{\alpha, m}$  denotes the matrix whose coefficients are given by

$$P^{\alpha, m}(x', x) = \lambda(x', x, m, \alpha(x')), \quad (x', x, m, \alpha) \in \mathcal{X} \times \mathcal{X} \times \mathcal{P}(\mathcal{X}) \times \mathcal{A}^{\mathcal{X}}.$$

From this formulation, we see that the problem fits in the framework of MFMDPs, or MDPs with finite horizon and continuous space, the state being the distribution.

In [176], the solution is learned using tabular Q-learning after discretizing the simplex: replacing  $\mathcal{P}(\mathcal{X})$  by an  $\epsilon$ -net with a finite number of distributions allows one to replace the MFMDP by a finite-state MFMDP on which tabular RL methods can be applied. This approach is convenient in that tabular methods typically have fewer hyperparameters and furthermore convergence results are easier to obtain. However, the main drawback is that such methods do not scale well to very large state space. In our case, discretizing the simplex requires a large number of points when the number of states increases.

Alternatively, the value function can be approximated directly on the simplex  $\mathcal{P}(\mathcal{S})$ , without any discretization. For example, we can replace the Q-function by a neural network and employ deep RL techniques to train the parameters. Here we follow the approach proposed in [58] and we focus on deterministic controls. The control and the value function are approximated by neural networks and trained using the DDPG method [186], which has been reviewed in Section 4.1.1.2. Since this method allows the control to take continuous values, we replace  $A = \{0, 1\}$  by  $A = [0, 1]$  (without changing the transition rate matrix), which amounts to letting the player choose the intensity with which she seeks to change her computer's level of protection.

We aim at learning the solution for various distributions. To train the neural networks, we sample at each iteration a random initial distribution  $\mu_0$  and generate a trajectory in the simplex by following the dynamics (4.3). Figure 20 displays the evolution of the population when using the learned control starting from five initial distributions of the testing set and one initial distribution of the training set. The testing set of initial distributions is:  $\{(0.25, 0.25, 0.25, 0.25), (1, 0, 0, 0), (0, 0, 0, 1), (0.3, 0.1, 0.3, 0.1), (0.5, 0.2, 0.2, 0.1)\}$ . We see that, in this setting, the distribution always evolves towards a configuration in which there is no defended agents, and the proportion of undefended infected and undefended susceptible are roughly 0.43 and 0.57, respectively.

## 4.2 Reinforcement learning for stochastic differential games

### 4.2.1 Multi-agent reinforcement learning (MARL)

Multi-agent reinforcement learning (MARL) studies reinforcement learning methods for multiple learners. The main difficulty is that, when several agents learn while interacting, from the point of view of each agent, the environment is non-stationary. Another issue is the question of scalability, which arises when the number of learners is very large. However, for a small number of agents, MARL has led to recent breakthrough results; see *e.g.* in autonomous driving [224], the game of Go [225], or video games such as Star Craft [233].

Several viewpoints can be adopted. Relying on dynamical systems theory, one approach is to consider that each agent uses a learning algorithm, and to study the resulting behavior of the group of agents viewed as a system evolving in discrete or continuous time. Another approach, based on game theory and closer to the topics discussed in Section 3, is to look for notions of solutions such as Nash equilibria and to design algorithms that let the agents learn such solutions. A typical example is Nash Q-learning, in which every player runs their own version of Q-learning simultaneously with the other players. Each player tries to compute its optimal Q-function, but the optimal policy of player  $i$  depends on the policies implemented by the other players. To be specific, consider an  $N$ -player game as in Section 3.1 but now in discrete time. Note that the problem faced by player  $i$  is not an MDP with state  $X^i$  because the cost and dynamics of player  $i$  depend on the other players. Assume the players use a strategy profile  $\boldsymbol{\pi} = (\pi^1, \dots, \pi^N)$ . Then the Q-function of player  $i$  is: for  $\mathbf{x} = (x^1, \dots, x^N)$  and  $\mathbf{a} = (a^1, \dots, a^N)$ ,

$$Q_{t_n}^{i, \boldsymbol{\pi}}(\mathbf{x}, \mathbf{a}) = \mathbb{E}^{\boldsymbol{\pi}} \left[ \sum_{j=n}^{N_T-1} f^i(t_j, \mathbf{X}_{t_j}, \boldsymbol{\alpha}_{t_j}) \Delta t + g^i(\mathbf{X}_T) \middle| \mathbf{X}_{t_n} = \mathbf{x}, \boldsymbol{\alpha}_{t_n} = \mathbf{a} \right].$$

Hu and Wellman proposed in [136] a version of Q-learning for (infinite horizon discounted)  $N$ -player games, called Nash Q-learning, and identified conditions under which this algorithm converges to a Nash

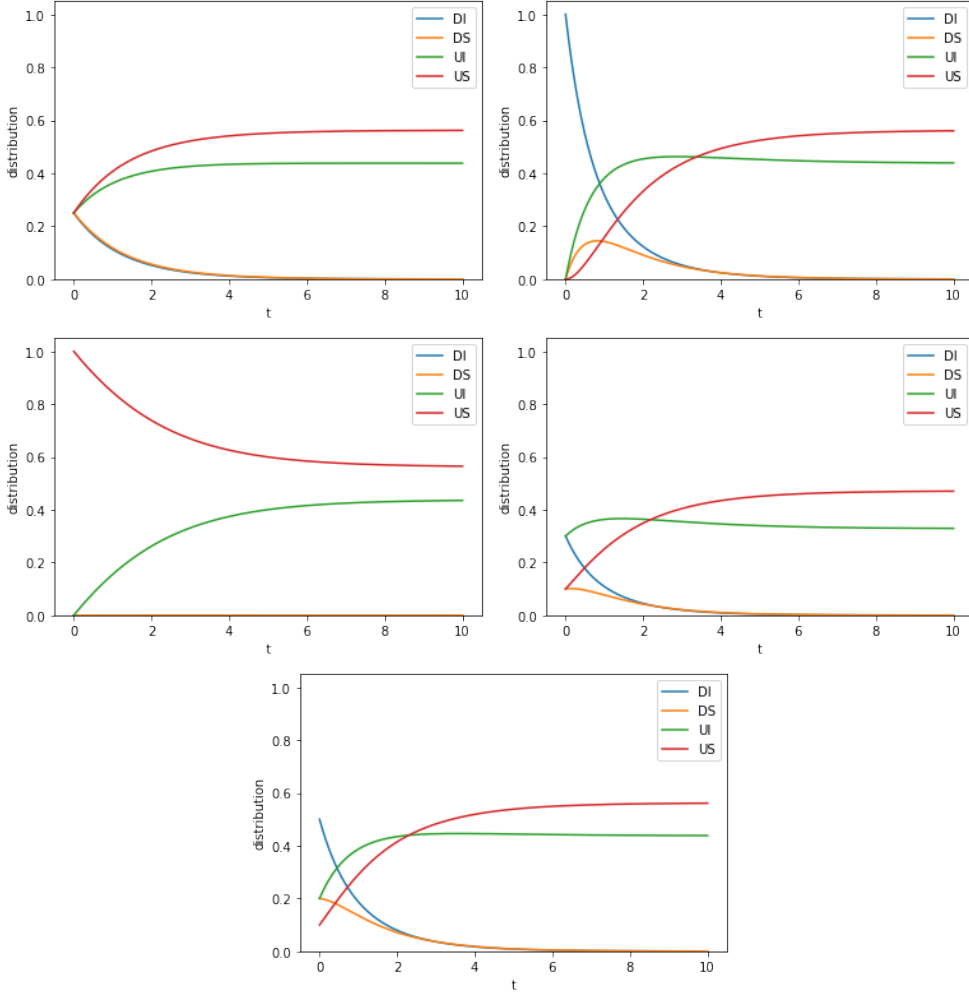


Figure 20: Cybersecurity MFC model solved with DDPG in Section 4.1.2: Evolution of the population distribution for five initial distributions.

equilibrium. The method can be adapted with deep neural networks, as done for instance in [62]. We refer the interested reader to, *e.g.*, [39, 231, 31, 170, 241, 243, 108] for more details on MARL. Recently, [111, 110] also studied mean-field control RL in a decentralized way using cooperative MARL.

#### 4.2.2 Reinforcement learning for mean-field games

We now turn our attention to RL methods for MFG. As pointed out in Section 3.2, finding a mean-field Nash equilibrium boils down to (1) finding a control that is optimal for a representative infinitesimal player facing the equilibrium distribution flow, and (2) computing the induced distribution flow, which should match the equilibrium one. These two elements can be tackled alternatively, as described in Section 3.1 in the  $N$ -player case and in Section 3.2.2 in the mean-field case. The first part is a standard optimal control problem, which can thus be tackled using standard RL techniques, see Section 4.1.1. In this setting, we assume that the agent who is learning can repeat experiments of the following form: given the current state, the agent chooses an action (or a sequence of actions), and the environment returns the new state as well as the reward (or a sequence of states and rewards). In the representative player’s MDP, the distribution enters as a parameter that influences the reward and dynamics, but is fixed when the player learns an optimal policy. During such experiments, we generally assume that the population distribution is fixed, and it is updated after a number of iterations; see *e.g.* [112, 84]. Alternatively, we can assume that it is

updated at every iteration but at a slow rate; see *e.g.* [228, 12, 238]. Most of the literature thus far focuses on tabular methods. A few works have used deep RL methods to compute the best response. For example, DDPG have been used in [84], soft actor-critic (SAC) has been used for a flocking model in [208], while deep Q-learning or some variants of it has been used in [71, 207, 178]. Recently, several works have studied the advantages and the limitations brought by the regularization of the policy through penalization terms in the cost function [10, 71, 113]. We refer to [177] for a survey of learning algorithms and reinforcement learning methods to approximate MFG solutions.

### Numerical illustration: an example with explicit solution.

For the sake of illustration, we consider an MFG model which admits an explicit solution in the continuous time ergodic setting. The mode has been introduced and solved in [9]. The MFG is defined as follows. The state space is the one-dimensional unit torus, *i.e.*,  $\mathbb{T} = [0, 1]$  with periodic boundary condition. The action space is  $\mathbb{R}$  (or in practice any bounded interval containing  $[-2\pi, 2\pi]$ , which is the range of the equilibrium control). The drift function is

$$b(x, m, a) = a.$$

The running cost is

$$f(x, m, a) = \tilde{f}(x) + \frac{1}{2}|a|^2 + \log(m),$$

where the first term is the following cost, which encodes spatial preferences for some regions of the domain

$$\tilde{f}(x) = -2\pi^2 \sin(2\pi x) + 2\pi^2 \cos(2\pi x)^2 - 2 \sin(2\pi x).$$

In the ergodic MFG setting, the objective of an infinitesimal representative player is to minimize

$$\lim_{T \rightarrow +\infty} \frac{1}{T} \mathbb{E} \left[ \int_0^T f(X_t, \mu_t(X_t), \alpha_t(X_t)) dt \right],$$

where  $X$  is controlled by  $\alpha$ . Here  $\mu_t$  is assumed to have a density for every  $t \geq 0$ , and we identify it with its density. So  $\mu_t(X_t)$  denotes the value of the density of  $\mu_t$  at  $X_t$ . The equilibrium control and the equilibrium mean-field distribution are respectively given by

$$a^* : x \mapsto 2\pi \cos(2\pi x) \quad \text{and} \quad \mu^* : x \mapsto \frac{e^{2\sin(2\pi x)}}{\int_{\mathbb{T}} e^{2\sin(2\pi y)} dy}.$$

We use fictitious play [43] combined with a deep RL algorithm to learn the best response at each iteration for the solution. The problem is in continuous state and action spaces and admits a deterministic equilibrium control. Hence, following [84], at each iteration, we solve the representative player's MDP using DDPG [186] reviewed in Section 4.1.1.2.

The left plot of Figure 21 displays (blue line) the population distribution learned by fictitious play, which corresponds to the distribution induced by the average of past best responses. This is to be compared with the ergodic distribution (red dashed line). The right plot displays the last iteration of the best response. This control is approximated by two neural networks: a target network (green dashed line) and an actor network (blue line). We also display the ergodic equilibrium control (red dashed line).

## 5 Conclusion and Perspectives

This paper provides a review of some of the recent development of machine learning methods for stochastic optimal control and games, with a special focus on emerging applications of deep learning and reinforcement learning to these problems. Despite the rapidly growing number of recent works, many questions remain to be investigated further. We hope this survey can trigger interest and attract more researchers to work on this topic. Besides the material already reviewed in this survey, we outline a few research directions below.

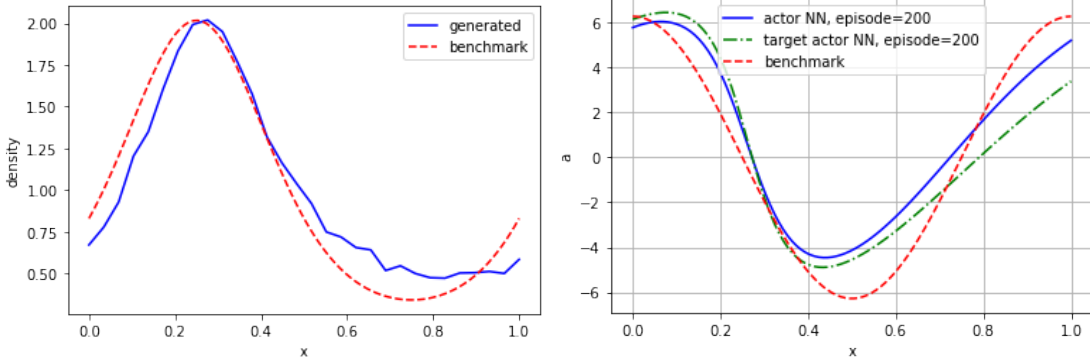


Figure 21: MFG with analytical solution for the ergodic setting in Section 4.2.2, solved with fictitious play and DDPG: stationary distribution and control.

First, most of the methods presented here lack full analysis on the theoretical side. The mathematical foundations of deep learning are attracting growing interest, and recent results could help analyze the methods described in this paper. The main motivation underlying the use of deep networks is their ability to cope with the curse of dimensionality. However, rigorously phrasing and proving such a statement has been done only in particular cases. Analyzing the generalization capability of neural networks is typically done by splitting the analysis into several types of errors, such as approximation, estimation, and optimization errors. Bounds on the approximation and estimation errors can generally be obtained based on the regularity of the function to be approximated, which can be difficult in the context of differential games. Furthermore, bounding the optimization error is even more challenging since it involves not only the definition of the game but also the optimization algorithm. Due to these difficulties, estimating these errors remains an open question for most methods discussed in this survey.

From a practical viewpoint, an important question related to neural network-based methods is the choice of hyperparameters. The most obvious one is the architecture of the neural network. In many cases, a feedforward fully connected architecture provides good performances (*e.g.*, for deep BSDE, DBDP, Sig-DFP). However, in other cases (*e.g.*, DGM, RNN for problems with delay, as discussed in this survey), ad hoc architectures seem necessary to reach the best results. In any case, architectures undoubtedly play a crucial role in the performance of every deep learning method, and a careful design is, in general, what leads to state of the art results in high dimension. So far, most deep learning methods for differential games have focused on providing proof of concepts. Given these baselines, it is now a natural question to try more sophisticated architectures in order to achieve better numerical performance. Once the architecture is fixed, the hyperparameters of the optimization method need to be determined. For example, the initialization of the network parameters, the learning rate, and the mini-batch size are important factors ensuring fast convergence. Their role is crucial for training deep and sophisticated architectures. However, finding a systematic rule for choosing these hyperparameters *a priori* remains difficult. A popular approach to identify suitable ranges of values is to try several values and measure the empirical convergence speed on problems for which the solution is known, using either an analytical formula or another numerical method. The task is quite complex because the hyperparameters' influences are interdependent. For problems without benchmarks, finding good hyperparameters values is even more challenging. To the best of our knowledge, the literature does not yet provide a detailed understanding of how to choose hyperparameters and how to measure algorithms' performance without knowing benchmark solutions. We did not discuss this aspect in the present survey for brevity, but finding efficient heuristics is certainly an interesting direction. A related question is how to assess convergence of algorithms computing Nash equilibria in games, since the goal is to find a fixed point and not an optimizer.

Regarding specific problems related to MFGs, a direction that has received little attention thus far is numerical methods that can work even when there is a common noise affecting the whole population. The type of difficulties that arise numerically is connected to the difficulty of solving such MFGs from a theoretical viewpoint. We have exposed the Sig-DFP method to tackle MFGs with common noise, focusing on mean-field interactions through moments. Common noise appears in applications, for instance, in

the form of aggregate shocks in macroeconomics. Hence it is worth developing further machine learning algorithms to deal with MFGs with common noise and general interactions. So far, we lack efficient ways to parameterize, represent, and discretize probability measures defined on a continuous-state space.

Another aspect related to concrete applications of the methods presented in this survey pertains to the resources needed to train deep neural networks. For model-based methods and even more for model-free reinforcement learning methods, sophisticated models typically need a vast number of training episodes, leading to two challenges. First, as the model complexity grows, the massive computational cost required to learn the solution becomes prohibitive. Second, for real-world applications, Monte Carlo simulations will be replaced by real data, but we generally have much fewer data points than the number of samples used by most deep learning methods described in this survey. It will thus be very interesting to design more sample-efficient methods and establish sharp estimates of their sample complexity.

Last but not least, to the best of our knowledge, the methods presented in this survey have been applied only to relatively simple models for the purpose of academic research. But a significant motivation for the development of machine learning methods is that they will allow us to efficiently solve more realistic optimal control problems and games. We hope that this survey can contribute to fostering interactions between theoretical research and applied research communities, and lead to concrete applications in real-world problems.

## Acknowledgement

R.H. was partially supported by the NSF grant DMS-1953035, the Faculty Career Development Award, the Research Assistance Program Award, the Early Career Faculty Acceleration funding, and the Regents' Junior Faculty Fellowship at University of California, Santa Barbara. Some parts of the review paper have been used for teaching special topic graduate classes at the University of California, Santa Barbara, and R.H. appreciates all the feedback from the audience of these classes. R.H. and M.L. are grateful to all their co-authors of the papers mentioned in this review.

## References

- [1] B. Acciaio, J. Backhoff-Veraguas, and R. Carmona. Extended mean field control problems: stochastic maximum principle and transport perspective. *SIAM journal on Control and Optimization*, 57(6):3666–3693, 2019.
- [2] Y. Achdou, F. Camilli, and I. Capuzzo-Dolcetta. Mean field games: numerical methods for the planning problem. *SIAM Journal on Control and Optimization*, 50(1):77–109, 2012.
- [3] Y. Achdou and I. Capuzzo-Dolcetta. Mean field games: numerical methods. *SIAM Journal on Numerical Analysis*, 48(3):1136–1162, 2010.
- [4] Y. Achdou and M. Laurière. On the system of partial differential equations arising in mean field type control. *Discrete & Continuous Dynamical Systems*, 35(9):3879, 2015.
- [5] Y. Achdou and M. Laurière. Mean field games and applications: Numerical aspects. *Mean field games*, pages 249–307, 2020.
- [6] Y. Achdou, M. Lauriere, and P.-L. Lions. Optimal control of conditioned processes with feedback controls. *Journal de Mathématiques Pures et Appliquées*, 2020.
- [7] N. Agram, A. Bakdi, and B. Oksendal. Deep learning and stochastic mean-field control for a neural network model. *SSRM preprint ssrn.3683722*, 2020.
- [8] A. Al-Aradi, A. Correia, D. Naiff, G. Jardim, and Y. Saporito. Solving nonlinear and high-dimensional partial differential equations via deep learning. *arXiv preprint arXiv:1811.08782*, 2018.
- [9] N. Almulla, R. Ferreira, and D. Gomes. Two numerical approaches to stationary mean-field games. *Dynamic Games and Applications*, 7(4):657–682, 2017.

- [10] B. Anahtarci, C. D. Kariksiz, and N. Saldi. Q-learning in regularized mean-field games. *arXiv preprint arXiv:2003.12151*, 2020.
- [11] D. Andersson and B. Djehiche. A maximum principle for SDEs of mean-field type. *Appl. Math. Optim.*, 63(3):341–356, 2011.
- [12] A. Angiuli, J.-P. Fouque, and M. Laurière. Unified reinforcement Q-learning for mean field game and control problems. *arXiv preprint arXiv:2006.13912*, 2020.
- [13] A. Angiuli, C. V. Graves, H. Li, J.-F. Chassagneux, F. Delarue, and R. Carmona. Cemracs 2017: numerical probabilistic approach to MFG. *ESAIM: Proceedings and Surveys*, 65:84–113, 2019.
- [14] P. K. Asea and P. J. Zak. Time-to-build and cycles. *Journal of Economic Dynamics and Control*, 23(8):1155–1175, 1999.
- [15] A. Aurell, R. Carmona, G. Dayanikli, and M. Laurière. Finite state graphon games with applications to epidemics. *Dynamic Games and Applications*, pages 1–33, 2022.
- [16] A. Aurell, R. Carmona, G. Dayanikli, and M. Lauriere. Optimal incentives to mitigate epidemics: a stackelberg mean field game approach. *SIAM Journal on Control and Optimization*, 60:S294–S322, 2022.
- [17] A. Bachouch, C. Huré, N. Langrené, and H. Pham. Deep neural networks algorithms for stochastic control problems on finite horizon: numerical applications. *Methodology and Computing in Applied Probability*, pages 1–36, 2021.
- [18] C. Barrera-Esteve, F. Bergeret, C. Dossal, E. Gobet, A. Meziou, R. Munos, and D. Reboul-Salze. Numerical methods for the pricing of swing options: a stochastic control approach. *Methodology and computing in applied probability*, 8:517–540, 2006.
- [19] H. Bauer and U. Rieder. Stochastic control problems with delay. *Mathematical Methods of Operations Research*, 62(3):411–427, 2005.
- [20] E. Bayraktar, N. Bauerle, and A. D. Kara. Finite approximations and Q learning for Mean Field Type Multi Agent Control. *arXiv preprint arXiv:2211.09633*, 2022.
- [21] E. Bayraktar, Q. Feng, and Z. Zhang. Deep signature algorithm for path-dependent american option pricing. *arXiv preprint arXiv:2211.11691*, 2022.
- [22] C. Beck, W. E, and A. Jentzen. Machine learning approximation algorithms for high-dimensional fully nonlinear partial differential equations and second-order backward stochastic differential equations. *Journal of Nonlinear Science*, 29(4):1563–1619, 2019.
- [23] S. Becker, P. Cheridito, and A. Jentzen. Deep optimal stopping. *Journal of Machine Learning Research*, 20:74, 2019.
- [24] S. Becker, P. Cheridito, and A. Jentzen. Pricing and hedging American-style options with deep learning. *Journal of Risk and Financial Management*, 13(7):158, 2020.
- [25] R. Bellman. A Markovian decision process. *Journal of mathematics and mechanics*, pages 679–684, 1957.
- [26] C. Bender, N. Schweizer, and J. Zhuo. A primal–dual algorithm for BSDEs. *Mathematical Finance*, 27(3):866–901, 2017.
- [27] C. Bender and J. Steiner. A posteriori estimates for backward SDEs. *SIAM/ASA Journal on Uncertainty Quantification*, 1(1):139–163, 2013.
- [28] A. Bensoussan, J. Frehse, and S. C. P. Yam. *Mean field games and mean field type control theory*. Springer Briefs in Mathematics. Springer, New York, 2013.

[29] J. Berner, P. Grohs, G. Kutyniok, and P. Petersen. *The Modern Mathematics of Deep Learning*, page 1–111. Cambridge University Press, 2022.

[30] D. P. Bertsekas and S. E. Shreve. *Stochastic optimal control: the discrete-time case*, volume 5. Athena Scientific, 1996.

[31] D. Bloembergen, K. Tuyls, D. Hennes, and M. Kaisers. Evolutionary dynamics of multi-agent learning: A survey. *Journal of Artificial Intelligence Research*, 53:659–697, 2015.

[32] H. Boedihardjo, X. Geng, T. Lyons, and D. Yang. The signature of a rough path: uniqueness. *Advances in Mathematics*, 293:720–737, 2016.

[33] P. Bonnier, P. Kidger, I. P. Arribas, C. Salvi, and T. Lyons. Deep signature transforms. In *Advances in Neural Information Processing Systems 32 (NeurIPS)*, 2019.

[34] B. Bouchard and N. Touzi. Discrete-time approximation and Monte-Carlo simulation of backward stochastic differential equations. *Stochastic Processes and their applications*, 111(2):175–206, 2004.

[35] A. Briani and P. Cardaliaguet. Stable solutions in potential mean field game systems. *Nonlinear Differential Equations and Applications*, 25(1):1, 2018.

[36] G. W. Brown. Some notes on computation of games solutions. Technical report, Rand Corp Santa Monica CA, 1949.

[37] G. W. Brown. Iterative solution of games by fictitious play. *Activity Analysis of Production and Allocation*, 13(1):374–376, 1951.

[38] A. Budhiraja and K. Ross. Convergent numerical scheme for singular stochastic control with state constraints in a portfolio selection problem. *SIAM Journal on Control and Optimization*, 45(6):2169–2206, 2007.

[39] L. Busoniu, R. Babuska, and B. De Schutter. A comprehensive survey of multiagent reinforcement learning. *IEEE Transactions on Systems, Man, and Cybernetics, Part C (Applications and Reviews)*, 38(2):156–172, 2008.

[40] H. Cao, X. Guo, and M. Laurière. Connecting GANs, mean-field games, and optimal transport. *arXiv preprint arXiv:2002.04112*, 2020.

[41] P. Cardaliaguet. Notes on mean field games, 2013.

[42] P. Cardaliaguet, F. Delarue, J.-M. Lasry, and P.-L. Lions. *The master equation and the convergence problem in mean field games*. Princeton University Press, 2019.

[43] P. Cardaliaguet and S. Hadikhanloo. Learning in mean field games: the fictitious play. *ESAIM: Control, Optimisation and Calculus of Variations*, 23(2):569–591, 2017.

[44] P. Cardaliaguet and C.-A. Lehalle. Mean field game of controls and an application to trade crowding. *Mathematics and Financial Economics*, 12(3):335–363, 2018.

[45] E. Carlini and F. J. Silva. A fully discrete semi-Lagrangian scheme for a first order mean field game problem. *SIAM Journal on Numerical Analysis*, 52(1):45–67, 2014.

[46] E. Carlini and F. J. Silva. On the discretization of some nonlinear Fokker–Planck–Kolmogorov equations and applications. *SIAM Journal on Numerical Analysis*, 56(4):2148–2177, 2018.

[47] R. Carmona. *Lectures on BSDEs, Stochastic Control, and Stochastic Differential Games with Financial Applications*, volume 1. SIAM, 2016.

[48] R. Carmona and F. Delarue. Probabilistic analysis of mean-field games. *SIAM Journal on Control and Optimization*, 51(4):2705–2734, 2013.

- [49] R. Carmona, J.-P. Fouque, and L.-H. Sun. Mean field games and systemic risk. *Communications in Mathematical Sciences*, 13(4):911–933, 2015.
- [50] R. Carmona, F. Delarue, and A. Lachapelle. Control of McKean-Vlasov dynamics versus mean field games. *Math. Financ. Econ.*, 7(2):131–166, 2013.
- [51] R. Carmona and F. Delarue. The master equation for large population equilibria. In *Stochastic analysis and applications 2014*, pages 77–128. Springer, 2014.
- [52] R. Carmona and F. Delarue. *Probabilistic Theory of Mean Field Games with Applications I*. Springer, 2018.
- [53] R. Carmona and F. Delarue. *Probabilistic Theory of Mean Field Games with Applications II*. Springer, 2018.
- [54] R. Carmona and D. Lacker. A probabilistic weak formulation of mean field games and applications. *Ann. Appl. Probab.*, 25(3):1189–1231, 2015.
- [55] R. Carmona and M. Laurière. Convergence analysis of machine learning algorithms for the numerical solution of mean field control and games: I—the ergodic case. *To appear in SIAM Journal on Numerical Analysis. arXiv preprint arXiv:1907.05980*, 2019.
- [56] R. Carmona and M. Laurière. Convergence analysis of machine learning algorithms for the numerical solution of mean field control and games: II—the finite horizon case. *arXiv preprint arXiv:1908.01613. To appear in Annals of Applied Probability*, 2019.
- [57] R. Carmona and M. Laurière. Deep learning for mean field games and mean field control with applications to finance. *Machine Learning in Financial Markets: A guide to contemporary practises, editors: A. Capponi and C.-A. Lehalle, Cambridge University Press (Preprint arXiv:2107.04568)*, 2022.
- [58] R. Carmona, M. Laurière, and Z. Tan. Model-free mean-field reinforcement learning: mean-field MDP and mean-field Q-learning. *arXiv preprint arXiv:1910.12802*, 2019.
- [59] R. Carmona and L. Leal. Optimal execution with quadratic variation inventories. Technical report, Princeton University, 2021.
- [60] R. Carmona and K. Webster. The self-financing equation in high frequency markets. *Finance & Stochastics*, 23:729 – 759, 2019.
- [61] A. Cartea and S. Jaimungal. Incorporating order-flow into optimal execution. *Math. Financ. Econ.*, 10(3):339–364, 2016.
- [62] P. Casgrain, B. Ning, and S. Jaimungal. Deep Q-learning for Nash equilibria: Nash-DQN. *arXiv preprint arXiv:1904.10554*, 2019.
- [63] S. Cen, C. Cheng, Y. Chen, Y. Wei, and Y. Chi. Fast global convergence of natural policy gradient methods with entropy regularization. *Operations Research*, 70(4):2563–2578, 2022.
- [64] Q. Chan-Wai-Nam, J. Mikael, and X. Warin. Machine learning for semi linear PDEs. *Journal of Scientific Computing*, 79(3):1667–1712, 2019.
- [65] J.-F. Chassagneux, D. Crisan, and F. Delarue. A probabilistic approach to classical solutions of the master equation for large population equilibria. Forthcoming in Memoirs of the AMS, arXiv:1411.3009, 2014.
- [66] J.-F. Chassagneux, D. Crisan, and F. Delarue. Numerical method for FBSDEs of McKean–Vlasov type. *The Annals of Applied Probability*, 29(3):1640–1684, 2019.
- [67] T. Chen, Z. O. Wang, I. Exarchos, and E. Theodorou. Large-scale multi-agent deep FBSDEs. In *International Conference on Machine Learning*, pages 1740–1748. PMLR, 2021.

[68] Z. Chen and P. A. Forsyth. A semi-Lagrangian approach for natural gas storage valuation and optimal operation. *SIAM Journal on Scientific Computing*, 30(1):339–368, 2008.

[69] P. Cheridito, H. M. Soner, N. Touzi, and N. Victoir. Second-order backward stochastic differential equations and fully nonlinear parabolic PDEs. *Communications on Pure and Applied Mathematics: A Journal Issued by the Courant Institute of Mathematical Sciences*, 60(7):1081–1110, 2007.

[70] K. Cho, B. Van Merriënboer, C. Gulcehre, D. Bahdanau, F. Bougares, H. Schwenk, and Y. Bengio. Learning phrase representations using RNN encoder-decoder for statistical machine translation. *arXiv preprint arXiv:1406.1078*, 2014.

[71] K. Cui and H. Koepll. Approximately solving mean field games via entropy-regularized deep reinforcement learning. In *proc. of AISTATS*, 2021.

[72] J. Cvitanić, D. Possamaï, and N. Touzi. Dynamic programming approach to principal-agent problems. *Finance Stoch.*, 22(1):1–37, 2018.

[73] J. Cvitanić and J. Zhang. *Contract theory in continuous-time models*. Springer Finance. Springer, Heidelberg, 2013.

[74] G. Cybenko. Approximation by superpositions of a sigmoidal function. *Mathematics of control, signals and systems*, 2(4):303–314, 1989.

[75] C. Daskalakis, P. W. Goldberg, and C. H. Papadimitriou. The complexity of computing a Nash equilibrium. *SIAM Journal on Computing*, 39:195–259, 2009.

[76] A. Davey and H. Zheng. Deep learning for constrained utility maximisation. *arXiv preprint arXiv:2008.11757*, 2020.

[77] T. De Ryck, A. D. Jagtap, and S. Mishra. Error estimates for physics informed neural networks approximating the navier-stokes equations. *arXiv preprint arXiv:2203.09346*, 2022.

[78] T. De Ryck and S. Mishra. Error analysis for physics-informed neural networks (PINNs) approximating Kolmogorov PDEs. *Advances in Computational Mathematics*, 48(6):1–40, 2022.

[79] T. De Ryck and S. Mishra. Generic bounds on the approximation error for physics-informed (and) operator learning. *arXiv preprint arXiv:2205.11393*, 2022.

[80] T. Degris, M. White, and R. S. Sutton. Off-policy actor-critic. *arXiv preprint arXiv:1205.4839*, 2012.

[81] W. E and B. Yu. The deep Ritz method: a deep learning-based numerical algorithm for solving variational problems. *Communications in Mathematics and Statistics*, 6(1):1–12, 2018.

[82] W. E, J. Han, and A. Jentzen. Deep learning-based numerical methods for high-dimensional parabolic partial differential equations and backward stochastic differential equations. *Commun. Math. Stat.*, 5(4):349–380, 2017.

[83] W. E, M. Hutzenthaler, A. Jentzen, and T. Kruse. On multilevel Picard numerical approximations for high-dimensional nonlinear parabolic partial differential equations and high-dimensional nonlinear backward stochastic differential equations. *Journal of Scientific Computing*, 79(3):1534–1571, 2019.

[84] R. Elie, J. Pérolat, M. Laurière, M. Geist, and O. Pietquin. On the convergence of model free learning in mean field games. In *Proceedings of the AAAI Conference on Artificial Intelligence*, volume 34, pages 7143–7150, 2020.

[85] I. Elsanosi and B. Larssen. Optimal consumption under partial observations for a stochastic system with delay. *Preprint series. Pure mathematics* <http://urn. nb. no/URN: NBN: no-8076>, 2001.

[86] M. Fazel, R. Ge, S. Kakade, and M. Mesbahi. Global convergence of policy gradient methods for the linear quadratic regulator. In *International conference on machine learning*, pages 1467–1476. PMLR, 2018.

- [87] S. Federico. A stochastic control problem with delay arising in a pension fund model. *Finance and Stochastics*, 15(3):421–459, 2011.
- [88] D. Firooz and S. Jaimungal. Exploratory LQG mean field games with entropy regularization. *Automatica*, 139:110177, 2022.
- [89] P. A. Forsyth and G. Labahn. Numerical methods for controlled Hamilton-Jacobi-Bellman PDEs in finance. *Journal of Computational Finance*, 11(2):1, 2007.
- [90] J.-P. Fouque and Z. Zhang. Deep learning methods for mean field control problems with delay. *Frontiers in Applied Mathematics and Statistics*, 6(11), 2020.
- [91] C. Gao, S. Gao, R. Hu, and Z. Zhu. Convergence of the backward deep BSDE method with applications to optimal stopping problems. *arXiv preprint arXiv:2210.04118*, 2022.
- [92] N. Gast, B. Gaujal, and J.-Y. Le Boudec. Mean field for Markov decision processes: from discrete to continuous optimization. *IEEE Transactions on Automatic Control*, 57(9):2266–2280, 2012.
- [93] M. Germain, M. Laurière, H. Pham, and X. Warin. DeepSets and their derivative networks for solving symmetric PDEs. *Journal of Scientific Computing*, 91(2):1–33, 2022.
- [94] M. Germain, J. Mikael, and X. Warin. Numerical resolution of McKean-Vlasov FBSDEs using neural networks. *Methodology and Computing in Applied Probability*, pages 1–30, 2022.
- [95] M. Germain, H. Pham, and X. Warin. Neural networks-based algorithms for stochastic control and PDEs in finance. *arXiv preprint arXiv:2101.08068*, 2021.
- [96] F. A. Gers, N. N. Schraudolph, and J. Schmidhuber. Learning precise timing with LSTM recurrent networks. *Journal of machine learning research*, 3(Aug):115–143, 2002.
- [97] E. Gobet and R. Munos. Sensitivity analysis using Itô-Malliavin calculus and martingales, and application to stochastic optimal control. *SIAM J. Control Optim.*, 43(5):1676–1713, 2005.
- [98] D. A. Gomes, S. Patrizi, and V. Voskanyan. On the existence of classical solutions for stationary extended mean field games. *Nonlinear Analysis: Theory, Methods & Applications*, 99:49–79, 2014.
- [99] D. A. Gomes and V. K. Voskanyan. Extended deterministic mean-field games. *SIAM Journal on Control and Optimization*, 54(2):1030–1055, 2016.
- [100] D. Gomes, J. Gutiérrez, and M. Laurière. Machine learning architectures for price formation models. *arXiv preprint arXiv:2204.03968*, 2022.
- [101] I. Goodfellow, Y. Bengio, and A. Courville. *Deep learning*. MIT press, 2016.
- [102] F. Gozzi, S. di Roma, and C. Marinelli. Stochastic optimal control of delay equations arising in advertising models. *Stochastic Partial Differential Equations and Applications-VII*, pages 133–148, 2005.
- [103] F. Gozzi, C. Marinelli, and S. Savin. On controlled linear diffusions with delay in a model of optimal advertising under uncertainty with memory effects. *Journal of Optimization Theory and Applications*, 142(2):291–321, 2009.
- [104] A. Graves. Generating sequences with recurrent neural networks. *arXiv preprint arXiv:1308.0850*, 2013.
- [105] A. Graves, A.-r. Mohamed, and G. Hinton. Speech recognition with deep recurrent neural networks. In *2013 IEEE International Conference on Acoustics, Speech and Signal Processing*, pages 6645–6649. IEEE, 2013.
- [106] A. Graves and J. Schmidhuber. Offline handwriting recognition with multidimensional recurrent neural networks. In *Advances in Neural Information Processing Systems*, pages 545–552, 2009.

- [107] P. Grohs, S. Ibragimov, A. Jentzen, and S. Koppensteiner. Lower bounds for artificial neural network approximations: A proof that shallow neural networks fail to overcome the curse of dimensionality. *arXiv preprint arXiv:2103.04488*, 2021.
- [108] S. Gronauer and K. Diepold. Multi-agent deep reinforcement learning: a survey. *Artificial Intelligence Review*, pages 1–49, 2021.
- [109] H. Gu, X. Guo, X. Wei, and R. Xu. Dynamic programming principles for mean-field controls with learning. *arXiv preprint arXiv:1911.07314*, 2019.
- [110] H. Gu, X. Guo, X. Wei, and R. Xu. Mean-field controls with Q-learning for cooperative MARL: convergence and complexity analysis. *SIAM Journal on Mathematics of Data Science*, 3(4):1168–1196, 2021.
- [111] H. Gu, X. Guo, X. Wei, and R. Xu. Mean-field multi-agent reinforcement learning: A decentralized network approach. *arXiv preprint arXiv:2108.02731*, 2021.
- [112] X. Guo, A. Hu, R. Xu, and J. Zhang. Learning mean-field games. In *Advances in Neural Information Processing Systems 32 (NeurIPS)*, 2019.
- [113] X. Guo, R. Xu, and T. Zariphopoulou. Entropy regularization for mean field games with learning. *Mathematics of Operations Research*, 2022.
- [114] S. Hadikhanloo. Ph. d. paris-dauphine thesis defence document. 2018.
- [115] S. Hadikhanloo and F. J. Silva. Finite mean field games: fictitious play and convergence to a first order continuous mean field game. *Journal de Mathématiques Pures et Appliquées*, 132:369–397, 2019.
- [116] B. Hambly, R. Xu, and H. Yang. Policy gradient methods for the noisy linear quadratic regulator over a finite horizon. *SIAM Journal on Control and Optimization*, 59(5):3359–3391, 2021.
- [117] B. Hambly, R. Xu, and H. Yang. Recent advances in reinforcement learning in finance. *arXiv preprint arXiv:2112.04553*, 2021.
- [118] J. Han, R. Hu, and J. Long. A class of dimensionality-free metrics for the convergence of empirical measures. *arXiv preprint arXiv:2104.12036*, 2021.
- [119] J. Han, R. Hu, and J. Long. Convergence of deep fictitious play for stochastic differential games. *Frontiers of Mathematical Finance*, 1(2):287–319, 2022.
- [120] J. Han, R. Hu, and J. Long. Learning high-dimensional McKean-Vlasov forward-backward stochastic differential equations with general distribution dependence. *arXiv preprint arXiv:2204.11924*, 2022.
- [121] J. Han and W. E. Deep learning approximation for stochastic control problems. *Deep Reinforcement Learning Workshop, NIPS, arXiv preprint arXiv:1611.07422*, 2016.
- [122] J. Han and R. Hu. Deep fictitious play for finding Markovian Nash equilibrium in multi-agent games. In *Mathematical and Scientific Machine Learning (MSML)*, volume 107, pages 221–245. PMLR, 2020.
- [123] J. Han and R. Hu. Recurrent neural networks for stochastic control problems with delay. *Mathematics of Control, Signals, and Systems*, 33(4):775–795, 2021.
- [124] J. Han, A. Jentzen, and W. E. Solving high-dimensional partial differential equations using deep learning. *Proceedings of the National Academy of Sciences*, 115(34):8505–8510, 2018.
- [125] J. Han and J. Long. Convergence of the deep BSDE method for coupled FBSDEs. *Probability, Uncertainty and Quantitative Risk*, 5(1):1–33, 2020.
- [126] J. Han, Y. Yang, and W. E. DeepHAM: A global solution method for heterogeneous agent models with aggregate shocks. *arXiv preprint arXiv:2112.14377*, 2021.

- [127] B. Hanin. Universal function approximation by deep neural nets with bounded width and ReLU activations. *Mathematics*, 7(10):992, 2019.
- [128] B. Hanin and D. Rolnick. Deep ReLU networks have surprisingly few activation patterns. *Advances in neural information processing systems*, 32, 2019.
- [129] B. Hanin and M. Sellke. Approximating continuous functions by ReLU nets of minimal width. *arXiv preprint arXiv:1710.11278*, 2017.
- [130] P. Henry-Labordere. Deep primal-dual algorithm for BSDEs: Applications of machine learning to CVA and IM. *Available at SSRN 3071506*, 2017.
- [131] P. Henry-Labordere, C. Litterer, and Z. Ren. A dual algorithm for stochastic control problems: Applications to uncertain volatility models and CVA. *SIAM Journal on Financial Mathematics*, 7(1):159–182, 2016.
- [132] C. F. Higham and D. J. Higham. Deep learning: An introduction for applied mathematicians. *Siam review*, 61(4):860–891, 2019.
- [133] S. Hochreiter and J. Schmidhuber. Long short-term memory. *Neural computation*, 9(8):1735–1780, 1997.
- [134] K. Hornik. Approximation capabilities of multilayer feedforward networks. *Neural networks*, 4(2):251–257, 1991.
- [135] K. Hornik, M. Stinchcombe, and H. White. Multilayer feedforward networks are universal approximators. *Neural networks*, 2(5):359–366, 1989.
- [136] J. Hu and M. P. Wellman. Nash Q-learning for general-sum stochastic games. *Journal of machine learning research*, 4(Nov):1039–1069, 2003.
- [137] R. Hu and M. Ludkovski. Sequential design for ranking response surfaces. *SIAM/ASA Journal on Uncertainty Quantification*, 5(1):212–239, 2017.
- [138] R. Hu. Deep learning for ranking response surfaces with applications to optimal stopping problems. *Quantitative Finance*, 20(9):1567–1581, 2020.
- [139] R. Hu. Deep fictitious play for stochastic differential games. *Communications in Mathematical Sciences*, 19(2):325–353, 2021.
- [140] R. Hu and T. Zariphopoulou.  $N$ -player and mean-field games in Itô-diffusion markets with competitive or homophilous interaction. In *Stochastic Analysis, Filtering, and Stochastic Optimization: A Commemorative Volume to Honor Mark HA Davis's Contributions*, pages 209–237. Springer, 2022.
- [141] M. Huang, P. E. Caines, and R. P. Malhamé. Large-population cost-coupled LQG problems with nonuniform agents: individual-mass behavior and decentralized  $\epsilon$ -Nash equilibria. *IEEE Transactions on Automatic Control*, 52(9):1560–1571, 2007.
- [142] M. Huang, R. P. Malhamé, and P. E. Caines. Large population stochastic dynamic games: closed-loop McKean-Vlasov systems and the Nash certainty equivalence principle. *Communications in Information and Systems*, 6(3):221–252, 2006.
- [143] K. J. Hunt, D. Sbarbaro, R. Źbikowski, and P. J. Gawthrop. Neural networks for control systems—a survey. *Automatica*, 28(6):1083–1112, 1992.
- [144] C. Huré, H. Pham, A. Bachouch, and N. Langrené. Deep neural networks algorithms for stochastic control problems on finite horizon: convergence analysis. *SIAM Journal on Numerical Analysis*, 59(1):525–557, 2021.
- [145] C. Huré, H. Pham, and X. Warin. Deep backward schemes for high-dimensional nonlinear PDEs. *Mathematics of Computation*, 89(324):1547–1579, 2020.

[146] M. Hutzenthaler, A. Jentzen, T. Kruse, and T. A. Nguyen. A proof that rectified deep neural networks overcome the curse of dimensionality in the numerical approximation of semilinear heat equations. *SN partial differential equations and applications*, 1:1–34, 2020.

[147] R. Isaacs. *Differential Games: A Mathematical Theory with Applications to Warfare and Pursuit, Control and Optimization*. London: John Wiley and Sons, 1965.

[148] S. Jaimungal, S. M. Pesenti, Y. S. Wang, and H. Tatsat. Robust risk-aware reinforcement learning. *SIAM Journal on Financial Mathematics*, 13(1):213–226, 2022.

[149] A. Jentzen, D. Salimova, and T. Welti. A proof that deep artificial neural networks overcome the curse of dimensionality in the numerical approximation of Kolmogorov partial differential equations with constant diffusion and nonlinear drift coefficients. *Communications in Mathematical Sciences*, 19(5):1167–1205, 2021.

[150] S. Ji, S. Peng, Y. Peng, and X. Zhang. Three algorithms for solving high-dimensional fully coupled FBSDEs through deep learning. *IEEE Intelligent Systems*, 35(3):71–84, 2020.

[151] Y. Jia and X. Y. Zhou. Policy evaluation and temporal-difference learning in continuous time and space: A martingale approach. *Available at SSRN 3905379*, 2021.

[152] Y. Jia and X. Y. Zhou. Policy gradient and actor-critic learning in continuous time and space: Theory and algorithms. *arXiv preprint arXiv:2111.11232*, 2021.

[153] Z. Jin, M. Qiu, K. Q. Tran, and G. Yin. A survey of numerical solutions for stochastic control problems: Some recent progress. *Numerical Algebra, Control and Optimization*, 12(2):213–253, 2022.

[154] L. P. Kaelbling, M. L. Littman, and A. W. Moore. Reinforcement learning: A survey. *Journal of artificial intelligence research*, 4:237–285, 1996.

[155] N. Keriven, A. Bietti, and S. Vaiter. On the universality of graph neural networks on large random graphs. *Advances in Neural Information Processing Systems*, 34:6960–6971, 2021.

[156] J. Kierzenka and L. F. Shampine. A BVP solver based on residual control and the Maltab PSE. *ACM Transactions on Mathematical Software (TOMS)*, 27(3):299–316, 2001.

[157] D. P. Kingma and J. Ba. Adam: A method for stochastic optimization. *arXiv preprint arXiv:1412.6980*, 2014.

[158] A. C. Kizilkale and R. P. Malhame. Collective target tracking mean field control for Markovian jump-driven models of electric water heating loads. *IFAC Proceedings Volumes*, 47(3):1867–1872, 2014. 19th IFAC World Congress.

[159] Z. Kobeissi. On classical solutions to the mean field game system of controls. *Communications in Partial Differential Equations*, 47(3):453–488, 2022.

[160] Z. Kobeissi and F. Bach. On a variance reduction correction of the temporal difference for policy evaluation in the stochastic continuous setting. *arXiv preprint arXiv:2202.07960*, 2022.

[161] M. Kohler, A. Krzyżak, and N. Todorovic. Pricing of high-dimensional American options by neural networks. *Mathematical Finance: An International Journal of Mathematics, Statistics and Financial Economics*, 20(3):383–410, 2010.

[162] M. Kohlmann and X. Y. Zhou. Relationship between backward stochastic differential equations and stochastic controls: a linear-quadratic approach. *SIAM J. Control Optim.*, 38(5):1392–1407, 2000.

[163] V. B. Kolmanovskii and L. E. Shaikhet. *Control of Systems with Aftereffect*, volume 157. American Mathematical Society, 1996.

[164] V. N. Kolokoltsov and A. Bensoussan. Mean-field-game model for botnet defense in cyber-security. *Appl. Math. Optim.*, 74(3):669–692, 2016.

[165] H. J. Kushner. Numerical methods for stochastic control problems in continuous time. *SIAM Journal on Control and Optimization*, 28(5):999–1048, 1990.

[166] F. E. Kydland and E. C. Prescott. Time to build and aggregate fluctuations. *Econometrica: Journal of the Econometric Society*, pages 1345–1370, 1982.

[167] D. Lacker. Limit theory for controlled McKean–Vlasov dynamics. *SIAM Journal on Control and Optimization*, 55(3):1641–1672, 2017.

[168] D. Lacker and A. Soret. Many-player games of optimal consumption and investment under relative performance criteria. *Mathematics and Financial Economics*, 14(2):263–281, 2020.

[169] D. Lacker and T. Zariphopoulou. Mean field and n-agent games for optimal investment under relative performance criteria. *Mathematical Finance*, 29(4):1003–1038, 2019.

[170] M. Lanctot, V. Zambaldi, A. Gruslys, A. Lazaridou, K. Tuyls, J. Pérolat, D. Silver, and T. Graepel. A unified game-theoretic approach to multiagent reinforcement learning. *Advances in neural information processing systems*, 30, 2017.

[171] B. Lapeyre and J. Lelong. Neural network regression for Bermudan option pricing. *Monte Carlo Methods and Applications*, 27(3):227–247, 2021.

[172] J.-M. Lasry and P.-L. Lions. Jeux à champ moyen. I. Le cas stationnaire. *C. R. Math. Acad. Sci. Paris*, 9:619–625, 2006.

[173] J.-M. Lasry and P.-L. Lions. Jeux à champ moyen. II. Horizon fini et contrôle optimal. *C. R. Math. Acad. Sci. Paris*, 10:679–684, 2006.

[174] J.-M. Lasry and P.-L. Lions. Mean field games. *Japanese Journal of Mathematics*, 2:229–260, 2007.

[175] J.-M. Lasry and P.-L. Lions. Mean field games. *Jpn. J. Math.*, 2(1):229–260, 2007.

[176] M. Laurière. On numerical methods for mean field games and mean field type control. Proc. AMS Short Course, 2020.

[177] M. Laurière, S. Perrin, M. Geist, and O. Pietquin. Learning mean field games: A survey. *arXiv preprint arXiv:2205.12944*, 2022.

[178] M. Laurière, S. Perrin, S. Girgin, P. Muller, A. Jain, T. Cabannes, G. Piliouras, J. Pérolat, R. Élie, O. Pietquin, et al. Scalable deep reinforcement learning algorithms for mean field games. *arXiv preprint arXiv:2203.11973*, 2022.

[179] M. Laurière and L. Tangpi. Convergence of large population games to mean field games with interaction through the controls. *SIAM Journal on Mathematical Analysis*, 54(3):3535–3574, 2022.

[180] L. Leal, M. Laurière, and C.-A. Lehalle. Learning a functional control for high-frequency finance. Preprint, arXiv:2006.09611, 2020.

[181] W. Lefebvre and E. Miller. Linear-quadratic stochastic delayed control and deep learning resolution. *Journal of Optimization Theory and Applications*, 191(1):134–168, 2021.

[182] C.-A. Lehalle and R. Azencott. Piecewise affine neural networks and nonlinear control. In *International Conference on Artificial Neural Networks*, pages 633–638. Springer, 1998.

[183] M. Leshno, V. Y. Lin, A. Pinkus, and S. Schocken. Multilayer feedforward networks with a nonpolynomial activation function can approximate any function. *Neural networks*, 6(6):861–867, 1993.

[184] K. Li and J. Liu. Portfolio selection under time delays: A piecewise dynamic programming approach. Available at SSRN 2916481, 2018.

[185] Y. Li. Deep reinforcement learning: An overview. *arXiv preprint arXiv:1701.07274*, 2017.

[186] T. P. Lillicrap, J. J. Hunt, A. Pritzel, N. Heess, T. Erez, Y. Tassa, D. Silver, and D. Wierstra. Continuous control with deep reinforcement learning. In *Proceedings of the International Conference on Learning Representations (ICLR 2016)*, 2016.

[187] A. T. Lin, S. W. Fung, W. Li, L. Nurbekyan, and S. J. Osher. APAC-Net: Alternating the population and agent control via two neural networks to solve high-dimensional stochastic mean field games. *arXiv preprint arXiv:2002.10113*, 2020.

[188] P.-L. Lions. Cours du Collège de France. [https://www.college-de-france.fr/site/en-pierre-louis-lions/\\_course.htm](https://www.college-de-france.fr/site/en-pierre-louis-lions/_course.htm), 2007-2011.

[189] Z. Lu, H. Pu, F. Wang, Z. Hu, and L. Wang. The expressive power of neural networks: A view from the width. *Advances in neural information processing systems*, 30, 2017.

[190] T. Lyons and Z. Qian. *System control and rough paths*. Oxford University Press, 2002.

[191] T. J. Lyons, M. Caruana, and T. Lévy. *Differential equations driven by rough paths*. Springer, 2007.

[192] J. L. Mathieu, S. Koch, and D. S. Callaway. State estimation and control of electric loads to manage real-time energy imbalance. *IEEE Transactions on Power Systems*, 28:430–440, 2013.

[193] M. Min and R. Hu. Signatured deep fictitious play for mean field games with common noise. In *International Conference on Machine Learning (ICML)*, pages 7736–7747. PMLR 139, 2021.

[194] S. Mishra and R. Molinaro. Estimates on the generalization error of physics-informed neural networks for approximating PDEs. *IMA Journal of Numerical Analysis*, 2022.

[195] S. Mishra and R. Molinaro. Estimates on the generalization error of physics-informed neural networks for approximating a class of inverse problems for PDEs. *IMA Journal of Numerical Analysis*, 42(2):981–1022, 2022.

[196] V. Mnih, K. Kavukcuoglu, D. Silver, A. A. Rusu, J. Veness, M. G. Bellemare, A. Graves, M. Riedmiller, A. K. Fidjeland, G. Ostrovski, S. Petersen, C. Beattie, A. Sadik, I. Antonoglou, H. King, D. Kumaran, D. Wierstra, S. Legg, and D. Hassabis. Human-level control through deep reinforcement learning. *Nature*, 518(7540):529–533, 2015.

[197] S.-E. A. Mohammed. *Stochastic Functional Differential Equations*, volume 99. Pitman Advanced Publishing Program, 1984.

[198] S.-E. A. Mohammed. Stochastic differential systems with memory: theory, examples and applications. In *Stochastic Analysis and Related Topics VI*, pages 1–77. Springer, 1998.

[199] M. Motte and H. Pham. Mean-field Markov decision processes with common noise and open-loop controls. *To appear in Annals of Applied Probability (arXiv preprint arXiv:1912.07883)*, 2019.

[200] R. Munos. Policy gradient in continuous time. *Journal of Machine Learning Research*, 7:771–791, 2006.

[201] J. Nash. Non-cooperative games. *Annals of mathematics*, pages 286–295, 1951.

[202] M. Nutz and Y. Zhang. Conditional optimal stopping: a time-inconsistent optimization. *Ann. Appl. Probab.*, 30(4):1669–1692, 2020.

[203] B. Øksendal and A. Sulem. A maximum principle for optimal control of stochastic systems with delay, with applications to finance. *Preprint series. Pure mathematics* <http://urn. nb. no/URN: NBN: no-8076>, 2000.

[204] E. Pardoux and S. Peng. Adapted solution of a backward stochastic differential equation. *Systems & Control Letters*, 14(1):55–61, 1990.

[205] S. Park, C. Yun, J. Lee, and J. Shin. Minimum width for universal approximation. In *International Conference on Learning Representations*.

[206] S. Peng. Stochastic Hamilton–Jacobi–Bellman equations. *SIAM Journal on Control and Optimization*, 30(2):284–304, 1992.

[207] S. Perrin, M. Laurière, J. Pérolat, R. Élie, M. Geist, and O. Pietquin. Generalization in mean field games by learning master policies. *AAAI'22 (arXiv preprint arXiv:2109.09717)*, 2021.

[208] S. Perrin, M. Laurière, J. Pérolat, M. Geist, R. Élie, and O. Pietquin. Mean field games flock! The reinforcement learning way. In *proc. of IJCAI*, 2021.

[209] H. Pham. *Continuous-time stochastic control and optimization with financial applications*, volume 61. Springer Science & Business Media, 2009.

[210] H. Pham. On some recent aspects of stochastic control and their applications. *Probability Surveys*, 2:506–549, 2005.

[211] H. Pham, X. Warin, and M. Germain. Neural networks-based backward scheme for fully nonlinear PDEs. *SN Partial Differential Equations and Applications*, 2(1):16, 2021.

[212] A. Pinkus. Approximation theory of the MLP model in neural networks. *Acta Numerica*, 8:143–195, 1999.

[213] W. B. Powell. *Approximate Dynamic Programming: Solving the curses of dimensionality*, volume 703. John Wiley & Sons, 2007.

[214] D. Psaltis, A. Sideris, and A. A. Yamamura. A multilayered neural network controller. *IEEE control systems magazine*, 8(2):17–21, 1988.

[215] M. Raissi, P. Perdikaris, and G. E. Karniadakis. Physics-informed neural networks: A deep learning framework for solving forward and inverse problems involving nonlinear partial differential equations. *Journal of Computational Physics*, 378:686–707, 2019.

[216] C. Reisinger, W. Stockinger, and Y. Zhang. A fast iterative PDE-based algorithm for feedback controls of nonsmooth mean-field control problems. *arXiv preprint arXiv:2108.06740*, 2021.

[217] C. Reisinger, W. Stockinger, and Y. Zhang. A posteriori error estimates for fully coupled McKean–Vlasov forward-backward SDEs. *arXiv preprint arXiv:2007.07731*, 2020.

[218] A. M. Reppen, H. M. Soner, and V. Tissot-Daguet. Deep stochastic optimization in finance. *arXiv preprint arXiv:2205.04604*, 2022.

[219] A. M. Reppen, H. M. Soner, and V. Tissot-Daguet. Neural optimal stopping boundary. *arXiv preprint arXiv:2205.04595*, 2022.

[220] D. E. Rumelhart, G. E. Hinton, and R. J. Williams. Learning representations by back-propagating errors. *Nature*, 323(6088):533–536, 1986.

[221] L. Ruthotto, S. J. Osher, W. Li, L. Nurbekyan, and S. W. Fung. A machine learning framework for solving high-dimensional mean field game and mean field control problems. *Proceedings of the National Academy of Sciences*, 117(17):9183–9193, 2020.

[222] Y. F. Saporito and Z. Zhang. Path-dependent deep Galerkin method: A neural network approach to solve path-dependent partial differential equations. *SIAM Journal on Financial Mathematics*, 12(3):912–940, 2021.

[223] A. M. Schäfer and H. G. Zimmermann. Recurrent neural networks are universal approximators. In *Artificial Neural Networks–ICANN 2006: 16th International Conference, Athens, Greece, September 10–14, 2006. Proceedings, Part I 16*, pages 632–640. Springer, 2006.

[224] S. Shalev-Shwartz, S. Shammah, and A. Shashua. Safe, multi-agent, reinforcement learning for autonomous driving. *arXiv preprint arXiv:1610.03295*, 2016.

[225] D. Silver, A. Huang, C. J. Maddison, A. Guez, L. Sifre, G. Van Den Driessche, J. Schrittwieser, I. Antonoglou, V. Panneershelvam, M. Lanctot, et al. Mastering the game of Go with deep neural networks and tree search. *Nature*, 529(7587), 2016.

[226] D. Silver, G. Lever, N. Heess, T. Degris, D. Wierstra, and M. Riedmiller. Deterministic policy gradient algorithms. In *Proceedings of the 31st International Conference on Machine Learning*, volume 32 of *Proceedings of Machine Learning Research*, pages 387–395. PMLR, 2014.

[227] J. Sirignano and K. Spiliopoulos. DGM: A deep learning algorithm for solving partial differential equations. *Journal of computational physics*, 375:1339–1364, 2018.

[228] J. Subramanian and A. Mahajan. Reinforcement learning in stationary mean-field games. In *in proc. of AAMAS*, 2019.

[229] R. S. Sutton and A. G. Barto. *Reinforcement learning: An introduction*. MIT press, 2018.

[230] A.-S. Sznitman. Topics in propagation of chaos. In *Ecole d’été de probabilités de Saint-Flour XIX—1989*, pages 165–251. Springer, 1991.

[231] K. Tuyls and G. Weiss. Multiagent learning: Basics, challenges, and prospects. *Ai Magazine*, 33(3):41–41, 2012.

[232] R. van der Meer, C. W. Oosterlee, and A. Borovykh. Optimally weighted loss functions for solving PDEs with neural networks. *Journal of Computational and Applied Mathematics*, 405:113887, 2022.

[233] O. Vinyals, I. Babuschkin, W. M. Czarnecki, M. Mathieu, A. Dudzik, J. Chung, D. H. Choi, R. Powell, T. Ewalds, P. Georgiev, et al. Grandmaster level in StarCraft II using multi-agent reinforcement learning. *Nature*, 575(7782), 2019.

[234] H. Wang, T. Zariphopoulou, and X. Y. Zhou. Reinforcement learning in continuous time and space: A stochastic control approach. *Journal of Machine Learning Research*, 21(198):1–34, 2020.

[235] H. Wang and X. Y. Zhou. Continuous-time mean–variance portfolio selection: A reinforcement learning framework. *Mathematical Finance*, 30(4):1273–1308, 2020.

[236] L. Wang, Q. Cai, Z. Yang, and Z. Wang. Neural policy gradient methods: Global optimality and rates of convergence. In *International Conference on Learning Representations*.

[237] R. J. Williams. Simple statistical gradient-following algorithms for connectionist reinforcement learning. *Reinforcement learning*, pages 5–32, 1992.

[238] Q. Xie, Z. Yang, Z. Wang, and A. Minca. Learning while playing in mean-field games: Convergence and optimality. In *International Conference on Machine Learning*, pages 11436–11447. PMLR, 2021.

[239] Y. Xuan, R. Balkin, J. Han, R. Hu, and H. D. Ceniceros. Optimal policies for a pandemic: A stochastic game approach and a deep learning algorithm. In *Mathematical and Scientific Machine Learning*, pages 145:987–1012. PMLR, 2022.

[240] Y. Xuan, R. Balkin, J. Han, R. Hu, and H. D. Ceniceros. Pandemic control, game theory and machine learning. *Notices of the AMS*, 69(11):1878–1887, December 2022.

[241] Y. Yang and J. Wang. An overview of multi-agent reinforcement learning from game theoretical perspective. *arXiv preprint arXiv:2011.00583*, 2020.

[242] Y. Zang, J. Long, X. Zhang, W. Hu, E. Weinan, and J. Han. A machine learning enhanced algorithm for the optimal landing problem. In *Mathematical and Scientific Machine Learning*, pages 319–334. PMLR, 2022.

- [243] K. Zhang, Z. Yang, and T. Başar. Multi-agent reinforcement learning: A selective overview of theories and algorithms. *Handbook of Reinforcement Learning and Control*, pages 321–384, 2021.
- [244] D.-X. Zhou. Universality of deep convolutional neural networks. *Applied and computational harmonic analysis*, 48(2):787–794, 2020.

## A Deep Learning Tools

In this section, we briefly review neural networks and stochastic gradient descent, which are two of the main tools of modern machine learning. We refer to [132] for a more comprehensive mathematical introduction to deep learning for applied mathematicians and to [101] for more background on deep learning.

### A.1 Neural network architectures

We start by introducing the feedforward fully connected architecture, before discussing recurrent neural networks and long short-term memory networks.

#### A.1.1 Feedforward fully connected neural networks

Feedforward neural networks (FNNs) are the most common type of neural networks. We denote by

$$\mathbf{L}_{d_1, d_2}^{\rho} = \left\{ \phi : \mathbb{R}^{d_1} \rightarrow \mathbb{R}^{d_2} \mid \exists (w, \beta) \in \mathbb{R}^{d_2 \times d_1} \times \mathbb{R}^{d_2}, \forall i \in \{1, \dots, d_2\}, \phi(x)_i = \rho \left( \beta_i + \sum_{j=1}^{d_1} w_{i,j} x_j \right) \right\}$$

the set of layer functions with input dimension  $d_1$ , output dimension  $d_2$ , and activation function  $\rho : \mathbb{R} \rightarrow \mathbb{R}$ . Typical choices for  $\rho$  are ReLU (positive part), identity, sigmoid, or hyperbolic tangent,

$$\rho_{\text{ReLU}}(x) = \max\{x, 0\}, \quad \rho_{\text{Id}}(x) = x, \quad \rho_s(x) = \frac{1}{1 + e^{-x}}, \quad \rho_{\tanh}(x) = \tanh(x). \quad (\text{A.1})$$

Building on this notation and denoting by  $\circ$  the composition of functions, we define

$$\mathbf{N}_{d_0, \dots, d_{\ell+1}}^{\rho, \tilde{\rho}} = \left\{ \phi_{\ell} \circ \phi_{\ell-1} \circ \dots \circ \phi_0 \mid (\phi_i)_{i=0, \dots, \ell-1} \in \bigtimes_{i=0}^{i=\ell-1} \mathbf{L}_{d_i, d_{i+1}}^{\rho}, \phi_{\ell} \in \mathbf{L}_{d_{\ell}, d_{\ell+1}}^{\tilde{\rho}} \right\}$$

as the set of regression neural networks with  $\ell$  hidden layers and one output layer, the activation function of the output layer being  $\tilde{\rho}$ . The number  $\ell$  of hidden layers, the numbers  $d_0, d_1, \dots, d_{\ell+1}$  of units per layer, and the activation functions, are the components of what is called the architecture of the network. Once it is fixed, the actual network function  $\varphi \in \mathbf{N}_{d_0, \dots, d_{\ell+1}}^{\rho, \tilde{\rho}}$  is determined by the remaining parameters

$$\theta = (\beta^{(0)}, w^{(0)}, \beta^{(1)}, w^{(1)}, \dots, \beta^{(\ell-1)}, w^{(\ell-1)}, \beta^{(\ell)}, w^{(\ell)}),$$

defining the functions  $\phi_0, \phi_1, \dots, \phi_{\ell-1}$  and  $\phi_{\ell}$  respectively. Let us denote by  $\Theta$  the set of values for such parameters. For each  $\theta \in \Theta$ , the function computed by the network will be denoted by  $\varphi^{\theta} \in \mathbf{N}_{d_0, \dots, d_{\ell+1}}^{\rho, \tilde{\rho}}$  when we want to stress the dependence on the parameters.

To alleviate the presentation, we will follow the convention to use vector and matrix notations, and here activation functions are implicitly applied coordinate-wisely. Then

$$\varphi^{\theta}(x) = \tilde{\rho} \left( \beta^{(\ell)} + w^{(\ell)} \rho \left( \beta^{(\ell-1)} + w^{(\ell-1)} \rho \left( \dots \beta^{(0)} + w^{(0)} x \right) \right) \right).$$

#### A.1.2 Recurrent neural networks

Although FNNs are universal approximators, they are not very suitable to handle path-dependent properties of the state process, which are important for instance when the stochastic control problem or the game has delay features. The idea of recurrent neural networks (RNNs) [220] is to make use of sequential

information, and thus provide a natural framework for overcoming these issues. In fact, RNNs have already shown great success in, *e.g.*, natural language processing and handwriting recognition [104, 105, 106]. Many variants exist and below we shall focus on one such variant, but the generic architecture can be described as follows: the neural network takes two inputs,  $x$  and  $h$ , and produces two outputs,  $y$  and  $h'$ , as follows:

$$h' = \rho \left( \beta^{(1)} + w^{(1,1)}h + w^{(1,2)}x \right),$$

$$y = \tilde{\rho} \left( \beta^{(2)} + w^{(2)}h' \right),$$

where  $\rho, \tilde{\rho}$  are two activation functions, and the parameters of the neural network are vectors  $\beta^{(1)}, \beta^{(2)}$  of suitable sizes, and matrices  $w^{(1,1)}, w^{(1,2)}, w^{(2)}$  of suitable sizes.

Given a sequence of data points  $(x_k)_{k \geq 0}$ , which can represent the discrete-time trajectory of state process for instance, and an initial input  $h_0$ , a RNN can be used recursively to produce the sequence  $(y_k, h_k)_{k \geq 1}$  defined by

$$h_k = \rho \left( \beta^{(1)} + w^{(1,1)}h_{k-1} + w^{(1,2)}x_{k-1} \right),$$

$$y_k = \tilde{\rho} \left( \beta^{(2)} + w^{(2)}h_k \right).$$

Here,  $h_{k+1}$  encodes information that is transmitted from iteration  $k$  to iteration  $k+1$ . This information is produced using previous information  $h_k$  and the current data point  $x_k$ . It is used to compute the output  $y_k$  associated to the current input  $x_k$ , and the future information  $h_{k+2}$ .

Based on the idea of using an architecture in a recurrent way, many generalizations of the above simple neural network have been proposed. We next present one of them.

### A.1.3 Long short-term memory

One of the most common types of RNN is the long short-term memory (LSTM) neural network [133]. The advantage of an LSTM is the ability to deal with the vanishing gradient problem and data with lags of unknown duration. An LSTM is composed of a series of units, each of which corresponds to a timestamp, and each unit consists of a cell  $c$  and three gates: input gate  $i$ , output gate  $o$ , and forget gate  $f$ . Among these components, the cell keeps track of the information received so far, the input gate captures to which extent new input information flows into the cell, the forget gate captures to which extent the existing information remains in the cell, and the output gate controls to which extent the information in the cell will be used to compute the output of the unit. Given a data sequence  $(x_k)_{k \geq 0}$  and an initial input  $h_0$ , the information flows are

$$\begin{aligned} \text{forget gate: } & f_k = \rho_s(W_f x_k + U_f h_{k-1} + b_f), \\ \text{input gate: } & i_k = \rho_s(W_i x_k + U_i h_{k-1} + b_i), \\ \text{output gate: } & o_k = \rho_s(W_o x_k + U_o h_{k-1} + b_o), \\ \text{cell: } & c_k = f_k \odot c_{k-1} + i_k \odot \rho_{\tanh}(W_c x_k + U_c h_{k-1} + b_c), \\ \text{output of the } k^{\text{th}} \text{ unit: } & h_k = o_k \odot \rho_{\tanh}(c_k), \end{aligned}$$

where the operator  $\odot$  denotes the Hadamard product,  $W_f, W_i, W_o, W_c, U_f, U_i, U_o, U_c, b_f, b_i, b_o$  and  $b_c$  are neural network parameters of compatible sizes, and  $\rho_s$  and  $\rho_{\tanh}$  are activation functions given in (A.1).

### A.1.4 Expressive power of neural networks

The first theories about neural networks date back to 1989 by Cybenko [74] and by Hornik, Stinchcombe and White [135], concerning the approximation capabilities of feedforward networks within a given function space of interest. Hornik [134] then extended the results to approximating function's derivatives, and Leshno, Lin, Pinkus and Schocken [183] proved results under arbitrary nonpolynomial activation functions. These results are referred to as universal approximation theorems. See also [212].

In the past decade, the mathematical theory has been greatly developed, which is complemented by unprecedented advances in highly parallelizable graphics processing units (GPUs), the introduction of new

network architectures, and the development of GPU-enabled algorithms. For instance, in terms of approximation theories, other types of neural networks have been investigated, including RNN [223], convolutional neural networks (CNNs) [244] and graph neural networks (GNNs) [155]. Concerning the expressive power of neural networks, [127] analyzed it from the depth point view, while [189, 129, 205] considered a width perspective. Several works tackle the question of how neural networks can tackle the curse of dimensionality; see, e.g., [128, 107, 149, 146]. For further discussion the onw mathematical theory of deep learning, we refer to, e.g., [29].

## A.2 Stochastic gradient descent and its variants

The process of adjusting the parameters of a parameterized system, such as a neural network, in order to optimize a loss function is called *training*. Stochastic gradient descent (SGD) is one of the most popular method to train neural network parameters, for example for the aforementioned FNNs, RNNs and LSTMs.

Consider a generic optimization problem: minimize over  $\varphi$ ,

$$J(\varphi) = \mathbb{E}_{\xi \sim \nu} [\mathcal{L}(\varphi, \xi)],$$

where  $\xi$  follows a distribution  $\nu$  and  $\mathcal{L}$  is a loss function. Using a neural network with a given architecture as an approximator for  $\varphi$ , the goal becomes to minimize over  $\theta$ ,

$$J(\theta) = \mathbb{E}_{\xi \sim \nu} [\mathcal{L}(\varphi_\theta, \xi)].$$

Even if  $\mathcal{L}$  is known, the loss cannot be computed exactly when  $\nu$  is unknown. If one does not have access to  $\nu$  but only to samples drawn from  $\nu$ , one can use SGD, described in Algorithm 1, which relies on an empirical risk minimization problem,

$$J^{S,N}(\theta) = \frac{1}{N} \sum_{i=1}^N \mathcal{L}(\varphi_\theta, \xi^i),$$

where  $N$  is the number of training samples of  $\xi$  and we denote the sample set by  $S = (\xi^1, \dots, \xi^N)$ .

---

### Algorithm 1 Stochastic Gradient Descent (SGD)

---

**Input:** An initial parameter  $\theta_0 \in \Theta$ . A mini-batch size  $N_{\text{Batch}}$ . A number of iterations  $M$ . A sequence of learning rates  $(\beta_m)_{m=0, \dots, M-1}$ .  
**Output:** Approximation of  $\theta^*$   
**for**  $m = 0, 1, 2, \dots, M-1$  **do**  
    Sample a minibatch of  $N_{\text{Batch}}$  samples  $S = (\xi^i)_{i=1, \dots, N_{\text{Batch}}}$  where  $\xi^i$  are i.i.d. drawn from  $\nu$   
    Compute the gradient  $\nabla J^{S, N_{\text{Batch}}}(\theta_m)$   
    Update  $\theta_{m+1} = \theta_m - \beta_m \nabla J^{S, N_{\text{Batch}}}(\theta_m)$   
**end for**  
    Return  $\theta_M$

---

SGD is generally used with a moderately large size of mini-batch, which reduces the computational cost of each iteration and can furthermore help escaping local minima. In practice, the choice of the learning rate can be crucial to ensure convergence. A popular way to adjust the learning rate is the Adam method [157] which is summarized in Algorithm 2 and can be viewed as an adaptive momentum accelerated SGD. The computation of the gradient  $\nabla J^{S,N}(\theta)$  with respect to  $\theta$  can be done automatically by libraries such as `TensorFlow` or `PyTorch`, which perform this computation efficiently by using backpropagation.

## B Preliminaries on SDDE

In this section, we provide some background on stochastic differential delay equations. Let  $\mathcal{C}_{-\delta} = C([-\delta, 0], \mathbb{R}^d)$  be the Banach space of all  $\mathbb{R}^d$ -valued continuous functions defined on  $[-\delta, 0]$  endowed with the supremum norm

$$\|y\|_{\mathcal{C}_{-\delta}} = \sup_{-\delta \leq s \leq 0} |y_s|, \quad \forall y \in \mathcal{C}_{-\delta}.$$

---

**Algorithm 2** ADAM: Adaptive Moment Estimation

---

**Input:** Stepsize  $\alpha$ . Exponential decay rates for the moment estimates  $\beta_1, \beta_2 \in [0, 1)$ . Initial parameter  $\theta_0$ . Small parameter for numerical stability  $\epsilon$ .

**Output:** Approximation of  $\theta^*$

Initialize first moment vector  $\bar{M}_0$  and second moment vector  $\bar{V}_0$

**for**  $m = 0, 1, 2, \dots, M-1$  **do**

    Sample a minibatch of  $N_{\text{Batch}}$  samples  $S = ((\xi^i)_{i=1, \dots, N_{\text{Batch}}})$  where  $x^i$  are i.i.d. drawn from  $\nu$

    Compute the gradient  $g_m = \nabla J^S(\theta_m)$

    Update biased first moment estimate:  $\bar{M}_m = \beta_1 \bar{M}_{m-1} + (1 - \beta_1)g_m$

    Update biased second moment estimate:  $\bar{V}_m = \beta_2 \bar{V}_{m-1} + (1 - \beta_2)g_m^2$

    Compute biased-corrected first moment estimate:  $\hat{M}_m = \bar{M}_m / (1 - \beta_1^m)$

    Compute biased-corrected second moment estimate:  $\hat{V}_m = \bar{V}_m / (1 - \beta_2^m)$

    Set  $\theta_{m+1} = \theta_m - \alpha \hat{M}_m / (\sqrt{\hat{V}_m} + \epsilon)$

**end for**

Return  $\theta_M$

---

This space represents portions of trajectories. The drift  $b$  and volatility  $\sigma$  coefficients, and the running  $f$  and terminal costs  $g$  are deterministic functionals

$$(b, \sigma, f) : [0, T] \times \mathcal{C}_{-\delta} \times \mathcal{A} \rightarrow (\mathbb{R}^d, \mathbb{R}^{d \times m}, \mathbb{R}); \quad g : \mathcal{C}_{-\delta} \rightarrow \mathbb{R}.$$

Denote by  $L^2(\Omega, \mathcal{C}_{-\delta})$  the space of all  $\mathcal{F}$ -measurable stochastic processes, *i.e.*,

$$\Omega \ni \omega \rightarrow X(\omega) \in \mathcal{C}_{-\delta} \text{ is in } L^2(\Omega, \mathcal{C}_{-\delta}), \text{ iff. } \int_{\Omega} \|X(\omega)\|_{\mathcal{C}_{-\delta}}^2 d\mathbb{P}(\omega) < \infty.$$

The space  $L^2(\Omega, \mathcal{C}_{-\delta})$  endowed with the semi-norm  $\|X\|_{L^2(\Omega, \mathcal{C}_{-\delta})} = [\int_{\Omega} \|X(\omega)\|_{\mathcal{C}_{-\delta}}^2 d\mathbb{P}(\omega)]^{1/2}$  is a complete space. We assume that the initial path  $\varphi \in L^2(\Omega, \mathcal{C}_{-\delta})$  and is independent of the Brownian motion  $W$ , and the existence of a solution  $X$  to the SDDE (2.12) is considered in  $L^2(\Omega, C([-\delta, T], \mathbb{R}^d))$ . Let  $(\mathcal{F}_t)_{t \geq 0}$  be the filtration supporting  $W$  and  $\varphi$ , and let  $C([0, T], L^2(\Omega, \mathcal{C}_{-\delta}))$  be the space of all  $L^2$ -continuous  $\mathcal{C}_{-\delta}$ -valued  $\mathcal{F}_t$ -adapted processes  $P : [0, T] \ni t \rightarrow \underline{P}_t \in L^2(\Omega, \mathcal{C}_{-\delta})$  endowed with the semi-norm

$$\|P\|_{C([0, T], L^2(\Omega, \mathcal{C}_{-\delta}))} = \sup_{0 \leq t \leq T} \|\underline{P}_t\|_{L^2(\Omega, \mathcal{C}_{-\delta})}.$$

The trajectory  $\underline{X}_t$  solving the SDDE (2.12) is considered in  $C([0, T], L^2(\Omega, \mathcal{C}_{-\delta}))$ .

Usually, one requires uniform Lipschitz conditions in the second variable of  $b$  and  $\sigma$  to ensure the existence and uniqueness of strong solutions to the SDDE (2.12), that is,

$$\|(b, \sigma)(t, y_1, \alpha) - (b, \sigma)(t, y_2, \alpha)\|_{L^2} \leq L \|y_1 - y_2\|_{L^2(\Omega, \mathcal{C}_{-\delta})}, \quad \forall t \in [0, T] \text{ and } y_1, y_2 \in L^2(\Omega, \mathcal{C}_{-\delta}).$$

See detailed analysis in Mohammed's monographs [197, 198]. Assumptions on  $f$  and  $g$  will ensure the expected cost (2.13) is finite.

## C Pseudo-codes of Algorithms

---

**Algorithm 3** Deep Fictitious Play for Finding Open-loop Nash Equilibrium

---

**Require:**  $N = \#$  of players,  $N_T = \#$  of subintervals on  $[0, T]$ ,  $M = \#$  of training paths,  $M' = \#$  of out-of-sample paths for final evaluation,  $\alpha^0 = \{\alpha_{t_n}^{i,0} \in \mathcal{A} \subset \mathbb{R}^k, i \in \mathcal{I}\}_{n=0}^{N_T-1}$  = initial belief,  $\mathbf{X}_0 = \{x_0^i \in \mathbb{R}^d, i \in \mathcal{I}\}$  = initial states

- 1: Create  $N$  separated deep neural networks as described in Eq. (3.6)
- 2: Generate  $M$  discrete sample path of BM:  $\mathbf{W} = \{W_{t_n}^i \in \mathbb{R}^m, i \in \mathcal{I} \cup \{0\}\}_{n=1}^{N_T}$
- 3:  $\mathbf{k} \leftarrow 0$
- 4: **repeat**
- 5:   **for all**  $i \in \mathcal{I}$  **do in parallel**
- 6:      $\mathbf{k} \leftarrow \mathbf{k} + 1$
- 7:     (Continue to) Train  $i^{th}$  NN with data  $\{\mathbf{X}_0, \alpha^{-i,\mathbf{k}-1} = \{\alpha_{t_n}^{j,\mathbf{k}-1}, j \in \mathcal{I} \setminus \{i\}\}_{n=0}^{N_T-1}, \mathbf{W}\}$
- 8:     Obtain the approximated optimal strategy  $\alpha^{i,\mathbf{k}}$  and cost  $J^i(\alpha^{i,\mathbf{k}}; \alpha^{-i,\mathbf{k}-1})$
- 9:   **end for**
- 10:   Collect optimal policies at stage  $\mathbf{k}$ :  $\alpha^{\mathbf{k}} \leftarrow (\alpha^{1,\mathbf{k}}, \dots, \alpha^{N,\mathbf{k}})$
- 11:   Compute relative change of cost  $err^{\mathbf{k}} = \max_{i \in \mathcal{I}} \left\{ \frac{|J^i(\alpha^{i,\mathbf{k}}; \alpha^{-i,\mathbf{k}-1}) - J^i(\alpha^{i,\mathbf{k}-1}; \alpha^{-i,\mathbf{k}-2})|}{J^i(\alpha^{i,\mathbf{k}-1}; \alpha^{-i,\mathbf{k}-2})} \right\}$
- 12:   **until**  $err^{\mathbf{k}}$  go below a threshold
- 13:   Generate  $M'$  out-of-sample paths of BM for final evaluation
- 14:    $\mathbf{k}' \leftarrow 0$
- 15:   **repeat**
- 16:      $\mathbf{k}' \leftarrow \mathbf{k}' + 1$
- 17:     Evaluate  $i^{th}$  NN with  $\{\mathbf{X}_0, \alpha^{-i,\mathbf{k}'-1}$ , out-of-sample paths $\}, \forall i \in \mathcal{I}$
- 18:     Obtain  $\alpha^{i,\mathbf{k}'}$  and  $J^{i,\mathbf{k}'} = J^i(\alpha^{i,\mathbf{k}'}; \alpha^{-i,\mathbf{k}'-1}) \forall i \in \mathcal{I}$
- 19:   **until**  $J^{i,\mathbf{k}'}$  converges in  $\mathbf{k}'$ ,  $\forall i \in \mathcal{I}$
- 20: **return** The optimal policy  $\alpha^{i,\mathbf{k}'}$ , and the final cost for each player  $J^{i,\mathbf{k}'}$

---



---

**Algorithm 4** Deep Fictitious Play for Finding Markovian Nash Equilibrium

---

**Require:**  $N = \#$  of players,  $N_T = \#$  of subintervals on  $[0, T]$ ,  $K = \#$  of total stages in fictitious play,  $N_{\text{sample}} = \#$  of sample paths generated for each player at each stage of fictitious play,  $N_{\text{SGD\_per\_stage}} = \#$  of SGD steps for each player at each stage,  $N_{\text{batch}}$  = batch size per SGD update,  $\alpha^0$ : the initial policies that are smooth enough

- 1: Initialize  $N$  deep neural networks to represent  $u^{i,0}, i \in \mathcal{I}$
- 2: **for**  $\mathbf{k} \leftarrow 1$  to  $K$  **do**
- 3:   **for all**  $i \in \mathcal{I}$  **do in parallel**
- 4:     Generate  $N_{\text{sample}}$  sample paths  $\{\check{\mathbf{X}}_{t_n}^i\}_{n=0}^{N_T}$  according to (3.18) and the realized optimal policies  $\alpha^{-i,\mathbf{k}-1}(t_n, \check{\mathbf{X}}_{t_n}^i)$
- 5:     **for**  $\ell \leftarrow 1$  to  $N_{\text{SGD\_per\_stage}}$  **do**
- 6:       Update the parameters of the  $i^{th}$  neural network one step with  $N_{\text{batch}}$  paths using the SGD algorithm (or its variant), based on the loss function (3.17)
- 7:     **end for**
- 8:     Obtain the approximate optimal policy  $\alpha^{i,\mathbf{k}}$  according to (3.13)
- 9:   **end for**
- 10:   Collect the optimal policies at stage  $\mathbf{k}$ :  $\alpha^{\mathbf{k}} \leftarrow (\alpha^{1,\mathbf{k}}, \dots, \alpha^{N,\mathbf{k}})$
- 11: **end for**
- 12: **return** The optimal policy  $\alpha^{\mathbf{k}}$

---

---

**Algorithm 5** The Sig-DFP Algorithm

---

**Input:**  $b, \sigma, \sigma_0, f, g, \iota$  and  $X_0(\omega_i), \{W_{t_n}(\omega_i)\}_{n=0}^{N_T}, \{\hat{W}_{t_n}^0(\omega_i)\}_{n=0}^{N_T}$  for  $i = 1, 2, \dots, N$ ;  $K$ : rounds for FP;  $B$ : minibatch size;  $N_{\text{batch}}$ : number of minibatches.

Compute the signatures of  $\hat{W}_{t_n}^0(\omega_i)$  for  $i = 1, \dots, N, n = 1, \dots, N_T$ ;

Initialize  $\hat{\nu}^{(0)}, \theta$ ;

**for**  $k = 1$  **to**  $K$  **do**

- for**  $r = 1$  **to**  $N_{\text{batch}}$  **do**
- Simulate the  $r^{\text{th}}$  minibatch of  $X^{(k)}(\omega_i)$  using  $\hat{\nu}^{(k-1)}$  and compute  $J_B(\theta, \hat{\nu}^{(k-1)})$ ;
- Minimize  $J_B(\theta, \hat{\nu}^{(k-1)})$  over  $\theta$ , then update  $\alpha(\cdot; \theta)$ ;
- end for**
- Simulate  $X^{(k)}(\omega_i)$  with the optimized  $\alpha(\cdot; \theta^*)$ , for  $i = 1, \dots, N$ ;
- Regress  $\iota(X_0^{(k)}(\omega_i), \alpha_0^{(k)}(\omega_i)), \iota(X_{T/2}^{(k)}(\omega_i), \alpha_{T/2}^{(k)}(\omega_i)), \iota(X_T^{(k)}(\omega_i), \alpha_T^{(k)}(\omega_i))$  on  $S^M(\hat{W}_0^0 \omega_i), S^M(\hat{W}_{t_{N_T/2}}^0(\omega_i)), S^M(\hat{W}_T^0(\omega_i))$  to get  $\tilde{l}^{(k)}$ ;
- Update  $\hat{l}^{(k)} = \frac{k-1}{k} \hat{l}^{(k-1)} + \frac{1}{k} \tilde{l}^{(k)}$ ;
- Compute  $\hat{\nu}^{(k)}$  by  $\hat{\nu}_{t_n}^{(k)}(\omega^i) = \langle \hat{l}^{(k)}, S^M(\hat{W}_{t_n}^0(\omega_i)) \rangle$ , for  $i = 1, 2, \dots, N, n = 1, \dots, N_T$ ;

**end for**

**Output:** the optimized  $\alpha_\varphi^*$  and  $\hat{l}^{(k)}$ .

---

## D List of Acronyms

ADAM	Adaptive Moments Gradient Descent
BSDE	Backward Stochastic Differential Equation
2BSDE	Second Order Backward Stochastic Differential Equation
CDC	Centers for Disease Control and Prevention
DNN	Deep Neural Networks
DBDP	Deep Backward Dynamic Programming
Deep BSDE	Deep Backward Stochastic Differential Equation
DDPG	Deep Deterministic Policy Gradient
DGM	Deep Galerkin Method
DFP	Deep Fictitious Play
DPG	Deterministic Policy Gradient
DPP	Dynamic Programming Principle
FBSDE	Forward Backward Stochastic Differential Equation
FNN	Feedforward Neural Network
FP	Fokker-Planck
GRU	Gated Recurrent Unit
HJB	Hamilton-Jacobi-Bellman
KFP	Kolmogorov-Fokker-Planck
LQ	Linear-Quadratic
LSTM	Long Short-term Memory
MARL	Multi-agent Reinforcement Learning
MC	Monte Carlo
MDP	Markov Decision Process
MFC	Mean-Field Control
MFG	Mean-Field Game
MFMDP	Mean-Field Markov Decision Process
MKV	McKean-Vlasov
MKV FBSDE	McKean-Vlasov Forward Backward Stochastic Differential Equation
NE	Nash Equilibrium
NN	Neural Network
ODE	Ordinary Differential Equation
PDE	Partial Differential Equations
PINN	Physics Informed Neural Network
ReLU	Rectified Linear Unit
RL	Reinforcement Learning
RNN	Recurrent Neural Network
SC	Stochastic Control
SDE	Stochastic Differential Equation

## E List of Frequently Used Notations

Deep learning related notations	
$\theta$	neural network parameters
$\varphi^\theta$	neural network with parameters $\theta$
$J(\theta)$	optimization function for training the parameters $\theta$
Optimal control related notations	
$x$	state variable
$(X_t)_{t \in [0, T]}$	state process
$(Y_t, Z_t)_{t \in [0, T]}$	backward and adjoint processes
$(\alpha_t)_{t \in [0, T]}, (\beta_t)_{t \in [0, T]}$	control process
$(W_t)_{t \in [0, T]}, (W_t^0)_{t \in [0, T]}$	Wiener process
$d$	dimension of the state
$k$	dimension of the action
$m$	dimension of the noise
$b(t, x, \alpha)$	drift coefficient of the state process
$\sigma(t, x, \alpha)$	diffusion coefficient of the state process
$f(t, x, \alpha)$	instantaneous cost function
$g(x)$	terminal cost function
$J(\alpha)$	total cost function associated with the control $\alpha$
$\check{J}(\theta)$	total cost function associated with the discretized stochastic control problem with neural network parameters $\theta$
$(\bar{X}_t)_{t \in [0, T]}$	empirical average of $N$ -players' states
$\underline{X}_t = (\underline{X}_t(s))_{s \in [-\delta, 0]}$	trajectory of $X_t$ from time $t - \delta$ to $t$
$T$	time horizon
$\text{Hess}_x u(t, x)$	Hessian matrix of $u$ with respect to $x$
$H$	Hamiltonian function
$u(t, x)$	value function
Stochastic games related notations	
$X_t^i$	state process for player $i$
$\alpha_t^i$	action function for player $i$
$\boldsymbol{\alpha} = [\alpha^1, \alpha^2, \dots, \alpha^N]$	a collection of all players' strategy profiles
$\boldsymbol{\alpha}^{-i} = [\alpha^1, \dots, \alpha^{i-1}, \alpha^{i+1}, \dots, \alpha^N]$	the strategy profiles excluding player $i$ 's
$\mathbf{W} = [W^0, W^1, \dots, W^N]$	$(N+1)$ -vector of $m$ -dimensional independent Brownian motions
$\mathbb{F} = \{\mathcal{F}_t, 0 \leq t \leq T\}$	the augmented filtration generated by $\mathbf{W}$
$J^i(\boldsymbol{\alpha})$	cost function for player $i$
$k$	stage index in deep fictitious play
$m$	mean process (or conditional mean if there is common noise)
$\mu$	state distribution process
$\mu^N$	empirical state distribution process
$\nu$	state-action distribution process
$\nu^N$	empirical state-action distribution process